Planning with Uncertainty in Position Using High-Resolution Maps

Juan Pablo Gonzalez

CMU-RI-TR-08-02

Submitted in partial fulfillment of the
requirements for the degree of
Doctor of Philosophy in Robotics

The Robotics Institute
Carnegie Mellon University
Pittsburgh, Pennsylvania 15213

April 2008

Thesis Committee:
Anthony Stentz (chair)
Martial Hebert
Drew Bagnell
Steven LaValle, University of Illinois at Urbana

Abstract

Navigating autonomously is one of the most important problems facing outdoor mobile robots. This task is extremely difficult if no prior information is available and is trivial if perfect prior information is available and the position of the robot is precisely known. Perfect prior maps are rare, but good-quality, high-resolution prior maps are increasingly available. Although the position of the robot is usually known through the use of the Global Position System (GPS), there are many scenarios in which GPS is not available, or its reliability is compromised by different types of interference such as mountains, buildings, foliage or jamming. If GPS is not available, the position estimate of the robot depends on dead-reckoning alone, which drifts with time and can accrue very large errors. Most existing approaches to path planning and navigation for outdoor environments are unable to use prior maps if the position of the robot is not precisely known. Often these approaches end up performing the much harder task of navigating without prior information.

This thesis addresses the problem of planning paths with uncertainty in position for large outdoor environments. The objective is to be able to reliably navigate autonomously in an outdoor environment without GPS through the use of high resolution prior maps and a good dead-reckoning system. Different approaches to the problem are presented, depending on the types of landmarks available, the accuracy of the map and the quality of the perception system. These approaches are validated in simulations and field experiments on an e-gator robotic platform.

Acknowledgments

I would like to thank my advisor Tony Stentz for his vision, guidance and ideas, which have shaped my research during these years and will help shape my future as well.

I also would like to thank my committee members Steven LaValle, Drew Bagnell and Martial Hebert, and other people who have made important contributions to this work. I would like to thank especially to Max Likhachev, David Ferguson and Nick Roy for the many thorough discussions and exchanges of ideas that prepared the way for the approaches presented here. I would also like to thank Marc Zinck, Balajee Kannan, Freddie Dias, Matthew Sarnoff, Eugene Marinelli and Ling Xu for their invaluable contribution to the field experiments.

Thank you, Red Whittaker for your endless drive to push the boundaries of robotics and for creating the Red Team, which was one of the best experiences of my life, and the inspiration of many aspects of this research.

Thanks to General Dynamics Robotic Systems and in particular Barbara Lindauer, Kevin Bonner, Scott Myers, Marc DelGiorno, and John Martin for their generous support and encouragement.

To CMU, and especially the Robotics Institute, for shaping the PhD in robotics in a way that not only provides knowledge, but also enables collaboration, friendship and a sense of community. To my friends at CMU, which have made these years so fun and exciting.

Thanks to Colombia en Pittsburgh which has given me a greater appreciation for my home country while getting to know some of the finest people I know and having great fun along the way.

To my family, for their support and for making life so fun and full of memories. To Larry and Carol for being my family. To my mom, for her love and support during all these years. To my dad, who always had time to answer my endless questions and who now is in a better place.

Thank you, Melissa for making life full of love, in spite of dissertations. And thank you, little Vanessa, for always having a happy face to brighten my day.

This work was sponsored by the U.S. Army Research Laboratory under contract "Robotics Collaborative Technology Alliance" (contract number DAAD19-01-2-0012). The views and conclusions contained in this document do not represent the official policies or endorsements of the U.S. Government.

Contents

List of Figures

Chapter 1

Introduction

Navigating autonomously is one of the most important problems facing outdoor mobile robots. This task is extremely difficult if no prior information is available and is trivial if perfect prior information is available and the position of the robot is precisely known. Perfect prior maps are rare, but good-quality, high-resolution prior maps are increasingly available. Although the position of the robot is usually known through the use of the Global Position System (GPS), there are many scenarios in which GPS is not available, or its reliability is compromised by different types of interference such as mountains, buildings, foliage or jamming. If GPS is not available, the position estimate of the robot depends on dead-reckoning alone, which drifts with time and can accrue very large errors. Most existing approaches to path planning and navigation for outdoor environments are unable to use prior maps if the position of the robot is not precisely known. Often these approaches end up performing the much harder task of navigating without prior information.

1.1 Applications

GPS is not available in underwater and underground environments, as well as in planetary environments. More frequently, however, GPS is available but its reliability is compromised. This happens in situations that require navigating through areas in which the sky is partially occluded such as urban areas, forests or canyons. It can also be affected by intentional jamming in battlefield operations.

In situations like these, planning with uncertainty in position complements existing path planning and navigation approaches by allowing safe navigation in the parts of the mission that lack reliable GPS coverage.

1.2 Prior Work

1.2.1 Classical path planning

Classical path planning deals with the problem of finding the best path between two locations, assuming the position of the robot is known at all times. Because of the deterministic nature of the problem, and the fact that good heuristics can be easily found, the problem can be efficiently addressed using deterministic search techniques. In general the problem consists in modeling the state space as a graph *G(V,E)*, and then finding an appropriate search algorithm to search such graph [57].

1.2.2 Classical path planning with uncertainty in position

In order to deal with uncertainty in position, classical path planning algorithms usually model uncertainty as a region of uncertainty that changes shape as states propagate in the search.

Indoors

Most of the prior work in classical path planning with uncertainty deals with indoor environments and as such represents the world as either *free* or *obstacle*. In most of the approaches from classical path planning, uncertainty is modeled as a set that contains all the possible locations within the error bounds defined by an uncertainty propagation model.

The first approach to planning with uncertainty, by Lozano-Perez, Mason and Taylor [64], was called *pre-image back chaining.* This approach was designed to plan fine motions in the presence of uncertainty in polygonal worlds. Latombe, Lazanas and Shekhar [55] expanded this approach by proposing practical techniques to calculate *pre-images*, still within the limitations of binary, polygonal worlds. Latombe [56][54] has an extensive review of other similar approaches as of 1991.

Lazanas and Latombe [59] later expanded the *pre-image backchaining* approach to robot navigation. For this purpose they define the bounds in the error of the position of the robot as a disk, and they use an uncertainty propagation model in which the error in the position of the model increases linearly with distance traveled. The idea of a landmark is also introduced as a circular region with perfect sensing. The world consists of free space with disks that can be either landmarks or obstacles.

Takeda and Latombe [93][94], proposed an alternative approach to planning with uncertainty using a sensory uncertainty field. In their approach, the landmarks in the environments are transformed into a sensory uncertainty field that represents the landmark's ability to localize the robot. Then they use Dijkstra's algorithm to find a path

that minimizes the uncertainty field or a combination of uncertainty and another objective function. The planner is limited to a polygonal representation of the world, and does not actually consider the uncertainty in position that the robot accrues as it executes the path.

Bouilly, Simeón and Alami [5][6] use a potential-field approach. In their approach the world is described by free space and polygonal obstacles and landmarks. They add the notion of localization with walls. The also introduce the notion of minimizing either the length of the resulting path or its uncertainty.

Page and Sanderson [73] extend Takeda and Latombe's approach [93][94] by modeling the uncertainty along the path, as well as considering the characteristics of the sensor uncertainty field when localizing with different types of landmarks. This allows for localization with walls and other polygonal obstacles. It also enables modeling cameras and other sensors as sources of localizing information.

Fraichard and Mermond [15][26][27] extend the approach of Bouilly *et al* by adding a third dimension to the search (for heading) and computing non-holonomic paths for car-like robots. They also use a more elaborate model for uncertainty propagation in which they calculate separately the uncertainty caused by errors in the longitudinal and steering controls.

Lambert and Fraichard [52] combine some of the previous approaches, introducing a non-holonomic planner for car-like robots that uses a perception uncertainty field to estimate the localization abilities of different landmarks. The approach, however, does not represent uncertainty as part of the search space.

Lambert and Gruyer [53] extend this approach with a planner that finds shortest safe paths by considering the non-holonomic constraints of a car-like robot and also representing uncertainty as part of the search space. They introduce the concept of "Towers of Uncertainty" which allows for multiple covariance matrices at a given *x,y* location to be preserved in the search.

Outdoors

Planning paths for outdoor applications represents additional challenges with respect to planning for indoor environments. The main challenges are the varying difficulty of the terrain, the lack of structure, and the size of the environment.

The varying difficulty of the terrain requires a representation of the environment that is able to represent terrain types other than *free space* and *obstacles.* Outdoor terrain has many variations with different implications for robot navigation: there are paved roads, unpaved roads, grass, tall grass, hilly areas, etc. The non-binary nature of outdoor terrain also requires a different spatial representation for the world. While polygonal representations are adequate and efficient for indoor environments, they are not practical or efficient for varying terrain types. The most common way to represent this varying

terrain is through a cost map. Cost maps are usually uniform grids of cells in which the cost at each cell represents the difficulty of traversing that cell. The main problem of uniform cost maps is that they can only represent the world up to the resolution of the cells in the map. If by reducing the size of the cells arbitrarily it is possible to solve a problem with an arbitrarily high precision, the solution is usually called *resolution-complete*. Although there are other representations that avoid this problem, most cost maps are implemented on a uniform grid. While there are many algorithms that can search the graph described by this grid, A*[68] expands the smallest number of nodes if all the edges have positive costs and an admissible heuristic can be found.

Haït, Siméon and Taïx were the first to consider the problem of planning with uncertainty in an outdoor environment. In the approach proposed in [36], the resulting path minimizes a non-binary cost function defined by a cost map, but the definition of uncertainty is limited to a fixed local neighborhood in which the planner checks for the validity of the paths. In [37] they expand their uncertainty model to be a disk with a radius that grows linearly with distance traveled, and they add landmarks as part of the planning process. Their approach performs a wave propagation search in a 2-D graph and attempts to minimize worst-case cost instead of path length. However, because their representation is limited to 2-D, it is unable to find solutions for problems in which uncertainty constraints require choosing a higher-cost path in order to achieve lower uncertainty. See section Chapter 4 for more details on the importance of modeling uncertainty as a third dimension.

Iagnemma *et al* [40] propose a two-stage approach in which a path is first planned in a 2-D cost map, and then the path is rigorously evaluated using a physical model of the robot. During this second evaluation stage, uncertainties in the terrain data, soil/tire interaction rover model and rover path are considered. If the model-base evaluation determines that the path is not safe, the cost in the high risk regions is increased and the process is repeated. While this approach is able to efficiently plan very safe paths, it does not model uncertainty in the planning stage, therefore suffering from some of the shortcomings of Haït's approach.

1.2.3 Planning with uncertainty using POMDPs

A Partially Observable Markov Decision Process (POMDP) is a representation in which both states and actions are uncertain [12][43] therefore providing a rich framework for planning under uncertainty. To handle partial state observability, plans are expressed over *information states*, instead of world states, since the latter ones are not directly observable. The space of information states is the space of all beliefs a system might have regarding the world state and is often known as the *belief space*. In POMDPs,

information states are typically represented by probability distributions over world states. POMDPs can be used for either belief tracking or policy selection.

When used for belief tracking, the solution of a POMDP is a probability distribution representing the possible world states. Most approaches to belief tracking perform only robot localization (see section 1.2.4), however a few perform planning based on the solution of the belief tracking POMDP. Nourbakhsh *et al*, [71] quantize the world into corridors and interleave planning and execution by using a POMDP to keep track of all possible states, and then find the shortest path to the goal from the most likely location of the robot. Their results are implemented in the DERVISH robot, allowing it to win the 1994 Office Delivery Event of in AAAI'94.

Simmons *et al* [86] use a similar approach of interleaving planning and execution on Xavier, but quantize the position of the robot in one-meter intervals along corridors. From the most likely position reported by the POMDP they plan an A* path that accounts for the probability of corridors being blocked or turns being missed.

When used for policy selection the solution of a POMDP is a policy that chooses what action to attempt at each information state based on the state estimate and the results of the previous actions. In this case, the optimal solution of a POMDP is the policy that maximizes the expected reward considering the probability distributions of states and actions. While the model is sufficiently rich to address most robotic planning problems, exact solutions are generally intractable for all but the smallest problems [76].

Because POMDPs optimize a continuous value function they could easily handle the continuous cost worlds typical of outdoor environments. However, because of their complexity, they have only been used for indoor environments where the structure and size of the environment significantly reduce the complexity of the problem. In spite of the reduced state space of indoor environments, POMDPs still require further approximations or simplifications in order to find tractable solutions.

Very few POMDP approaches can handle large-enough environments that would be suitable for outdoor environments. One of the leading approaches to extend POMDP's to larger environments is Pineau's Point-Based Value Iteration (PBVI) [75][76]. This approach selects a small set of belief points to calculate value updates, enabling it to solve problems with 10^3-10^4 states, at least an order of magnitude larger than conventional techniques. However, this algorithm still takes several hours to find such solution.

Roy and Thrun implemented an approach called Coastal Navigation [79][81] that models the uncertainty of the robot's position as a state variable and minimizes the uncertainty at the goal. They model the uncertainty through a single parameter which is the entropy of a Gaussian distribution and then use Value Iteration to find an optimal policy in this compressed belief space. Their algorithm has a lengthy pre-processing stage

but is able to produces results in a few seconds after the initial pre-processing state. The total planning time (including the pre-processing stage) can take from several minutes to a few hours [82] in a world with approximately 10^4 states in *(x,y)*. If the prior map that the robot uses is accurate, the initial pre-processing only needs to be performed once. However, if there are significant changes in the world, the pre-processing would have to be repeated, or the solution to the problem may no longer be valid.

Roy and Gordon build on this approach using Exponential Family Principal Component Analysis (E-PCA) [80], and take advantage of belief space sparsity. The dimensionality of the belief space is reduced by exponential family Principal Components Analysis, which allows them to turn the sparse, high-dimensional belief space into a compact, low-dimensional representation in terms of learned features of the belief state. They then plan directly on the low-dimensional belief features. By planning in a low-dimensional space, they can find policies for POMDPs that are orders of magnitude larger than what can be handled by conventional techniques. Still, for a world with 10^4 states E-PCA takes between two and eight hours to find a solution, depending on the number of bases used.

1.2.4 Robot localization

Localization is a fundamental problem in robotics. Using its sensors, a mobile robot must determine its localization within some map of the environment. There are both passive and active versions of the localization problem:

Passive robot localization

In passive localization the robot executes actions and its position is inferred from the sensor outputs collected during the traverse.

Kalman filter

The earliest and most common form of passive robot localization is the Kalman filter [44], which combines relative (dead-reckoning) and absolute position estimates to get a global position estimate. The sources for the absolute position estimates can be landmarks, map features, Global Positioning System (GPS), laser scans matched to environment features, etc.

The Kalman Filter is an optimal estimator for a linear dynamic process. Each variable describing the state of the process to be modeled is represented by a Gaussian distribution and the Kalman filter predicts the mean and variance of that distribution based on the data available at any given time. Because the Gaussian distribution is unimodal, the Kalman filter is unable to represent ambiguous situations and requires an initial estimate of the position of the robot. Approaches like the Kalman filter that can

only handle single hypotheses and require and initial estimate of the position of the robot are considered *local approaches*.

If the process to be estimated is not linear, as often happens in real systems, the standard Kalman filter cannot be used. Instead, other versions of the Kalman filter such as the Extended Kalman Filter need to be implemented. The Extended Kalman filter linearizes the system process model every time a new position estimate is calculated, partially addressing the non-linearities of the system. However the estimate produced by the Extended Kalman filter is no longer optimal. See Gelb [29] for an in-depth analysis of the theory and practical considerations of Kalman Filters.

In spite of its limitations, Kalman filters are the most widely used passive localization approach, because of its computational efficiency and the quality of the results obtained when there is a good estimate of the initial position and unique landmarks are available.

Map matching

One of the earliest forms of passive localization is map matching, which originated in the land vehicle guidance and tracking literature [28][38][95]. The vehicle is usually constrained to a road network and its position on the road network is estimated based on odometry, heading changes, and initial position. Because an estimate of the initial position is needed, this method is also considered a *local approach.* The main application of map matching is to augment GPS in tracking the position of a vehicle.

While the first approaches were limited to grid-like road networks, later approaches such as [42] extended the idea to more general road geometries by using pattern recognition techniques. These algorithms attempt to correlate the pattern created by the recent motion of the vehicle with the patterns of the road network. El Najaar [19] uses belief theory to handle the fusion of different data sources and select the most likely location of the vehicle. Scott [83] models map-matching as an estimation process within a well defined mathematical framework that allows map information and other sources of position information to be optimally incorporated into a GPS-based navigation system. Abbott [1] has an extensive review of the literature in map-matching as well as an analysis of its influence on the performance of the navigation system.

Markov localization

Markov localization uses a POMDP to track the possible locations of the robot (belief tracking). Tracking the belief state of a POMDP is a computationally intensive task, but unlike planning with POMDPs it is tractable even for relatively large worlds. POMDPs are a *global approach* to localization. They can track multiple hypotheses (modes) about the belief space of the robot and are able to localize the robot without any information about the initial state of the robot. They also provide additional robustness to localization failures.

Nourkbakhsh *et al*, [71] introduced the notion of Markov localization, quantizing the world into corridors and using a POMDP to keep track of all possible states. Simmons *et al* [86] use a similar approach on Xavier, but quantize the position of the robot in one-meter intervals along corridors.

Burgard *et al* [7][9][20] introduced grid-based Markov localization. In their approach, they accumulate in each cell of the position probability grid the posterior probability of this cell referring to the current position of the robot. This approach is able to take raw data from range sensors and is therefore able to take advantage of arbitrary geometric features in the environment. Its main disadvantage is that it needs to store a full 3-D grid containing the likelihoods for each position in x, y and θ. The approach is experimentally validated in worlds of about 200x200 cells, but should work in much larger worlds.

Dellaert *et al* [15][24] introduced Monte Carlo Localization. In this approach the probability density function is represented by maintaining a set of samples that are randomly drawn from it (a *particle filter*) instead of a grid. By using a sampling-based representation they significantly improve speed and space efficiency with respect to grid-based approaches, while maintaining the ability to represent arbitrary distributions. It is also more accurate than grid-based Markov localization, and can integrate measurements at a considerably higher frequency.

Markov localization is a powerful and mature technique for robot localization. It is a reliable and fast way to globally localize a robot. However, it is a passive technique and it cannot control the trajectory of the vehicle to choose a path that either guarantees localization or satisfies other mission objectives.

Active robot localization

In active localization a plan must be designed to reduce the localization uncertainty as much as possible. Active localization does not plan trajectories that improve localization while simultaneously achieving some goal, but instead dictates the optimal trajectory only for discovering the true location of the robot [20].

Non deterministic

Non-deterministic approaches to active robot localization model the position of the robot as a set of states. The localization task consists of reducing the set to a singleton (a single state). Most approaches assume that the initial position is unknown and there is no uncertainty in sensing or acting.

Koenig and Simmons use real-time heuristic search (Min-Max Learning Real Time A* - LRTA*) [46][50], which is an extension of LRTA* to handle non-deterministic domains. They are able to produce worst-case optimal results in a maze by modeling the task as a large, non-deterministic domain whose states are sets of poses.

If the robot has a range sensor and a compass then the environment can be modeled as a polygon and use visibility tests to identify hypotheses about the location of the robot followed by a hypothesis elimination phase. Dudek *et al* [15] proved that localizing a robot in this way with minimum travel is NP-hard, and proposed a greedy approach that is complete but that can have very poor performance. Rao *et al* [77] builds on that result and uses the best of a set of randomly selected points to eliminate hypotheses, which produces much better average performance.

O'Kane and La Valle [72] showed that the localization problem in a polygonal world could be solved in a suboptimal fashion with just a compass and a contact sensor. They also showed that this was the minimal robot configuration that would allow localization is such worlds.

Probabilistic

Probabilistic methods for active localization model the distribution of possible states as a probability density function, and then find a set of actions to localize the robot. The POMDP-based planning approaches described in section 1.2.3 could in theory be used to solve this problem, but they also have the limitations caused by the complexity of POMDPs.

The approach proposed by Burgard *et al* [10][23] is similar to the one by Roy and Thrun described in section 1.2.3. They use entropy as a single-parameter statistic that summarizes the localization of the robot and perform value iteration selecting actions that minimize entropy at each step. Even though the solution uses a non-sufficient statistic to describe the probability distribution and uses greedy action selection, the algorithm performs very well and is able to work in reasonably large worlds. The approach, however, requires a long pre-processing stage in which the likelihoods of all sensor readings are calculated.

1.2.5 Active exploration and SLAM

Simultaneous Localization and Mapping (SLAM), attempts to build a map of an unknown environment while simultaneously using this map to estimate the absolute position of the vehicle. While in general SLAM is a passive approach in which the robot moves and data is collected to build the map and localize the robot, there exists a complementary approach called *active exploration*. In *active exploration* the objective is to find an optimal exploration policy to reduce the uncertainty in the map. As in active localization the optimal solution is intractable, but suboptimal solutions often produce satisfactory results.

One approach to the active localization problem is to attempt to maximize the information gain throughout the map by using gradient descent on the information gain

(or change in the relative entropy) [7][100]. The main problem with this approach is that is only locally optimal and is subject to local minima.

Staunchis and Burgard [90] describe one of the few global exploration algorithms. Their approach uses *coverage maps*, an extension of occupancy maps in which each cell represents not only the occupancy of the cell but also a probabilistic belief about the coverage of the cell. In this way they are able to compute the information available at all locations in the environment which allows them to calculate a maximally informative location.

Sim and Roy [85] propose using the *a-optimal* information measure instead of the *d-optimal* information measure (relative entropy), as the measure for information gain. Whereas the *d-optimal* information measure uses the product of the eigenvalues of the distribution, the *a-optimal* information measure uses the sum of the eigenvalues. They then use pruned breadth-first search over all robot positions to search for the expected sequence of estimates the lead to the maximum information gain. While their approach is not optimal, it produces a significantly more accurate map than the map obtained using *d-optimal* information gain.

1.2.6 Summary

Planning with uncertainty in position in outdoor environments is a difficult and computationally expensive problem that presents a number of important challenges such as the varying difficulty of the terrain, the lack of structure, and the size of the environment. The most general solution to planning paths with uncertainty in position requires finding the optimal policy for a POMDP, which is intractable for all but the smallest problems.

Most of the current approaches take advantage of the structure and size of indoor environments to make the problem tractable. While a few approaches handle outdoor environments, they do not model uncertainty in the planning space, which significantly limits the quality of the solutions that can be obtained.

1.3 Problem Statement

This thesis addresses the problem of planning paths with uncertainty in position for large outdoor environments. The objective is to be able to reliably navigate autonomously in an outdoor environment without GPS through the use of accurate, high resolution prior maps and a good dead-reckoning system.

The initial position of the robot is assumed to be known within a few meters and the initial heading is also assumed to be known within a few degrees. The dead reckoning

estimate in the position of the robot is assumed to drift slowly, at a rate lower than 10% of distance traveled, which is typical of an outdoor robot with wheel encoders and a fiber-optic gyro.

We assume a high-resolution map that allows the identification of landmarks and the approximate estimation of terrain types by automatic or manual methods. The high-resolution map is translated into a cost grid, in which the value of each cell corresponds to the cost of traveling from the center of the cell to its nearest edge. Non-traversable areas are assigned infinite cost and considered obstacles. We also assume that the robot has an on-board perception system with a limited detection range R, and is able to reliably detect landmarks and avoid small obstacles not present in the prior map.

The resulting path should minimize the expected traversability cost along the path, while ensuring that the uncertainty in the position of the robot does not compromise its safety or the reachability of the goal.

Additionally we explore some extensions such as dealing with imperfect landmark maps or imperfect landmark perception, and using linear landmarks for localization.

1.4 Technical approach

We present an approach that takes advantage of the low drift rate in the inertial navigation system of many outdoor mobile robots. The planner uses a Gaussian distribution to model position uncertainty and uses deterministic search to efficiently find paths that minimize expected cost while considering uncertainty in position.

We model the world as a continuous-cost map derived from a high-resolution prior map. This model allows us to model the varying difficulty of the terrain typical of outdoor environments. We model uncertainty as an additional dimension that constrains the feasible solutions to the problem and use deterministic search techniques such as A*, heuristics, lazy evaluation, state dominance and incremental search to efficiently find solutions in this larger state representation.

Our approach also uses landmarks to reduce uncertainty as part of the planning process. Landmarks are carefully chosen such that they can be reliably detected and their detection can be modeled as a deterministic event. Because landmarks that can be reliably detected such as trees and electric poles are not unique, we use an estimate of the position of the robot in order to disambiguate them and prevent aliasing as part of the planning process.

This thesis is structured as follows. Chapter 2, Background, introduces techniques and mathematical tools necessary to implement and understand the different approachs presented. Chapter 4, Planning with Uncertainty in Position , describes the core

approach to planning with uncertainty in position, based on a simplified error propagation model. While this approach is of limited use because it assumes no sensing, it provides the foundations for the other approaches presented later. Chapter 5, Planning with Uncertainty in Position Using Point Landmarks extends the previous approach by using landmarks. The approach is able to use non-unique landmarks by combining planning and perception in order to create unique landmarks. Chapter 6, Replanning with Uncertainty in Position (RPUP) uses D*Lite to repair the search graph and improve the performance of the algorithm by up to two orders of magnitude. It also introduces the idea of sensor and prior map updates, which deal with the two most common types of updates available for replanning. Chapter 7, Planning with Uncertainty in Position using an Inaccurate Landmark Map or Imperfect Landmark Perception, explores the impact of imperfect landmarks and proposes an approach that guarantees that the robot will not get lost if it fails to detect a landmark, while still allowing for fast replanning because of world updates. Chapter 8, Planning with Uncertainty in Position using Linear Landmarks, extends the uncertainty propagation model to use the full error covariance matrix, thus enabling the use of linear landmarks for localization.

Chapter 2

Background

2.1.1 Analysis of uncertainty propagation due to dead-reckoning

The first-order motion model for a point-sized robot moving in two dimensions is:

$$\begin{aligned} \dot{x}(t) &= v(t)\cos\theta(t) \\ \dot{y}(t) &= v(t)\sin\theta(t) \\ \dot{\theta}(t) &= \omega(t) \end{aligned} \tag{2.1}$$

where the state of the robot is represented by x(t), y(t) and θ(t) (x-position, y-position and heading respectively), and the inputs to the model are represented by v(t) and ω(t) (longitudinal speed and rate of change for the heading respectively). Equation (2.1) can also be expressed as:

$$\dot{\mathbf{q}}(t) = f(\mathbf{q}(t), \mathbf{u}(t)) \tag{2.2}$$

where $\mathbf{q}(t) = (x(t), y(t), \theta(t))$ and $\mathbf{u}(t) = (v(t), \omega(t))$.

A typical sensor configuration for a mobile robot is to have an odometry sensor and an onboard gyro. We can model the errors in the odometry and the gyro as errors in the inputs where $w_v(t)$ is the error in $v(t)$ (error due to the longitudinal speed control), and $w_\omega(t)$ is the error in $\omega(t)$ (error due to the gyro random walk).

Incorporating these error terms into (2.1) yields:

$$\begin{aligned} \dot{x}(t) &= (v(t) + w_v(t))\cos\theta(t) \\ \dot{y}(t) &= (v(t) + w_v(t))\sin\theta(t) \\ \dot{\theta}(t) &= \omega(t) + w_\omega(t) \end{aligned} \tag{2.3}$$

or, in discrete-time:

$$\begin{aligned} x(k+1) &= x(k) + (v(k) + w_v(k))\cos\theta(k)\Delta t \\ y(k+1) &= y(k) + (v(k) + w_v(k))\sin\theta(k)\Delta t \\ \theta(k+1) &= \theta(k) + (\omega(k) + w_\omega(k))\Delta t \end{aligned} \tag{2.4}$$

Using the extended Kalman filter (EKF) analysis for this system, which assumes that the random errors are zero-mean Gaussian distributions, we can model the error propagation as follows:

$$\Sigma(k+1) = \mathbf{F}(k) \cdot \Sigma(k) \cdot \mathbf{F}(k)^T + \mathbf{L}(k) \cdot \mathbf{Q}(k) \cdot \mathbf{L}(k)^T \tag{2.5}$$

where

$$\Sigma(k) = E(\hat{\mathbf{q}}(k)\hat{\mathbf{q}}(k)^T) \qquad \mathbf{Q}(k) = \frac{1}{\Delta t}\begin{pmatrix} {\sigma_v}^2 & 0 \\ 0 & {\sigma_\omega}^2 \end{pmatrix} \tag{2.6}$$

$$\mathbf{F}_{ij} = \frac{\partial f(q_i(k), u_j(k))}{\partial q_i}$$
$$\mathbf{F} = \begin{pmatrix} 1 & 0 & -v(k\Delta t)\sin(\theta(k)) \cdot \Delta t \\ 0 & 1 & v(k\Delta t)\cos(\theta(k)) \cdot \Delta t \\ 0 & 0 & 1 \end{pmatrix} \tag{2.7}$$

$$\mathbf{L}_{ij} = \frac{\partial f(q_i(k), u_j(k))}{\partial u_j}$$
$$\mathbf{L} = \begin{pmatrix} \cos(\theta(k)) \cdot \Delta t & 0 \\ \sin(\theta(k)) \cdot \Delta t & 0 \\ 0 & \Delta t \end{pmatrix} \tag{2.8}$$

Although there are no general closed-form solutions for these equations, Kelly [42] calculated closed-form solutions for some trajectories, and showed that a straight line trajectory maximizes each one of the error terms. We can use the results for this trajectory as an upper bound on the error for any trajectory. For a straight trajectory along the x-axis keeping all inputs constant, the error terms behave as follows. The error due to the longitudinal speed control w_v is reflected in the x direction, and is given by $\sigma_x^2 = \sigma_v^2 \cdot vt$, or $\sigma_x = \sigma_v\sqrt{vt}$. The error due to the gyro random walk w_ω is reflected in the y direction, and is given by $\sigma_y^2 = \sigma_\omega^2 \cdot v^2t^3$, or $\sigma_y = \sigma_\omega \cdot v \cdot t^{3/2}$.

Additionally, there are errors in the initial position of the robot. Errors in x and y do not increase unless there is uncertainty in the model or in the controls. Errors in the heading angle, however, propagate linearly with t. For small initial angle errors, the approximation $\sin\theta \approx \theta$ can be used to obtain the expression $\sigma_y = \sigma_{\theta_o}.vt$. As long as the total heading error is small, the first order approximation of the EKF will be a good approximation of the error propagation.

The dominant terms in the error propagation model depend on the navigation system and on the planning horizon for the robot. A typical scenario for a mobile robot with good inertial sensors is to have a planning horizon of up to 3km, at a speed of 5 m/s, with longitudinal control error of 10% of the commanded speed (σ_v= $0.1v = 0.5\,m/s$)

and gyro drift (random walk) of $20°/h/\sqrt{Hz}$ ($\sigma_\omega = 0.005°/s \;\; = 8.72 \cdot 10^{-5} rad/s$). In this scenario, the dominant term is the error in the longitudinal control. However, if there is uncertainty in the initial angle, this term becomes the dominant one for errors as small as 0.5 degrees (See Figure 1).

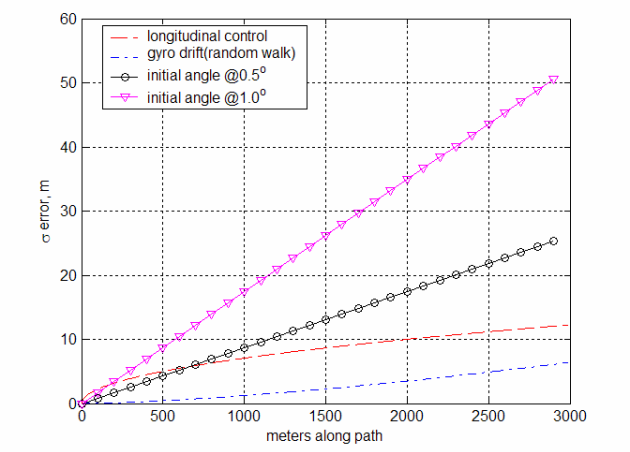

Figure 1. Comparison between different values of initial angle error and longitudinal control error

If we were to model the uncertainty propagation with a single parameter, the most appropriate model would be that of the dominant term. In this case, that dominant term is the error in the initial heading, which varies linearly with distance traveled.

Figure 2 shows the error propagation combining all the types of error (with the values mentioned above, and an initial heading error of 0.5 degrees) for a straight trajectory. The figure uses the results of a Monte Carlo simulation as a reference and it also shows the 2σ contours for the full EKF model and the 2σ contours for a single-parameter (isometric) Gaussian. Figure 3 shows the same analysis for a random trajectory. Notice how the single-parameter Gaussian is now a looser bound for the error propagation, and how the full EKF model is still a good approximation. See [31] for a more detailed analysis of the different modes of error propagation.

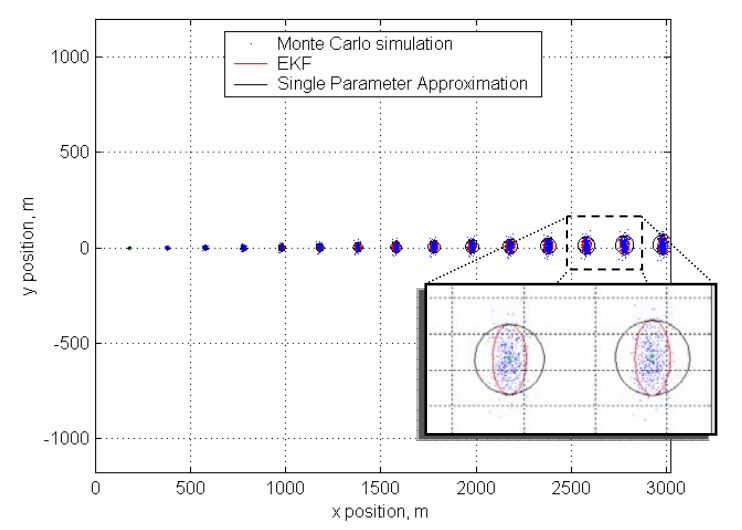

Figure 2. Error propagation for a straight trajectory with all error sources combined and inset showing detail. The blue dots are the Monte Carlo simulation, the red ellipse is the EKF model (2σ), and the black circle is the single parameter approximation (2σ)

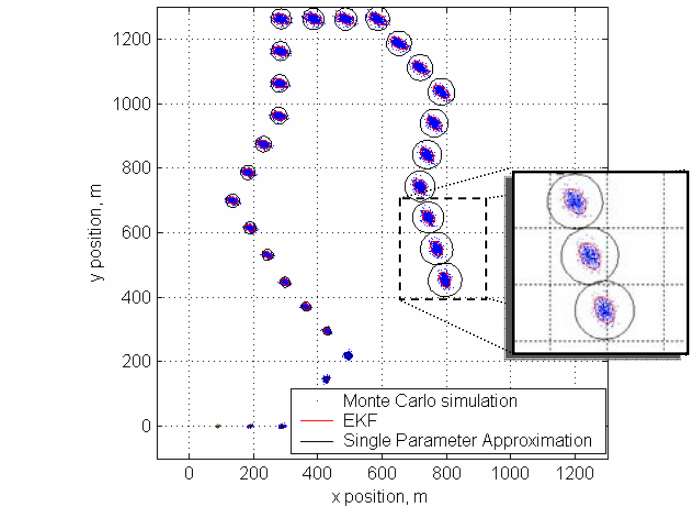

Figure 3. Error propagation for a random trajectory with all error sources combined and inset showing detail. The blue dots are the Monte Carlo simulation, the red ellipse is the EKF model (2σ), and the black circle is the single parameter approximation (2σ).

2.1.2 Prior maps

The task of navigating autonomously is extremely difficult if no prior information is available and is trivial if perfect prior information is available and the position of the robot is precisely known. Perfect prior maps are rare, but good-quality, high-resolution

prior maps are increasingly available. Although the position of the robot is usually known through the use of the Global Position System (GPS), there are many scenarios in which GPS is not available, or its reliability is compromised by different types of interference such as mountains, buildings, foliage or jamming. If GPS is not available, the position estimate of the robot depends on dead-reckoning alone, which drifts with time and can accrue very large errors. Most existing approaches to path planning and navigation for outdoor environments are unable to use prior maps if the position of the robot is not precisely known. Often these approaches end up performing the much harder task of navigating without prior information.

The approach presented here requires prior maps to estimate the cost to traverse different areas and to provide landmarks for navigation.

Cost map

The cost map is the representation of the environment that the planner uses. It is represented as a grid, in which the cost of each cell corresponds to the cost of traveling from the center of the cell to its nearest edge. Non-traversable areas are assigned infinite cost and considered obstacles. The cost of traveling is usually measured in terms of traversal time, energy required, mobility risk, etc.

The procedure to create a cost map from a prior map depends on the type of prior map used. If elevation maps are available, cost is usually calculated from the slope of the terrain. When only aerial maps are available, machine learning techniques such as those in [84][88][89] can be used. Figure 4 shows the cost map for the test area used in the experimental results presented here. The cost map was created by training a Bayes classifier and adding manual annotations to the resulting map. The table below shows the cost assigned to the different terrain types. In this example, the preferred type of terrain for navigation is paved roads that have been manually labeled. It is twice as expensive to travel on an automatically identified road, as the confidence in such road is not as high. Dirt roads are three times as expensive, as the robot is more likely to encounter obstacles that could block its path, or that could cause the robot to slow down.

TABLE I

COST VALUES FOR DIFFERENT TERRAIN TYPES.

Terrain Type	***Cost***
Paved Road*	5
Paved Road 2	10
Dirt Road	15
Grass	30
Trees	40
Water	250
Buildings*	255

* Items manually labeled.

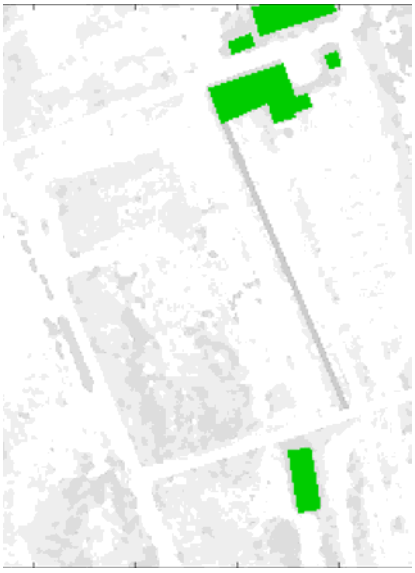

Figure 4. Cost map: lighter regions represent lower cost, and darker regions represent higher cost. Green areas are manually labeled buildings.

Map registration

A prior map that is not correctly registered to the position of the vehicle is of little use for most planning approaches. The error in map registration usually comes from two main sources: error in the estimation of the position of the vehicle, and error in the estimation of the position of the map. The approach presented here uses the prior map as the reference for all planning and execution. Since the planner considers uncertainty in position, the error in map registration can be modeled as being part of the error in the position of the robot, therefore making use of the information of the map in a way that includes the total uncertainty in the position of the robot

2.1.3 Landmarks

Landmarks are features that can be identified in the prior map and that can be detected with the on-board sensors. The selection of landmarks depends on the quality and type of the prior map, the characteristics of the environment and the detection capabilities of the robot.

Landmarks can come from a separate database of features, or can be extracted directly from the prior map if the resolution of the map is high enough. In our approach, we use aerial maps with a resolution of 0.3 meters per cell. At this resolution, many features are clearly visible and can be identified using manual labeling or automatic techniques.

We classify landmarks based on their appearance on a map. *Point landmarks* are geographic or man-made features such as tree trunks and electric poles that can be represented in a map by a point. *Linear landmarks* are geographic or man-made features such as walls and roads that can be represented in a map by a line or set of lines (a poly line).

While some landmarks can be easily classified as point or linear landmarks, many can be seen as either one, depending on the characteristics of the feature and the detection range of the vehicle. A house with four walls, for example, can be seen as four linear landmarks (the straight parts of the walls) plus four point features (the four corners). Furthermore, because the corners differ by a rotation of more than 90 degrees, they can often be seen as four separate types of point landmarks. A line of trees can be seen a either a set of point landmarks or a single linear landmark, depending on the separation of the trees and the detection range of the vehicle.

Figure 5 shows a small section of our test area with landmarks manually labeled. Features 1 through 7 are point landmarks (electric poles); features 8 through 11 are linear landmarks (walls of a building), and features 12 through 15 are less obvious point landmarks (corners of a building).

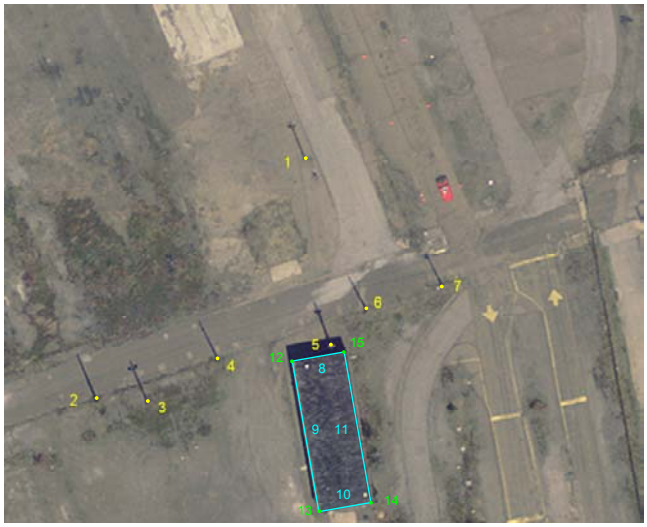

Figure 5. Detail of test area showing features of interest

2.1.4 Perception

One of the most challenging aspects of autonomous navigation is perception in unstructured or weakly structured outdoor environments such as forests, small dirt roads and terrain covered by tall vegetation [16]. While there has been great progress in perception in recent years, perception is still an area where, in general, only limited reliability has been achieved.

While general terrain classification and feature identification still have significant shortcomings, the detection of simple features such as tree trunks and poles can be performed in a more reliable way [51][99].

Simple features, however, are insufficient to provide unique location information because of aliasing and the fact that they are not unique. But we can make them unique and more reliable by combining them with an estimate of the position of the robot. By combining prior map information and planning with perception are able to improve the performance of the perception in the same way that using prior maps improves the navigation capabilities of robotic system.

For planning purposes the vehicle is assumed to have a range sensor with a maximum detection range R and 360^{o} field of view. We use electric poles as landmarks since they are widely available in our test location and can be reliably detected at distances of up to 10 meters. With little modification the approach could be modified to detect tree trunks and other similar features.

For execution purposes the vehicle is assumed to be able to detect small obstacles not present in the prior map, and most importantly, to be able to reliably detect the landmarks in the map. We use a simplified version of the approach by Vandapel [99]. Our approach finds areas that have high variance in elevation and low horizontal variance (narrow and tall objects). Although in theory any object with this description would be detected, the height threshold is such that in practice only electric poles are usually detected. In order to uniquely identify each landmark, we only attempt to detect a landmark when our position estimate indicates that we are within its *unique detection region.* See Chapter 5 for more details.

Chapter 3

Modeling Uncertainty as Additional Dimensions

Planning with uncertainty in position for indoor environments is usually approached as a special case of shortest path planning. Because a binary representation of the world (*free space* or *obstacles*) is usually sufficient for indoor navigation, the best path to follow is usually the shortest path, which is often the path that also minimizes uncertainty in position. This path can be found using 2-D planning approaches such as those described in section 1.2.2.

For outdoor environments, however, the varying difficulty of the terrain requires a representation of the environment that is able to represent terrain types other than *free space* and *obstacles,* such as a cost map. When cost maps are used as the objective function to be minimized by a planner, the lowest cost path is no longer the same as the shortest path or the path with lowest uncertainty. While in binary worlds uncertainty is directly proportional to the objective function that is being minimized (path length), in continuous cost worlds it is not. A 2-D representation is unable to find solutions for problems in which uncertainty constraints require choosing a higher-cost path in order to achieve lower uncertainty. To represent the constraint imposed by uncertainty in the planning problem, it is therefore necessary to add at least one more dimension to the planning problem.

Figure 6 shows an example that highlights the importance of adding a dimension to represent uncertainty. It describes a sample world with a long obstacle (green) that has a small opening. While most of the space has low cost (5), there is a small region near the goal with higher cost (30). Figures (a) and (b) show an intermediate step in planning a path from the start location (S) to the goal location (G). Figure (a) shows the lowest expected cost path from S to the intermediate state, and (b) shows the lowest uncertainty path, which is more expensive. A 2-D planner attempting to minimize expected cost would only be able to represent the state from (a). While this is often correct, if the larger uncertainty of that state prevents the path from going through the opening in the obstacle, the intermediate state from (a) is no longer the better choice. The intermediate state shown in (b), in spite of having higher cost, is the only way for the path to fit through the opening in the obstacle and find the lowest cost path shown in (c). Only by

modeling uncertainty as an additional dimension is it possible to find the lowest expected cost path in such continuous cost domains.

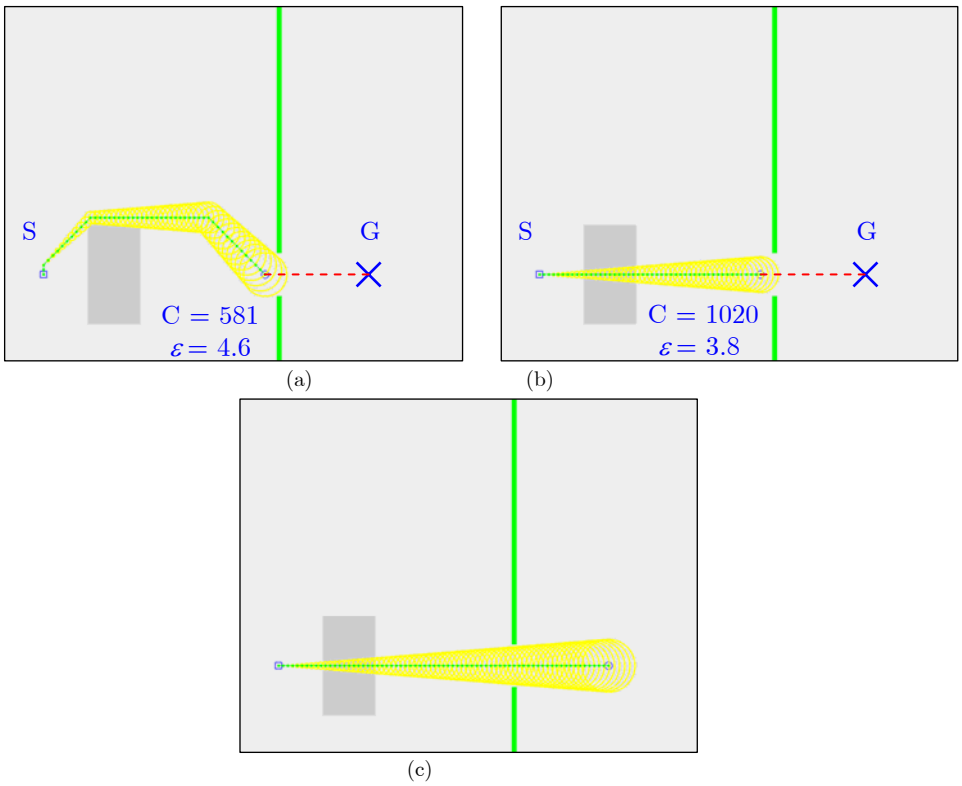

Figure 6. Importance of modeling uncertainty as a separate dimension. Light gray areas are low cost (5), dark gray areas are higher cost (30), and green areas are non-traversable (obstacles). (a) Intermediate state with low cost but high uncertainty. (b) Intermediate state with low uncertainty but high cost. (c) optimal path from start to goal

In order to use uncertainty as additional dimensions, we construct a configuration-uncertainty state space in which

$$\mathbf{r} = (\mathbf{q}, \boldsymbol{\varepsilon}) = (\mathbf{p}, \theta, \boldsymbol{\varepsilon}) \tag{3.1}$$

where $\mathbf{p} = (x,y)$ is the position of the robot in the workspace $\mathcal{W}$, $\mathbf{q} = (\mathbf{p},\theta)$ defines the configuration of the robot in the configuration space $\mathcal{C}$, and $\boldsymbol{\varepsilon} = (\varepsilon_1, \varepsilon_2, \ldots \varepsilon_n)$ is a parameterization that defines the uncertainty of the robot.

The uncertainty of the robot changes as the robot moves in response to an input u. If there exist deterministic functions f_q and $f_{\boldsymbol{\varepsilon}}$ such that $\mathbf{q}_{k+1} = f_q(\mathbf{q}_k, \boldsymbol{\varepsilon}_k, u_k)$ and $\boldsymbol{\varepsilon}_{k+1} = f_{\boldsymbol{\varepsilon}}(\mathbf{q}_k, \boldsymbol{\varepsilon}_k, u_k)$, then the transition of the robot from $\mathbf{r}_k$ to $\mathbf{r}_{k+1}$ is deterministic as well. We can then model the transitions of the robot at each state $\mathbf{r}_k$ in response to each possible u with a graph $G(V,E)$ such that

$$\begin{aligned} V &= \mathbf{r}_k \\ E &= L(\mathbf{r}_k, u_k) = L_{\mathbf{r}}(\mathbf{r}_k, \mathbf{r}_{,k+1}) \end{aligned} \tag{3.2}$$

where $L(\mathbf{r}_k,u_k) = L_{\mathbf{r}}(\mathbf{r}_k, \mathbf{r}_{k+1})$ is the cost of moving from $\mathbf{r_k}$ to $\mathbf{r_{k+1}}$ under input u_k.

In general we are interested in finding the lowest-cost path to go from an initial configuration $\mathbf{q_o}$ with uncertainty $\boldsymbol{\varepsilon}_o$ to a final configuration $\mathbf{q}_f$ with uncertainty less than or equal to $\boldsymbol{\varepsilon}_f$. We can use most forward graph search algorithms to find this path in the graph. In general, A* is a good choice since the transition cost is usually positive and we can use the Euclidean distance in (x,y) as an admissible heuristic.

While in principle the implementation of the formulation presented above is straightforward, there are significant challenges because of the dimensionality of the search space. There are two important aspects to consider: the number of dimensions in the search space, and the size of the space along each dimension. For outdoor environments, the size of the space along the x and y dimensions is usually greater than 100, and often greater than 1000. This limits significantly the number of dimensions that can be used to parameterize uncertainty.

There are two broad models of uncertainty that can be considered: non-deterministic uncertainty and probabilistic uncertainty [57][58]. The uncertainty model determines how to parameterize uncertainty, and the interpretation of the resulting path.

3.1 Non-deterministic uncertainty model

A non-deterministic uncertainty model usually represents uncertainty as the region $\mathcal{C}_{\mathcal{U}}$ in the configuration space of the robot in which the robot could be. In this model all that is known about the configuration of the robot at path step k is that is contained within $\mathcal{C}_{\mathcal{U}_k}$

$$\mathbf{q}_k = (x_k, y_k, \theta_k) \in \mathcal{C}_{\mathcal{U}_k} \tag{3.3}$$

In general $C_{\mathcal{U}}$ can be any shape or volume in the configuration space of the robot. In order to use a given representation of $C_{\mathcal{U}}$ to plan paths, we need to be able to parameterize it with a finite number of parameters such that

$$C_{\mathcal{U}} = f(\boldsymbol{\varepsilon}) = f(\varepsilon_1, \varepsilon_2, ...\varepsilon_n) \tag{3.4}$$

and there needs to be a deterministic function $f_{\boldsymbol{\varepsilon}}$ such that

$$\boldsymbol{\varepsilon}_{k+1} = f_{\boldsymbol{\varepsilon}}(\mathbf{q}_k, \boldsymbol{\varepsilon}_k, u_k). \tag{3.5}$$

However, each additional dimension in the parameter $\boldsymbol{\varepsilon}$ increases the dimensionality of the search space, which makes the search problem more spatially and computationally

intensive. With these elements we can define the configuration-uncertainty state space $\mathbf{r} = (\mathbf{q},\boldsymbol{\varepsilon})$, and the transitions between states. The transition cost is usually calculated as

$$L(\mathbf{r}_k, u_k) = \max_{\mathbf{q}_i \in C_{\mathcal{U}_k}} \{ L(\mathbf{q}_i, u_k) \} \tag{3.6}$$

where $L(\mathbf{q}_k,u_k)$ is the deterministic cost of applying input u_k at each configuration $\mathbf{q}_i$ that belongs to the uncertainty region $\mathcal{C}_{\mathcal{U}_k}$. If this transition cost is used to create the edges of the graph *G,* then the resulting path will minimize the worst case cost.

3.2 Probabilistic uncertainty model

While the previous model is very general and has few restrictions, its results are usually too conservative because it is minimizing the worst case scenario along the path. If there is enough information about the position of the robot to define a probability density function (*pdf)*, then we can use a probabilistic uncertainty model instead. In such case,

$$\begin{aligned} \mathbf{q}_k &= (x_k, y_k, \theta_k) \\ \mathbf{q}_k &: p_{\boldsymbol{\varepsilon}_k}(\mathbf{q}_k) \end{aligned} \tag{3.7}$$

where $p_{\boldsymbol{\varepsilon}_k}(\mathbf{q}_k)$ is the *pdf* of the configuration of the robot defined in terms of a finite set of parameters such that

$$p_{\boldsymbol{\varepsilon}} = f(\boldsymbol{\varepsilon}) = f(\varepsilon_1, \varepsilon_2, ...\varepsilon_n) \tag{3.8}$$

In order to have deterministic transitions, there needs to be a deterministic function $f_{\boldsymbol{\varepsilon}}$ such that

$$\boldsymbol{\varepsilon}_{k+1} = f_{\boldsymbol{\varepsilon}}(\mathbf{q}_k, \boldsymbol{\varepsilon}_k, u_k). \tag{3.9}$$

As in the non-deterministic case, each additional dimension in the parameter $\boldsymbol{\varepsilon}$ increases the dimensionality of the search space, making the search problem more spatially and computationally intensive. The configuration-uncertainty space is still $\mathbf{r} = (\mathbf{q},\boldsymbol{\varepsilon})$, and the transition cost is usually calculated as

$$L(\mathbf{r}_k, u_k) = E_{\mathbf{q}_k} \left\{ L(\mathbf{q}_{k,i}, u_k) \right\} \tag{3.10}$$

where $L(\mathbf{q}_k,u_k)$ is the deterministic cost of applying input u_k at each possible configuration $\mathbf{q}_{k,i}$. If this transition cost is used to create the edges of the graph *G,* then the resulting path will minimize the expected cost.

3.2.1 Gaussian uncertainty model

One of the most useful probabilistic uncertainty models is the Gaussian. It is widely used not only because of its mathematical properties, but also because many processes in nature are the result of adding multiple sub-processes. If the sub-processes have finite variance and are independent, identically distributed, then the resulting process will have a Gaussian distribution (Central Limit Theorem).

The uncertainty propagation model presented in section 2.1.1 takes advantage of the Gaussian nature of the errors in the dead-reckoning process. In this case,

$$\begin{aligned} \mathbf{q}_k &= (x_k, y_k, \theta_k) \\ \mathbf{q}_k &: N(\boldsymbol{\mu}_k, \Sigma_k) \end{aligned} \tag{3.11}$$

where $\boldsymbol{\mu}_k = (\mu_{x_k}, \mu_{y_k}, \mu_{\theta_k})$ is the most likely location of the robot at step k, and Σ_k is the covariance matrix of the distribution:

$$\Sigma_k = \begin{bmatrix} \sigma_{xx} & \sigma_{xy} & \sigma_{x\theta} \\ \sigma_{xy} & \sigma_{yy} & \sigma_{y\theta} \\ \sigma_{x\theta} & \sigma_{y\theta} & \sigma_{\theta\theta} \end{bmatrix}_k \tag{3.12}$$

The representation for the robot's position is

$$p_{\boldsymbol{\mu}_k, \Sigma_k}(\mathbf{q}_k) = \frac{1}{2\pi^{3/2} |\Sigma_k|^{3/2}} e^{-\frac{1}{2}(\mathbf{q}_k - \boldsymbol{\mu}_k)^T \Sigma^{-1} (\mathbf{q}_k - \boldsymbol{\mu}_k)} \tag{3.13}$$

and the uncertainty propagation is given by the Kalman filter update (2.5), which is a deterministic relationship that defines Σ_{k+1} as a function of the previous state's uncertainty.

The 3-D covariance matrix contains 9 parameters, of which 6 are independent. The configuration-uncertainty state space created by augmenting the state space with the covariance matrix therefore has a total of 9 dimensions. The augmented representation of the state space is

$$\mathbf{r} = (\boldsymbol{\mu}, \boldsymbol{\varepsilon}) \tag{3.14}$$

where $\boldsymbol{\varepsilon} = (\sigma_{xx}, \sigma_{xy,} \sigma_{yy}, \sigma_{\theta\theta}, \sigma_{x\theta}, \sigma_{y\theta})$.

While this approach enables a rich representation of the uncertainties present in many systems, it is not practical for outdoor environments, as the x and y dimensions of the planning space can be in excess of 1000 cells each. For this reason, in this thesis, we will focus on the simpler model presented in the following section. However, the use of a full Gaussian error model will be revisited in Chapter 8 in order to use linear landmarks for reducing uncertainty.

3.2.2 Simplified Gaussian error model

One of the simplest probabilistic models is a 2-D isometric Gaussian such that

$$\begin{aligned} \mathbf{q}_k &= (x_k, y_k) \\ \mathbf{q}_k &: N(\boldsymbol{\mu}_k, \sigma_k) \end{aligned} \tag{3.15}$$

where $\boldsymbol{\mu}_k = (\mu_{x_k}, \mu_{y_k})$ is the most likely location of the robot at step k, and $\sigma_k = \sigma_{x_k} = \sigma_{y_k}$ is the standard deviation of the distribution. Under this assumption, the representation for the robot's position is

$$p_{\boldsymbol{\mu}_k, \sigma_k}(\mathbf{q}_k) = \frac{1}{\sqrt{2\pi\sigma_k{}^2}} e^{-\frac{1}{2}\frac{(\mathbf{q}_k - \boldsymbol{\mu}_k)^T(\mathbf{q}_k - \boldsymbol{\mu}_k)}{\sigma_k{}^2}} \tag{3.16}$$

Let us define:

$$\varepsilon_k = 2 \cdot \sigma_k \tag{3.17}$$

we can then model the boundary of the uncertainty region as a disk centered at μ_k with a radius ε_k that corresponds to the 2σ contour for the underlying Gaussian distribution. With this simplified model, the augmented representation of the state space is

$$\mathbf{r} = (\boldsymbol{\mu}, \varepsilon) \tag{3.18}$$

which is a complete representation of the belief space under the assumption that all beliefs are isometric Gaussians.

As shown in section 2.1.1, this model is a conservative estimate of the true error propagation model and can provide an accurate approximation of the true model. This model assumes that the dominant term in the error propagation is the error in the initial heading. It also assumes that changes in direction do not affect the heading error therefore it is not necessary to include θ in the planning space.

Since the dominant term in the error propagation for our planning horizon is linear with distance traveled, we use the following model to propagate the uncertainty:

$$\varepsilon_{k+1} = \varepsilon_k + \alpha_u d(\mu_{k+1}, \mu_k) \tag{3.19}$$

where α_u is the uncertainty accrued per unit of distance traveled, μ_k is the position along the path, and $d(\mu_{k+1}, \mu_k)$ is the distance between the two adjacent path locations μ_{k+1} and μ_k. The uncertainty rate α_u is typically between 0.01 and 0.1 (1% to 10%) of distance traveled.

This belief space is a 3-D graph with deterministic transitions. In order to use a deterministic planner to plan over this space we need to define the transition cost between adjacent cells. Let us recall that

$$L(\mathbf{r}_k, u_k) = E_{\mathbf{q}_k}\left\{L(\mathbf{q}_{k,i}, u_k)\right\} \tag{3.20}$$

There are different ways to calculate this expected cost. The most general way is to perform a Monte Carlo simulation of the motion of each possible state $\mathbf{q}_{k,i}$ under input u_k. This simulation will draw samples from the initial distribution $N(\boldsymbol{\mu}_k, \sigma_k)$ and will calculate the next distribution $N(\boldsymbol{\mu}_{k+1}, \sigma_{k+1})$ as well as the expected cost of applying the input u_k. However, since the traversal costs are associated with an existing cost map grid, it is more efficient to represent the transition cost by extending the definition of traversal cost from the grid to include uncertainty.

When costs maps are used to model traversal costs for deterministic search, the cost of each cell in the cost map represents the cost of traveling from the center of the cell to its nearest edge. In our 3-D configuration-uncertainty space, this can be modeled as the expected cost of going from the center of each of the cells in distribution to their nearest edge:

$$C_{\mathbf{r}}(\mathbf{r}_k) = C_{\mathbf{r}}((\boldsymbol{\mu}_k, \varepsilon_k)) = E_{\mathbf{q}_k}\{C_o(\mathbf{q}_k)\} = \sum_i C_o(\mathbf{q}_{k,i}) p_{\boldsymbol{\mu}_k, \varepsilon_k}(\mathbf{q}_{k,i}) \tag{3.21}$$

Where $\mathbf{q}_{k,i}$ is each of the states within ε_k=2σ_k of $p_{\mu,\varepsilon}(\mathbf{q})$ and $C_o(\mathbf{q}_{k,i})$ is the deterministic cost of traveling from the center of the cell $\mathbf{q}_{k,i}$ to its nearest edge (see Figure 7). Using this definition, the cost to transition between two adjacent configurations $\mathbf{r}_k$ and $\mathbf{r}_{k+1}$ is given by

$$L_{\mathbf{r}}(\mathbf{r}_k, \mathbf{r}_{k+1}) = aC_{\mathbf{r}}(\mathbf{r}_k) + bC_{\mathbf{r}}(\mathbf{r}_{k+1}) = aC_{\mathbf{r}}((\boldsymbol{\mu}_k, \varepsilon_k)) + bC_{\mathbf{r}}((\boldsymbol{\mu}_{k+1}, \varepsilon_{k+1})) \tag{3.22}$$

where a and b are either 1 or $\sqrt{2}$ depending on the relative position μ_k and μ_{k+1}.

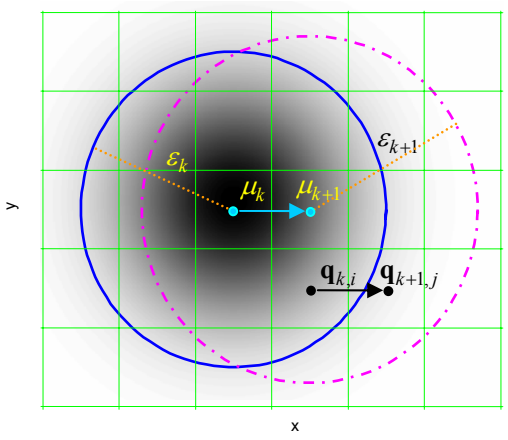

Figure 7. $p_{\mu_k,\varepsilon_k}(\mathbf{q}_k)$ and the state transitions from $\mathbf{r}_k = (\mu_k, \varepsilon_k)$ to $\mathbf{r}_{k+1} = (\mu_{k+1}, \varepsilon_{k+1})$

Chapter 4

Planning with Uncertainty in Position without Using Landmarks

The graph *G(V,E)* defined in (3.2) can be searched using most deterministic search algorithms. However, because of the size of the search space, most approaches will be impractical for outdoor environments. For outdoor environments, we would like to be able to have worlds that are about 1kmx1km, with a resolution of approximately one meter. A world of this size significantly limits the number of dimensions that can be used to represent uncertainty.

This chapter presents an approach to planning with uncertainty in position that uses a single parameter to represent uncertainty. The approach can be used with any single-parameter uncertainty representation. However, we use a simplified Gaussian error model as described in section 3.2.2, in order to integrate the results of the planner with Kalman Filter used for position estimation.

4.1 Planning in the configuration-uncertainty space

Even with only one dimension to represent uncertainty, the size of the search space can be very large. If we use 100 cells to represent uncertainty, and 1000 cells to represent each of the x and y dimensions, the search space is of size 10^8. Additionally, the calculation of traversal costs is usually a computationally expensive operation that has to be performed in all of the cells included in the search.

For these reasons, it is important to use an approach that expands as few states as possible. We use a modified version of forward A* in 3-D in which the successors of each state are calculated only in a 2-D plane, and state dominance is used to prune unnecessary states.

The planner works as follows: we have a start configuration $\mathbf{q}_0$ with uncertainty ε_0, a goal configuration $\mathbf{q}_f$ with uncertainty ε_f, and a 2-D cost map C. We form the augmented

state variable $\mathbf{r}_o = (\mathbf{q}_o, \varepsilon_o)$ and place it in the OPEN list. States in the OPEN list are sorted by their total cost to the goal:

$$L_T(\mathbf{q}_k, \varepsilon_k) = L^*\left((\mathbf{q}^0, \varepsilon^0), (\mathbf{q}^k, \varepsilon^k)\right) + L_h(\mathbf{q}_k, \mathbf{q}_f) \tag{4.1}$$

where $L^*((\mathbf{q}_0, \varepsilon_0), (\mathbf{q}_k, \varepsilon_k))$ is the cost of the best path from the initial state $\mathbf{r}_0 = (\mathbf{q}_0, \varepsilon_0)$ to the current state $\mathbf{r}_k = (\mathbf{q}_k, \varepsilon_k)$, and $L_h(\mathbf{q}_k, \mathbf{q}_f)$ is the heuristic cost from the current state to the goal . The heuristic used is the Euclidean distance between $\mathbf{q}_k$ and $\mathbf{q}_f$.

The state $\mathbf{r}_k$ with lowest total cost to the goal is popped from the OPEN list. Next, $\mathbf{r}_k$ is expanded. To determine if a successor $\mathbf{r}_j = (\mathbf{q}_j, \varepsilon_j)$ should be placed in the OPEN list, we use state dominance as follows: a state $\mathbf{r}_j$ is placed in the OPEN list only if it is not dominated by another state $\mathbf{r}_i$:

$$(\mathbf{r}_i \trianglerighteq \mathbf{r}_j) \Leftrightarrow (\mathbf{q}_i = \mathbf{q}_j) \wedge (L^*(\mathbf{r}_o, \mathbf{r}_i) \leq L^*(\mathbf{r}_o, \mathbf{r}_j)) \wedge (\varepsilon_i \leq \varepsilon_j) \tag{4.2}$$

In other words, a state is expanded as long as there is no other path to the same location (*x*,*y*) with lower uncertainty and lower cost from the start location. Additionally, since $\boldsymbol{\varepsilon}$ is a function of $\mathbf{q}$, the successors of $\mathbf{r_k}$ may be calculated in the 2-D configuration defined by $\mathbf{q_k}$, instead of the full 3-D configuration-uncertainty space defined by $\mathbf{r_k}$ (See Figure 8).

As the states are placed in the OPEN list, their uncertainty is updated using (3.19). However, if any states within 2σ in the uncertainty region of $\mathbf{r}_j$ are labeled as obstacles then the expected total path cost of $\mathbf{r}_j$ is set to infinity, thereby preventing any further expansion of that state.

As in A*, the process described above is repeated until a cell $\mathbf{r}_k$ with the same (*x*,*y*) coordinates as the goal position ($\mathbf{q}_k = \mathbf{q}_f$), and uncertainty less or equal to the target uncertainty ($\varepsilon_k \leq \varepsilon_f$) is popped off the OPEN list. The path connecting the backpointers from $\mathbf{r}_{k+1}$ to $\mathbf{r}_0$ is the lowest cost path in the graph G between $\mathbf{q}_0$ and $\mathbf{q}_f$ with a final uncertainty lower than ε_f. If the OPEN list becomes empty and no such state has been found, then there is not a path between $\mathbf{q}_0$ and $\mathbf{q}_f$ such that the final uncertainty is lower than ε_f.

Although the approach described above can be used in forward or backward search, it is much more efficient when used in forward search. When using forward search, the initial state $\mathbf{r}_0 = (\mathbf{q}_0, \varepsilon_0)$ in the configuration-uncertainty state space is known. With the use of state dominance, the search space is usually a thin volume as dominated states are easily pruned. In contrast, when using backward search, the initial state for the search is not known. Any state $\mathbf{r}_k = (\mathbf{q}_k, \varepsilon_k)$ with uncertainty less than ε_f should be placed in the OPEN list at the beginning of the search, therefore defining a thick volume of possible states from the beginning of the search.

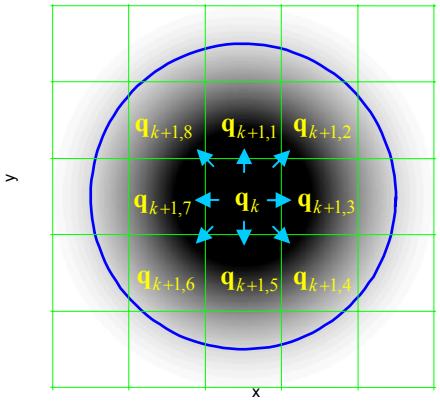

Figure 8. Successors of state $\mathbf{q}^k$

4.2 Topological analysis of search space

Under the assumption of low uncertainty rate, the uncertainty in the position of the robot evolves slowly. When using the single-parameter (isometric Gaussian) uncertainty propagation model described in the previous chapters combined with state dominance, the uncertainty evolution describes a local 2-D manifold.

For short transitions the uncertainty can be considered constant with little or no impact in the result. In some cases the whole search space is also a 2-D manifold. If this manifold is homeomorphic with a plane, the uncertainty dimension is not needed to find the optimal solution. In general, however, uncertainty cannot be ignored. Scenarios involving localization and narrow passages are some of the cases where ignoring uncertainty can lead to very suboptimal solutions, and to not being able to find existing solutions.

When using an isometric Gaussian to represent uncertainty, the combination of (x,y,ε) is a complete representation of the belief space for any environment. This representation can also be used to understand the topology of the search space. We will use the following example to illustrate some of the important characteristics of the search space when planning with uncertainty in position. Figure 9 shows a sample world with low and high cost regions (light gray and black color respectively). The uncertainty at the goal is required to be smaller than 10 meters. The lowest cost path is achieved by following the shortest path within the low cost regions. The final uncertainty at the goal is 6.4 meters, which satisfies the imposed constraint.

In this environment, and with the constraints imposed, the resulting search space defines a 2-D manifold. Figure 10 shows this manifold in 3-D and Figure 11 shows some

2-D views of it. This manifold is homeomorphic with the *xy* plane (each point in *xy* has at most one uncertainty value)

Since the search space for this example is homeomorphic with the *xy* plane, the uncertainty dimension is not really necessary. If we solve the same problem using a single uncertainty value for all the search space, the same solution is found. Figure 12 shows the resulting path when ignoring the uncertainty dimension. Figure 13 and Figure 14 show the search space for this example.

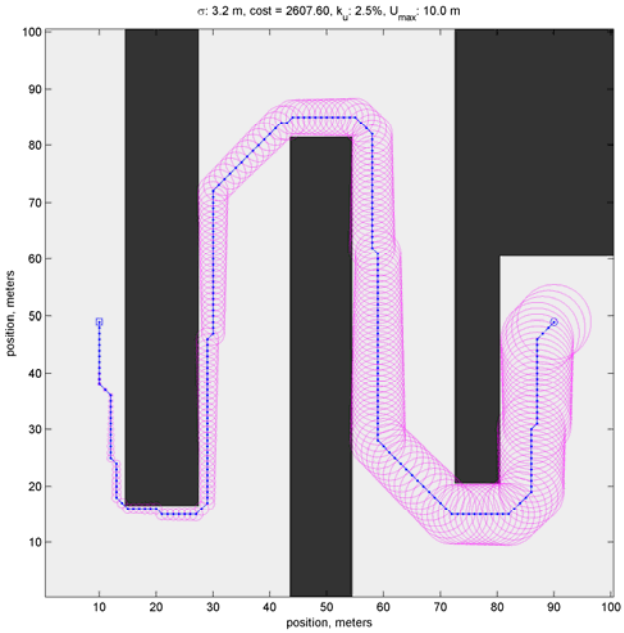

Figure 9. Sample world to analyze the topology of search spaces when planning with uncertainty in position. Light gray areas are low cost regions and black areas are high cost regions. The planning goal requires a final uncertainty of less than 10 meters. The blue and magenta lines show the mean and 2σ contours for the resulting path.

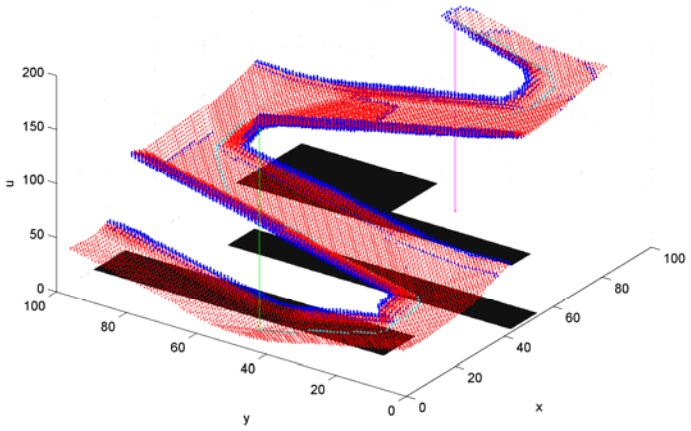

Figure 10. Search space for Figure 9. Red dots are states in the CLOSED list. Blue dots are states in the OPEN list. The resulting path is in cyan. x and y are in meters, u is in quantization units.

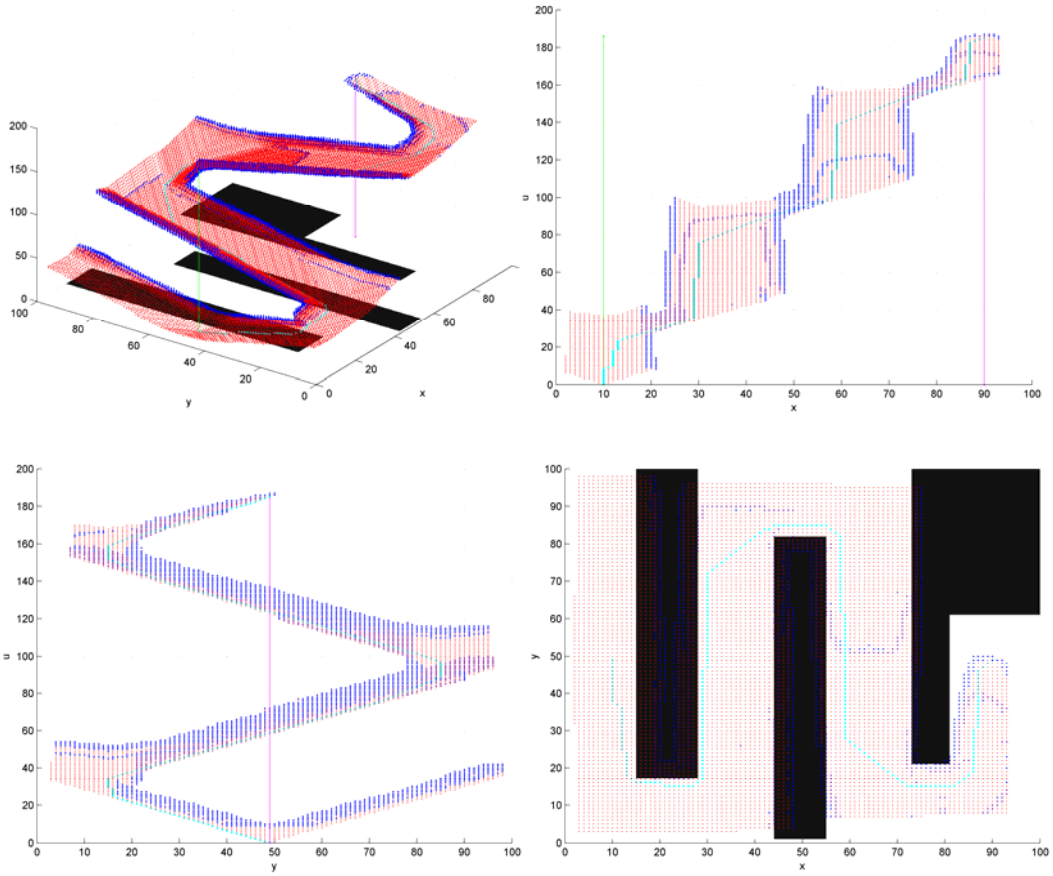

Figure 11. Axis views of the search space.

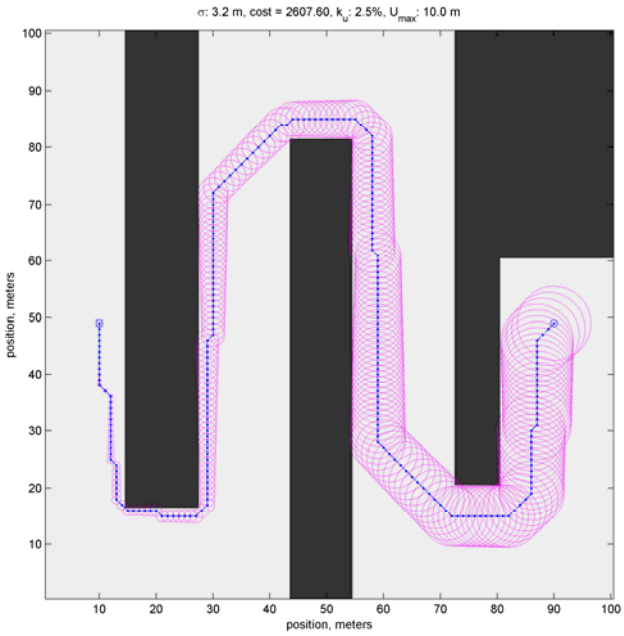

Figure 12. Resulting path when ignoring uncertainty. Because the search space is homeomorphic with the xy plane the uncertainty dimension is not necessary and the same solution is found whether uncertainty is used or not.

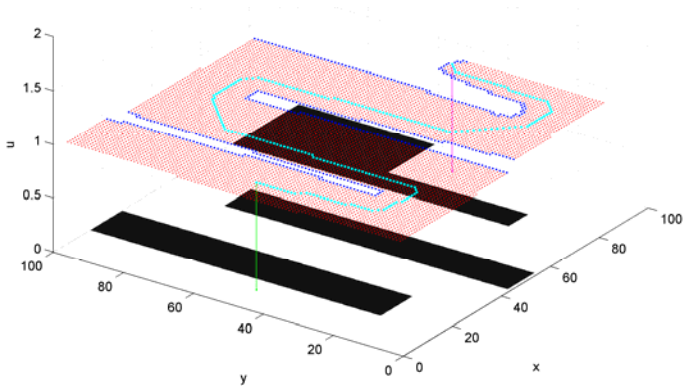

Figure 13. Search space for Figure 12. Red dots are states in the CLOSED list. Blue dots are states in the OPEN list. The resulting path is in cyan. x and y are in meters, u is in quantization units.

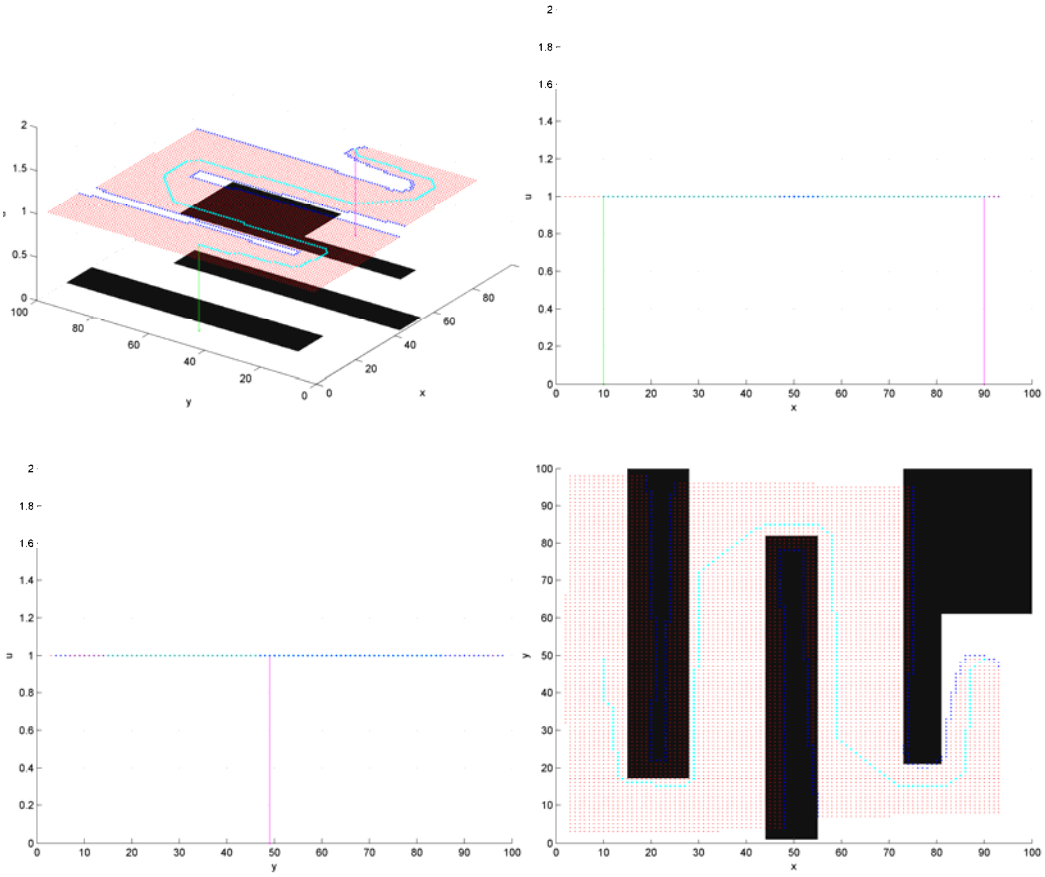

Figure 14. Axis views of the search space

While the previous examples illustrate some of the characteristics of the topology of the search space, the more general case is not as well defined or easy to represent. Figure 15 shows an example of a more complex topology in the search space. The environment is the same as in the previous two examples, but now the uncertainty at the goal has been reduced to be 3 meters. The solution to this problem requires going through some of the high cost regions, as staying in the low cost regions would accrue too much uncertainty. Finding this solution requires expanding most of the search space. While the search space is still a local 2-D manifold, the overall space is now a complex 3-D volume in which most xy locations have multiple uncertainty values. Figure 16 and Figure 17 show the search space for this problem. Since the search space is no longer homeomorphic with the xy plane, a planner that minimizes expected cost but does not include the uncertainty dimension will most likely be unable to find the solution to this problem.

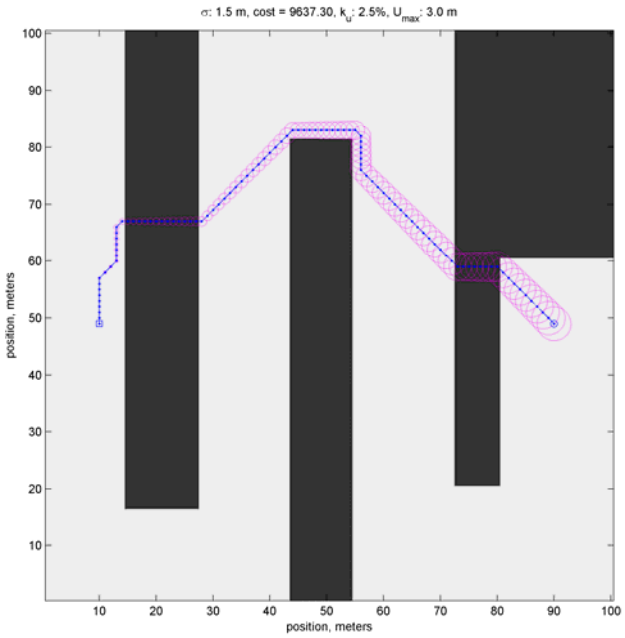

Figure 15. Resulting path when the constraint at the goal is reduced to 3 meters.

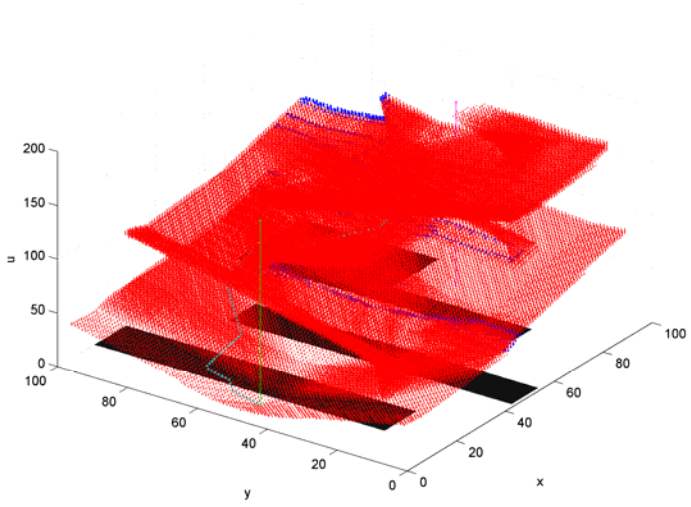

Figure 16. Search space for Figure 12. Red dots are states in the CLOSED list. Blue dots are states in the OPEN list. The resulting path is in cyan. x and y are in meters, u is in quantization units

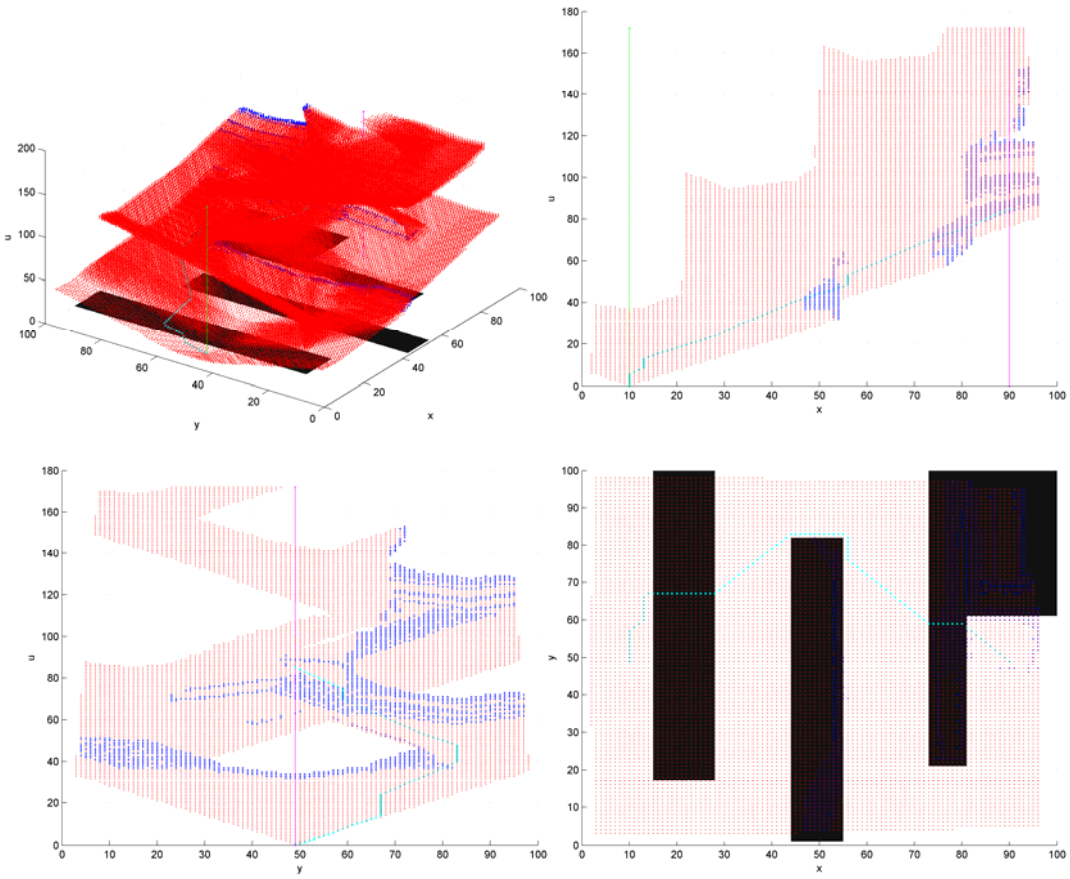

Figure 17. Axis views

4.3 Simulation results

The following is an example of our planner applied to the problem of finding the best path between two locations on opposite sides of Indiantown Gap, PA. The required task is to find the path with lowest cost from the start to the end location, with a final uncertainty smaller than 500 m, and which avoids all known obstacles in the map (within 2σ). The cost map used is defined as the mobility cost of traveling through each cell in the map, and is proportional to the slope of the terrain. Slopes greater than 30^{o} are considered obstacles. This example shows the results of using our planner to calculate a path with uncertainty rates of 0%, 2% and 4% of distance traveled, and uses the results of a Monte Carlo simulation to illustrate the importance of planning with uncertainty.

In Figure 18(a) we can see the results when uncertainty is not being considered. Figure 18 (b) shows the resulting path when we use our planner and a propagation model

with an uncertainty rate of 2%. Figure 18 (c) shows the resulting path when the uncertainty rate is increased to 4%.

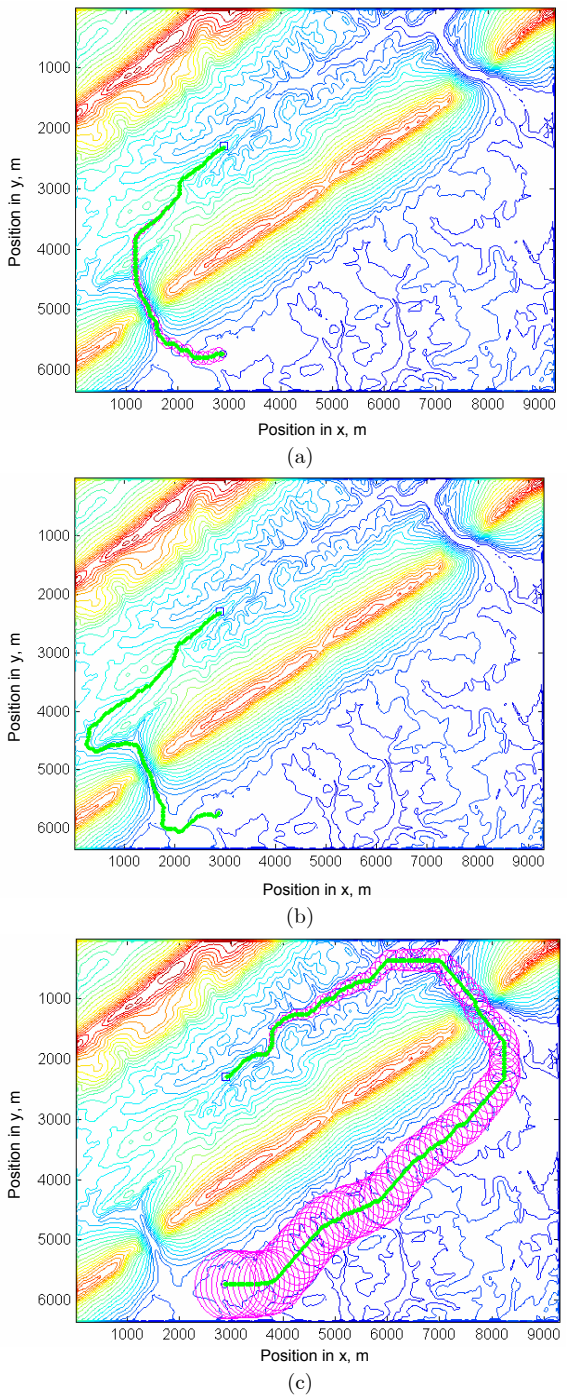

(a)

(b)

(c)

Figure 18. Comparison between paths found without uncertainty (a) and with uncertainty rates of 2% (b) and 4%. (c)

In order to understand the importance of planning with uncertainty, a set of Monte Carlo simulations were run for each of the previous three scenarios with and without considering uncertainty:

- Planning without considering uncertainty: we planned a path without uncertainty, and simulated executions with uncertainty rates of 0%, 2% and 4%.
- Planning considering uncertainty: we planned and simulated executions with uncertainty rates of 0%, 2% and 4%.

In both cases, we calculated the probability of collision as the percentage of simulations that resulted in a trajectory through obstacles. Table II shows the results of the simulations.

When there is no uncertainty (for example, if there is good GPS coverage throughout the path), the planner that considers uncertainty produces the same path as the planner without uncertainty (as expected).

If there is a 2% uncertainty rate in the motion model, and we fail to account for it, the average cost of the resulting path is 27705, and the probability of collision is 11% (The expected cost of this path as reported by the planner with no uncertainty is 9337). If we use our planner with uncertainty, the average cost is 19052 (30% lower). The expected cost calculated by the planner (18679), is also much closer to the average cost of the simulations, and the probability of collision is significantly lower (5%).

If there is a 4% uncertainty rate in the motion model but we do not account for it, the average cost of the resulting path is 37726, while the expected cost as calculated by the planner is still 9337. The probability of collision is now 36%. When we use the planner that considers uncertainty to solve this case, the average cost is 49727, the expected cost 42677, and the probability of collision 5%. The collision checking criterion for the planner with uncertainty is 2σ, which implies that paths with probabilities of collision of more than 15% would be rejected. Under this criterion, the path returned by the planner without uncertainty considerations is not a feasible path (36% probability of collision).

TABLE II

COMPARISON BETWEEN PLANNER WITH AND WITHOUT UNCERTAINTY

	Planner without uncertainty			Planner with uncertainty		
Uncert. rate	Expected cost	Average cost	Prob. of collision	Expected cost	Average cost	Prob. of collision
0%	9337	9353	0%	9337	9353	0%
2%	9337	27705	11%	18679	19052	5%
4%	9337	37726	36%	42677	49727	5%

4.4 Performance

The worst-case space complexity of the current implementation of the planner is $O(n_x \cdot n_y \cdot n_u)$, where n_x, n_y and n_u are the number of cells along the x, y and u directions. The average time complexity is $O(Q+R)$, where $Q = \alpha_u \cdot (n_x \cdot n_y)^2 \cdot n_u$ is the number of operations required to calculate the expected cost, $R = n_x \cdot n_y \cdot n_u \cdot \log(n_x \cdot n_y \cdot n_u))$ is the number of operations required by A* to calculate the path, and α_u is the uncertainty rate. For $\alpha_u > 0$, the Q term dominates the time complexity of the algorithm. If $\alpha_u = 0$, or the calculation of the expected value is performed beforehand, then the R term becomes the dominant one.

Our algorithm takes significant advantage of several tools available for deterministic search, namely heuristics, lazy evaluation and state dominance. In practice, the search space for the algorithm is not the full 3-D volume defined by the state space representation $n_x \cdot n_y \cdot n_u$, but a thin volume $n_x \cdot n_y \cdot \overline{n}_u$, where $\overline{n}_u$ is the average number of propagations along the uncertainty axis (the thickness of the search space). $\overline{n}_u$ is typically much smaller than the size of the uncertainty dimension (n_u). Because the search space is just a fraction of the complete search space and expected costs are only calculated when needed (lazy evaluation), the average performance of the algorithm is much faster than that of algorithms that calculate all states in the search space.

Figure 19 shows the planning time for the algorithm for a batch of 1800 simulations in 10 random fractal worlds such as the one shown in Figure 20, with α_u varying between 1% and 10%, and $n_x = n_y$ varying from 50 to 250 cells. We can see a strong dependence on n_x, n_y, and α_u, and a significantly weaker dependence on n_u. Figure 21 shows a similar plot, but only for α_u=5%, with $n_x = n_y$ varying from 100 to 1000 cells. The simulations were performed on an Intel(R) Xeon(TM) CPU running at 3.80GHz, with 4GB of memory

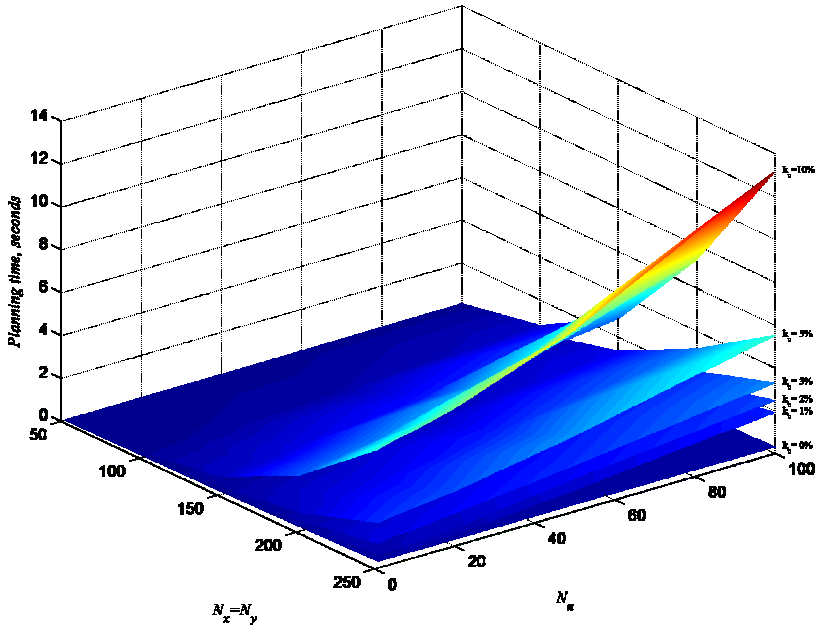

Figure 19. Planning time vs. world size (N_x=N_y) and number of uncertainty levels (N_u) for different uncertainty rates.

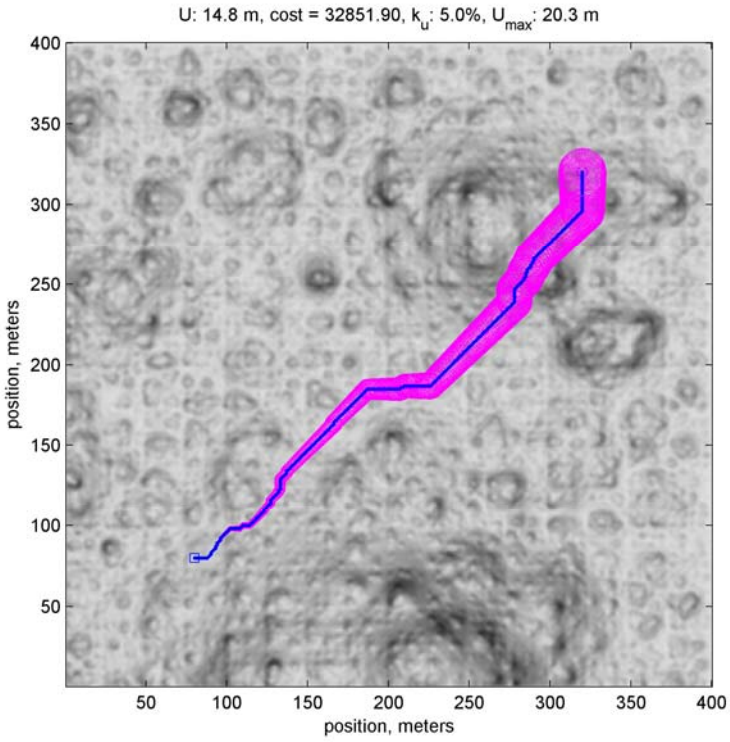

Figure 20. Fractal world used for performance simulations. Elevations are shown as a shaded-relief grayscale. The actual traversal cost is calculated based on the slope of the terrain.

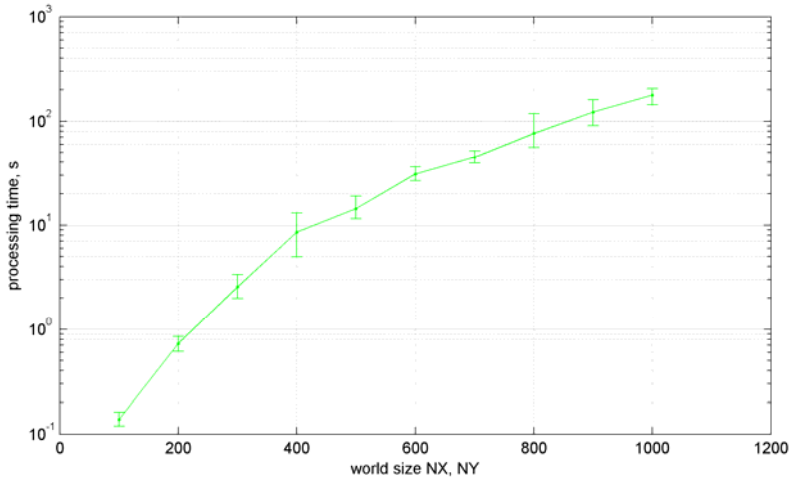

Figure 21.Planning time vs. world size (N_x=N_y) for $\alpha_u = 5\%$

Figure 22 shows the average number of uncertainty levels per state ($\overline{n}_u$) vs. the actual number of uncertainty levels (n_u). We can see that even though $\overline{n}_u$ does increase with n_u, it is always a small fraction of n_u. For $n_u = 100$ the average value of $\overline{n}_u$ is 3.4, and the maximum value is 7.9.

Our algorithm requires significantly fewer state expansions than processing all the states in the search space. Depending on the size of the world and the uncertainty rate the speed-up factor of our algorithm is between 8 and 80, depending on the size and characteristics of the world (see Figure 23).

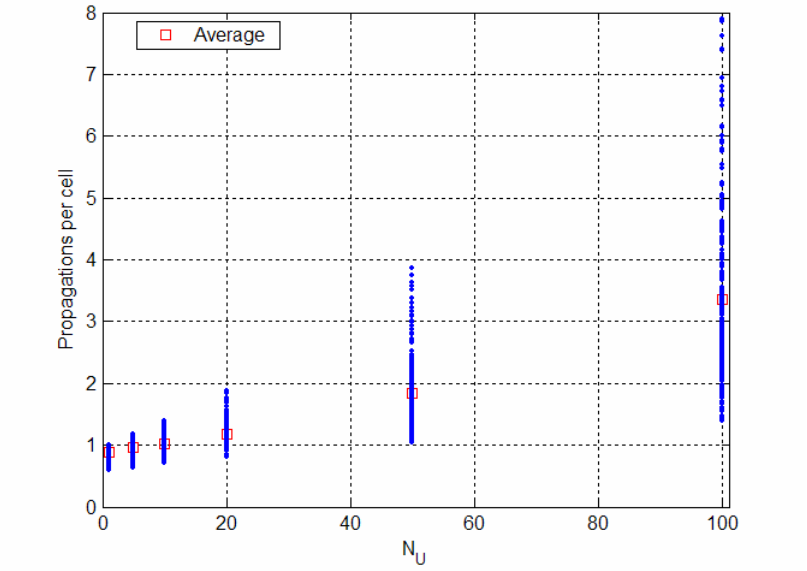

Figure 22. Propagations per cell ($\overline{n}_u$) vs. number of uncertainty levels n_u. The red squares indicate the mean value at for each value of n_u.

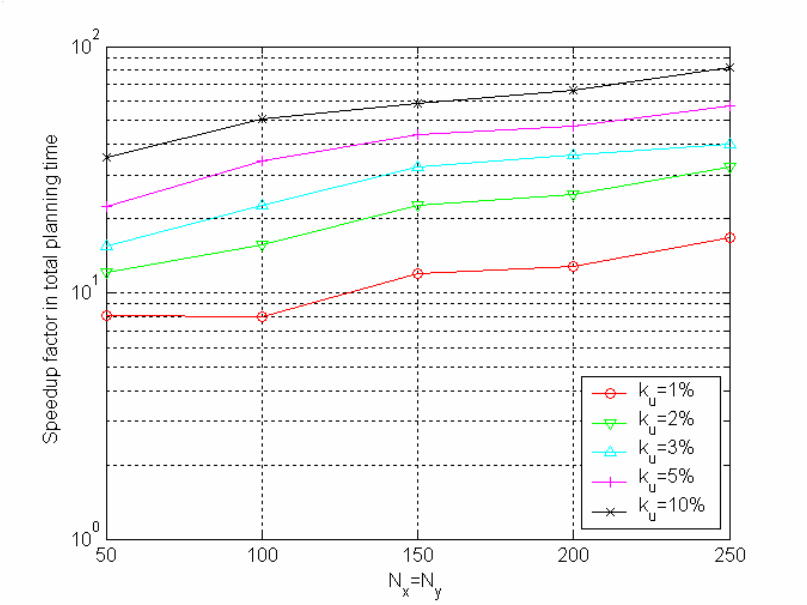

Figure 23.Speed up factor in total planning time compared to preprocessing all states

4.5 Discussion

We have introduced an efficient path planner that considers uncertainty in position for large outdoor environments[31][33]. The resulting paths are safer and have lower average execution costs than paths calculated without considering uncertainty.

Our approach models a stochastic problem as a deterministic search over a simplified belief space, enabling the use of a deterministic planner such as A* to solve the planning problem. Because of the characteristics of the search space and the motion model, there are significant performance gains from the use of state dominance and lazy evaluation. The approach calculates optimal paths in the configuration-uncertainty graph. While many representations of this graph are possible, the representation presented here is a 3-D grid. Such grid allows very efficient computations, but has limited connectivity. As such, the resulting paths can only follow 8 directions when projected in the 2-D plane.

The main two limitations of the approach presented are that it does not use any perception information to reduce the error growth, and that it has a very restrictive probability distribution for the position of the robot. These limitations will be addressed in the following chapters.

Chapter 5

Planning with Uncertainty in Position Using Point Landmarks

If landmarks are available, the robot can use them to reduce the uncertainty in its position. Most approaches to planning with uncertainty in position using landmarks assume that landmarks are unique, therefore finding a landmark immediately resolves the position of the robot. In outdoor environments, however, reliably identifying and detecting unique landmarks is very difficult. A more tractable problem is that of finding non-unique landmarks such as trees, electric poles, etc. Non-unique landmarks abound in outdoor environments, and some of them can be reliably identified in prior maps and with on-board sensors [99].

If we know that the position of the robot is within certain error distribution, then the number of features that are visible within the current detection range are known to be significantly fewer. And if we choose our features and our positions well, we can often make sure that there is only one feature within the detection range of the robot, in which case the feature detected becomes a unique feature.

The key idea is to identify those areas in which a given point feature can be uniquely identified. We call these regions *unique detection* regions. Assuming flat terrain, 360° field of view, and a detection range R, the detection region for a point feature i such as an electric pole is a circle of radius R. If the robot is located within this region we can guarantee that only feature i can be detected.

If there is no overlap between detection regions, each circle would be a *unique detection* region. However, if there are other features within a $2R$ radius of the feature, the other features would reduce the unique detection region of the original feature. These overlapping regions are in turn the unique detection regions for groups of two or more features.

Figure 24 shows the same area as Figure 5, with the unique detection regions for the electric poles in the area highlighted for a detection range R=10 meters. The dark (blue) shading shown in feature number 1 indicates *unique detection* regions. In this case, since there are no other features in a $2R$ radius the whole circular detection region is a *unique detection* region. The light shading (red) shown in parts of the detection regions of all the

other features indicates a part of the detection region where more than one feature can be detected, therefore excluding that area from the *unique detection* region.

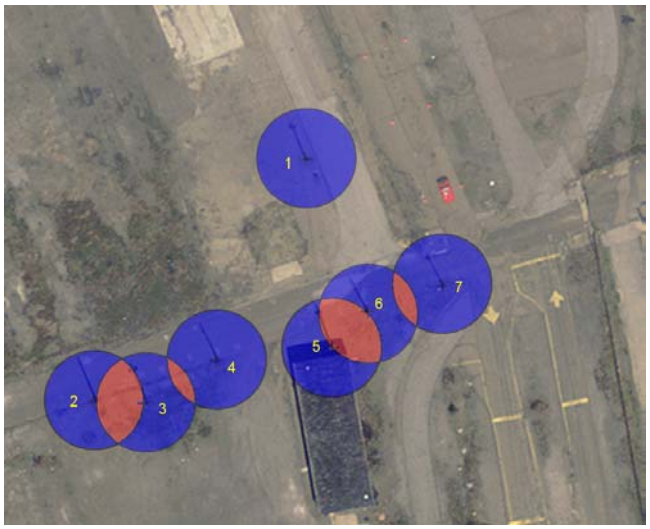

Figure 24. Unique detection regions for electric poles.

We could repeat this procedure for groups of two, three and more point features. If we were to use pairs of point features as another type of feature, the red regions in Figure 24 would be the *unique detection* regions for pairs of electric poles. However, detecting more than one feature at a time is less reliable than detecting individual features because of occlusions. For this reason, even though our algorithm can use of groups of point features, the results presented here only use individual point features as landmarks.

5.1 Modeling detections as deterministic transitions

In general, the detection of landmarks is a stochastic event that is not guaranteed to happen. There are three main situations in which landmarks are not detected: if the landmark is not present, if the landmark is not detected by the perception system and if the landmark is not in the vicinity. We address those three cases as follows: We assume that landmarks are present (accurate landmark map); we use simple landmarks that can be reliably detected; and we only attempt to detect a landmark when we are in the vicinity of one: If all the possible locations for a configuration $\mathbf{r}_k$ are inside a *unique detection* region, we can guarantee that the feature that created the region can be detected, and that no other features will be visible within the field of view of the robot.

When using a non-deterministic probabilistic model, a landmark can only be detected with certainty if whole uncertainty region $\mathcal{C}_\mathcal{U}$ is contained within the *unique detection*

region. When using a probabilistic uncertainty model, the complete probability distribution of the position of the robot should be contained within the *unique detection region.* In practice, some probability distributions (such as the Gaussian) have infinite extent and can only be considered within a given threshold. This approach allows modeling the detection of landmarks as a deterministic event, while introducing a conservative approximation that ignores detections that take place when the uncertainty region or the pdf of the position of the robot are not completely contained within the *unique detection region.*

We use the simplified Gaussian error model, and assume that a circle with radius $\varepsilon_k = 2 \cdot \sigma_k$ completely contains all possible locations on (x,y) of a given state $\mathbf{r}_k$. Therefore, if a circle of radius ε_k centered at $\boldsymbol{\mu}_k$ is completely contained within a *unique detection* region i, we can guarantee that feature i will be detected. This approximation allows us to model the detection of landmarks in a deterministic way, therefore allowing the use of deterministic search for this part of the state propagation as well.

When a landmark is detected, the next state in the state propagation is set to have the same mean as the state before the detection, which is the most likely location for the robot at that step. The uncertainty at this step will be set to a small value ε_L.

While in general a single landmark detected does not reduce the uncertainty in all directions, because of the small heading error assumed for our problem, it is correct to assume that the uncertainty in x and y will be reduced to a small value. The uncertainty in heading, however, remains the same as before the detection.

5.2 Simulation results

Figure 25 shows a sample cost map with some landmarks. Shades of gray indicate different costs in the cost map: areas with lighter color have lower cost, and areas with darker color have higher cost. Solid green areas are obstacles. The start location is a small square on the left, and the goal is a small circle on the right. As a reference, this figure also shows the shortest path that guarantees reachability of the goal for this cost map. The uncertainty rate is 10% of distance traveled. The yellow circles indicate the $\varepsilon = 2\sigma$ contours of the error distribution at each step along the path. The expected cost for this path is 8586.9 and the uncertainty at the goal is $\varepsilon_f = 2\sigma_f = 3.8$ m.

The following figures show the paths found by our approach under different constraints for uncertainty at the goal. They also illustrate the advantages of minimizing the expected cost of the path instead of minimizing the path length or the uncertainty of the path.

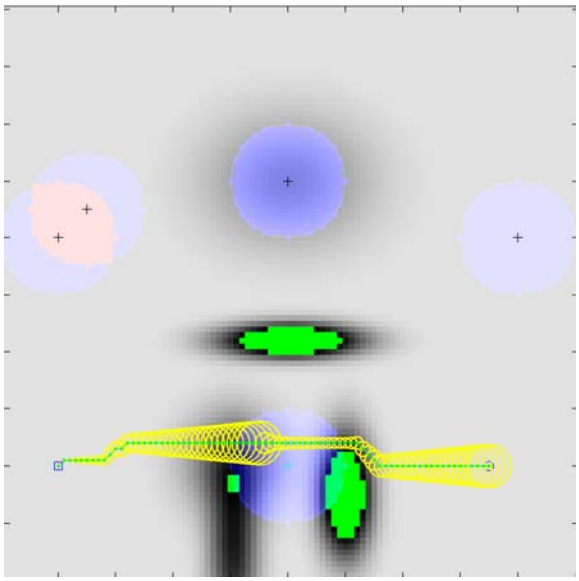

Figure 25. Planning with uncertainty rate ku=10% and using landmarks for localization (shortest path).

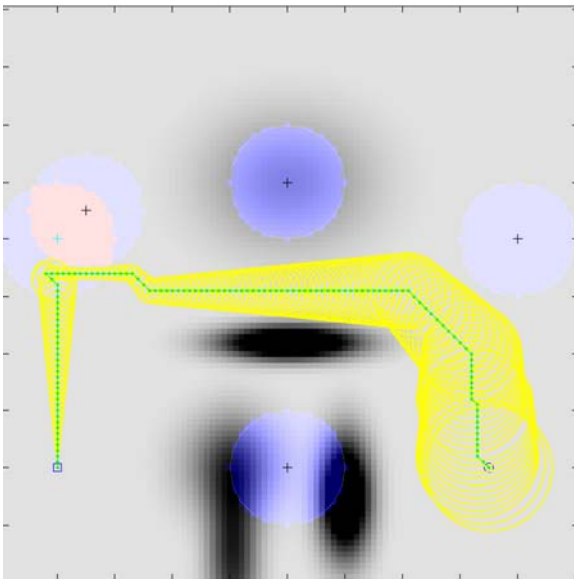

Figure 26. Planning with uncertainty rate k_u=10% and maximum uncertainty at the goal of 12 m.

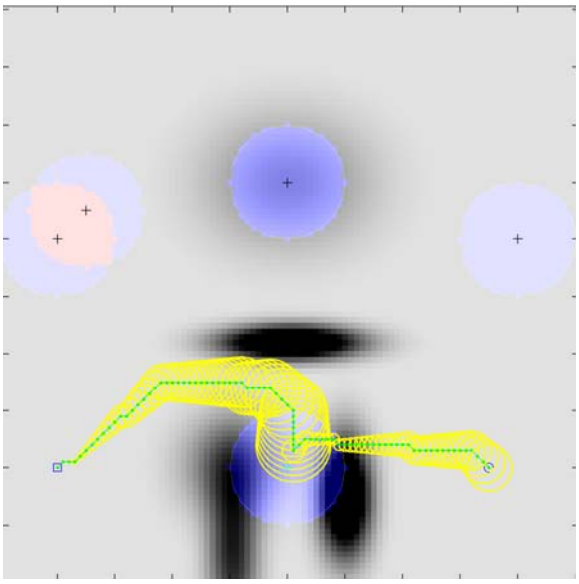

Figure 27. Planning with uncertainty rate k_u=10% and maximum uncertainty at the goal of 3.8 m

Figure 26 shows the lowest expected cost path with an uncertainty rate k_u=10% if the maximum uncertainty allowed at the goal is 12 m. The path found has an expected cost of 1485 (82% lower than the shortest path) and the uncertainty at the goal is 11 m. Because the uncertainty allowed at the goal is large, the planner has enough freedom to look for a low cost path, even if a low cost path is longer and has higher uncertainty. Only one of the localization regions can provide an improvement in the total cost, therefore the planner only includes that landmark in the final path. The planner also avoids the aliased region between the two landmarks on the left, and localizes only with the leftmost landmark.

If the maximum uncertainty allowed at the goal is small, the planner trades off lower cost solutions in order to satisfy the uncertainty constraint. Figure 27 shows the lowest expected cost path when the maximum uncertainty allowed at the goal is reduced to 3.8 m. Even with a maximum uncertainty at the goal equal to that of the shortest path there can be significant advantages in minimizing the expected cost instead of the uncertainty or the path length. The expected cost is now 4710 (still 47% lower than the shortest path) and the final uncertainty is ε =3.8 m. Although the last segment of the path is the shortest path for that segment, the first segment is able to look for a less expensive path than the shortest path and the resulting path is significantly less costly than the shortest path.

5.3 Field tests

In order to validate the results experimentally the following field test was carried out on the e-gator autonomous vehicle shown in Figure 28: a path was planned between a location S and a location G, assuming initial uncertainty σ=2.5m, uncertainty rate of 5% of distance traveled and maximum uncertainty of 10 m, using electric poles for localization (Figure 29). Notice how the path follows a road in order to minimize the expected cost along the path (instead of just minimizing the length of the path). The path also visits detection regions as needed to maintain a low cost path within the uncertainty constraints, and avoids narrow areas that could not be safely avoided if the position of the robot is not accurately known.

Also notice that the final uncertainty of the path is relatively high ($\varepsilon = 5.4$ m). This is because the maximum uncertainty allowed was set to 10 meters, and the planner will only try to reduce the uncertainty if the reduction in uncertainty will reduce the expected cost of the path. In the last segment the path is going through a large paved area and there is no increase in cost because of the higher uncertainty. For this reason, the planner does not try to detect any features in last 50 meters of the path.

Figure 28. E-gator autonomous vehicle used for testing and electric poles used for localization at test site. The vehicle equipped with wheel encoders and a KVH E- core 1000 fiber-optic gyro for dead reckoning, and a tilting SICK ladar and onboard computing for navigation and obstacle detection

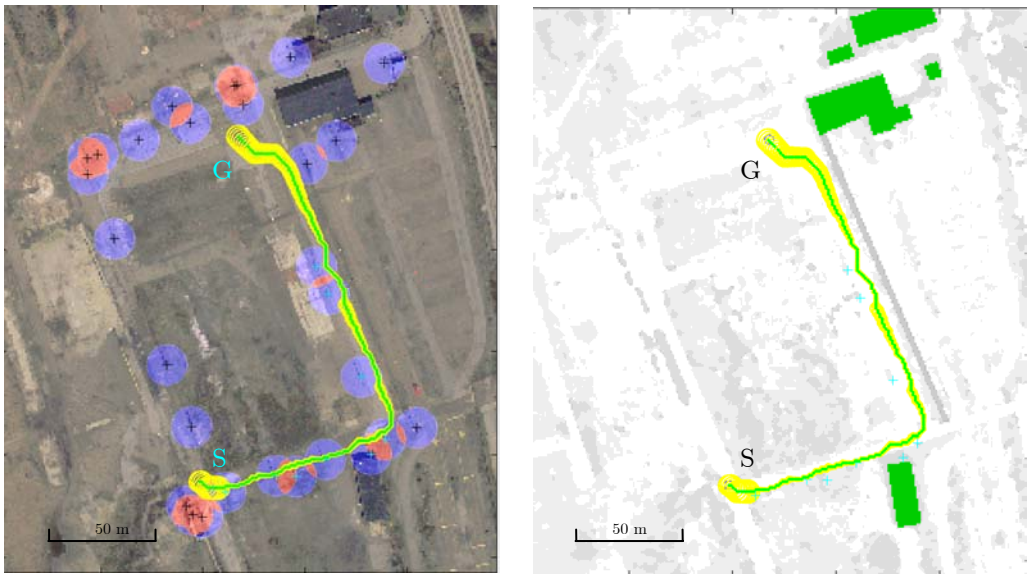

Figure 29. Path planned assuming initial uncertainty σ=2.5m, uncertainty rate of 5% of distance traveled and maximum uncertainty of 10 m. The expected cost of the path is 3232, and the final uncertainty is σ=2.7m. Left: aerial image and unique detection regions. Right: cost map used.

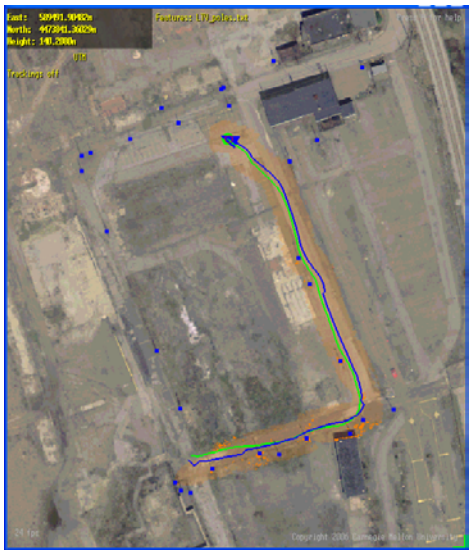

Figure 30.Path planned and executed without GPS. Blue dots show the location of landmarks. The blue line is the position estimate of the Kalman filter on the robot and the green line is the position reported by a WAAS differential GPS with accuracy of approximately 2 meters (for reference only).

Figure 30 shows the path executed by the robot. The blue line is the position estimate of the robot according to the onboard Kalman filter that combines the dead reckoning sensors and the landmark detections (no GPS). The green line shows the position estimate according to the GPS (shown as a reference only). Notice how the blue line stays very close to the GPS estimate, and jumps in a few places after detecting a landmark.

5.4 Discussion

The approach presented here [31][34][35] allows robust and efficient navigation without GPS. It uses landmarks in the environment that have been manually identified in a high-resolution prior map to reduce the uncertainty in the robot's position as part of the planning process. The resulting path minimizes the expected cost along the route considering the uncertainty in the position of the robot. We have also shown experimental results of the system, showing navigation capabilities similar to those of a robot equipped with GPS. The current version of the algorithm uses light poles as its landmarks, and assumes that the landmarks will always be detected in both planning and execution.

5.4.1 Performance

This approach has very similar performance to the planner presented in the previous chapter. However, two aspects affect the performance in different ways. On one hand, the search space and the dominance relationships are more complicated when adding detection regions. On the other hand, because of the periodic relocalizations, the uncertainty levels throughout the planning process remain lower. The net effect depends on the specific configuration, but on average it seems to be two to three times faster than the planner without landmarks. Figure 31 shows the results of running multiple simulations on fractal worlds of sizes between 100x100 and 1000x1000, for an uncertainty rate of 5% and randomly chosen landmarks. Figure 32 shows one of these fractal worlds. The planner is able to plan in less than 10 seconds for worlds up to 400x400, and in about 80 seconds in worlds of size 1000x1000. To the best of out knowledge this is the fastest planner for planning with uncertainty in position for continuous cost domains.

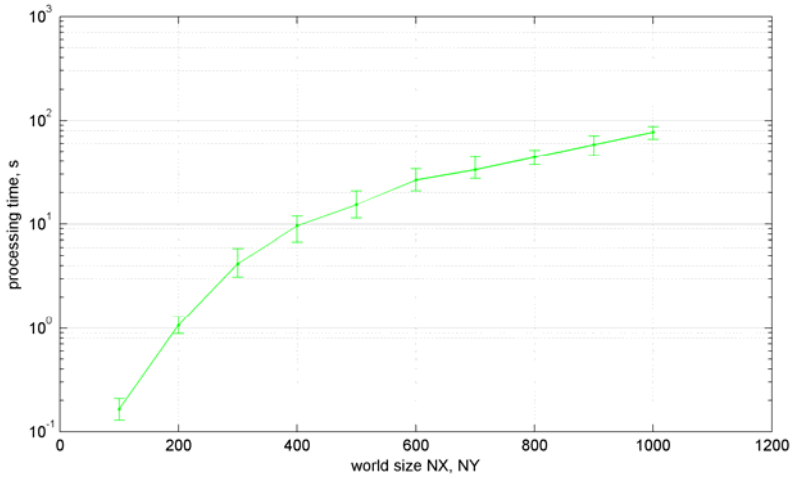

Figure 31. Planning time in fractal worlds with $\alpha_u = 5\%$ and varying world sizes.

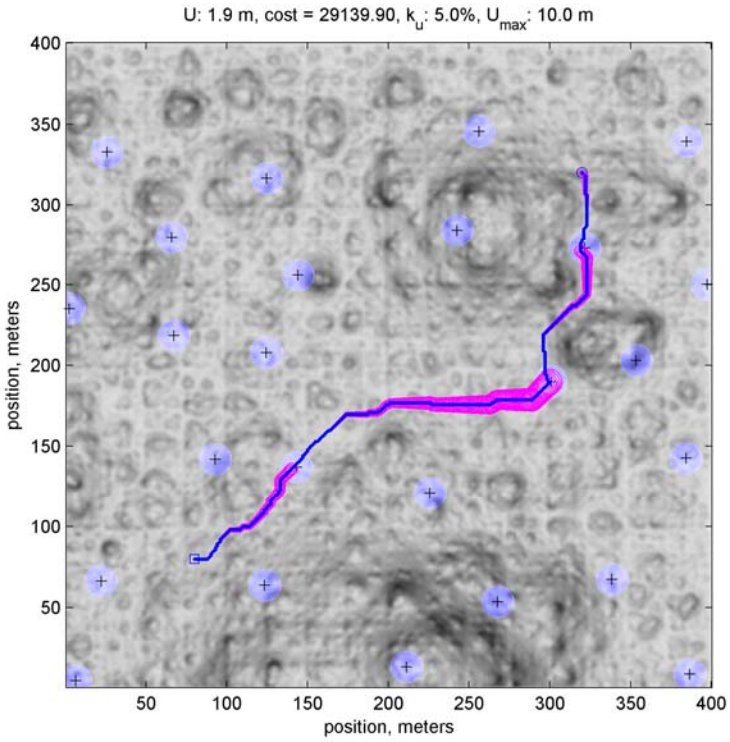

Figure 32. Fractal world used for performance simulations. Elevations are shown as a shaded-relief grayscale. The actual traversal cost is calculated based on the slope of the terrain. The blue circles indicate the detection regions of thelandmarks ("+").

5.4.2 Limitations

Although algorithms in the literature (such as the one of Lazanas and Latombe [59]) claim optimality when using landmarks in a similar fashion, the optimality of the algorithm is significantly limited by the representation and the approximations made. The most limiting approximation is the inability to use landmarks when the detection range is smaller than the uncertainty of the robot. Figure 33 shows an example where by performing a local search for a landmark L it is possible to find a lower cost path than the one found by our algorithm. In order to find this solution, the algorithm would need to have the ability to represent the local search for a landmark. While this is an important limitation it only affects the optimality of the solution when there are no other alternatives for the path and the uncertainty when reaching the landmark is slightly larger than the detection range. If the uncertainty at the landmark is much larger than the detection range, the solution found by the local search would be too complex and unreliable to be a feasible one.

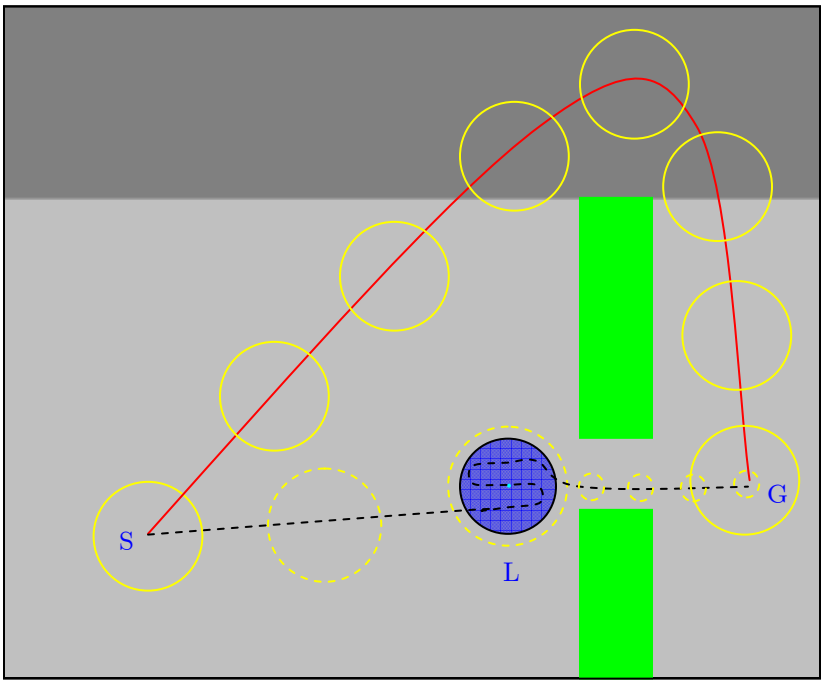

Figure 33. Limitations of the current approach. Light gray areas are low cost regions, dark gray areas are high cost regions, green regions are obstacles. The yellow circles represent the uncertainty at each step, the blue circle is the unique detection region for landmark *L*. The solid line is the path that our approach would find, and the dotted line is an approach that has lower cost while still guaranteeing reachability of the goal.

Another important limitation is that the approach proposed here finds the path that has the lowest expected cost and guarantees the reachability of the goal within the given error bounds. However, in some scenarios, the best approach would be to have a policy instead of a path. A policy would consider the detection of features as a non-deterministic event and would produce a set of actions to be performed depending on the outcome of the detection of features. Because of this added flexibility a policy could have a lower expected cost than the path found by our approach. But finding an optimal policy would require solving a POMDP, which would be intractable to solve or would take significantly longer to plan. Coastal Navigation, proposed by Roy and Thrun [79][97] is the closest approach in the existing literature that uses a POMDP to solve a similar problem in relatively large worlds. Their solution produces a policy that can find lower cost solutions, at the expense of longer processing times.

Coastal Navigation uses an *Augmented Markov Decision Process* (AMDP) to approximate the underlying POMDP. This AMDP uses entropy to describe the belief state of the robot at each location, therefore creating a search space that is *(x,y,H).* Instead of discrete landmarks, they use a sensor map of the environment to localize the

robot. They then use a probabilistic sensing model based on a map of previously sensed features. This approach is able to model the increasing likelihood that a feature will be detected as the robot gets closer to it, instead of waiting until the whole uncertainty region for the robot is completely contained within the detection region.

This solution can produce lower cost policies, at the expense of longer processing times. The processing of the prior sensor map, in particular, can take from several minutes to a few hours [82]. If the prior map that the robot uses is accurate, the initial pre-processing only needs to be performed once. However, if there are significant changes in the world, the pre-processing would have to be repeated, or the solution to the problem may no longer be valid. Even if the prior-map can be re-used, it is likely that Coastal Navigation would be slower than PUP, as it uses value iteration to process the complete state space (x,y,H), while PUP only searches a small fraction of the space in typical problems.

Chapter 6

Replanning with Uncertainty in Position (RPUP)

Even the best prior maps have inaccurate cost estimates. One of the most common causes for inaccurate cost estimates is the difference in resolution between the prior map and the onboard sensor map. While large terrain features will likely be present in both maps, smaller obstacles are often only found by onboard sensors. Other causes of inaccuracy in cost estimates are outdated maps, and errors in the process of converting the prior map into a cost map.

If these errors are significant, the path found by the planner will be suboptimal and could even be non traversable. The solution to this problem is to replan the path once the discrepancy is detected. The most basic (and least efficient) form of replanning the path is to repeat the planning process from scratch. The most complex (and most efficient) form of replanning is to use an algorithm that is able to repair the search graph and reuse as much as possible of the initial calculations such as D*[91][92] or D*Lite [46][47][48]. Unfortunately these algorithms require backward search and our approach derives significant performance gains from the use of forward search.

We propose an approach called Replanning with Uncertainty in Position (RPUP), that implements D*-lite within the Planning with Uncertainty in Position (PUP) approach described in the previous chapter. D*-lite reuses previous search results and minimizes the changes in the search graph that take place when costs change. However, there are significant challenges when implementing such approach.

The main limitation is that many of the performance gains in PUP come from using forward search and state dominance. However, when replanning for goal-directed navigation, it is much more efficient to plan backward from the goal than forward from the start. While in forward search the uncertainty at the beginning of the search (the start location) is known, in backward search the uncertainty at the beginning of the search (the goal location) is unknown. Instead of having a single start state with known uncertainty, all possible uncertainty values at the goal have to be considered in the search. Furthermore, most of the search will take place near the goal, where the uncertainty is higher (as opposed to planning forward, in which case the uncertainty near the start is usually lower).

We propose two ways to incorporate updates in the prior map when the uncertainty model is a simplified Gaussian: *prior map updates* and *sensor updates*.

6.1 Prior map updates

This approach assumes that the updates in the prior map are provided by a source that is well registered with the original map. For example, if the original map is a satellite image, updates to this map will also come from a satellite image that is well registered to the original satellite image. These updates, like the initial prior map, are not perfectly registered to the position of the robot.

As described in the previous chapters, planning with uncertainty in position can be modeled as planning in a 3-D configuration space where the cost at each location μ_x,μ_y,ε is given by:

$$C_{\mathbf{r}}(\mu_x,\mu_y,\varepsilon) = \sum_{\forall i} C_o(x_i,y_i)\cdot p_{\boldsymbol{\mu},\varepsilon}(x_i,y_i) \tag{6.1}$$

Where (μ_x,μ_y) is the most likely location for the robot, ε is the 2σ uncertainty contour, C_o is the traversal cost from the prior map, and p is the probability distribution of the position of the robot

$$p_{\boldsymbol{\mu},\varepsilon}(x,y) \triangleq N((\mu_x,\mu_y),\varepsilon/2) \tag{6.2}$$

Changes in the prior map C_o at location x_k, y_k require changing $C_{\mathbf{r}}(\mu_x,\mu_y,\varepsilon)$ at all locations such that

$$(\mu_x - x_k)^2 + (\mu_y - y_k)^2 \le \varepsilon^2 \tag{6.3}$$

D*-Lite is then used to update the 3-D search graph considering all the changed cells. While D*-lite is a natural extension of the A*-based approach used in planning with uncertainty in position, some aspects of the problem domain make implementing D*-lite not as efficient as it would be in a traditional 2-D planning domain. D*-lite for goal-directed navigation searches backward from the goal, in order to reuse a larger portion of previous searches. PUP, on the contrary, uses forward search in order to limit the number of states expanded in each search and take advantage of the known initial position.

The resulting D*-lite implementation with PUP plans backward from the goal to the start location of the search. However, because the uncertainty at the goal is not known, the search has to include all the allowable uncertainties at the goal. Furthermore state dominance is of limited use, as the states pruned at a given time, may not be dominated at a later stage and the overhead required to check for dominance cancels out the

performance gains. While in forward PUP the expanded states defined a thin volume, in backward PUP with D*-Lite the search space is usually a full 3-D volume.

Paths found by replanning with prior map updates are equivalent to the paths that would have been found if the new information had been present in the original prior map. Figure 34 (a) shows a path planned in using uncertainty in position. Figure 34 (b) shows the resulting path after replanning because a prior map update is received showing an obstacle to the left of the workspace. Notice how the new obstacle is avoided with the 2σ uncertainty contour of the robot's position, as are all other obstacles in the map.

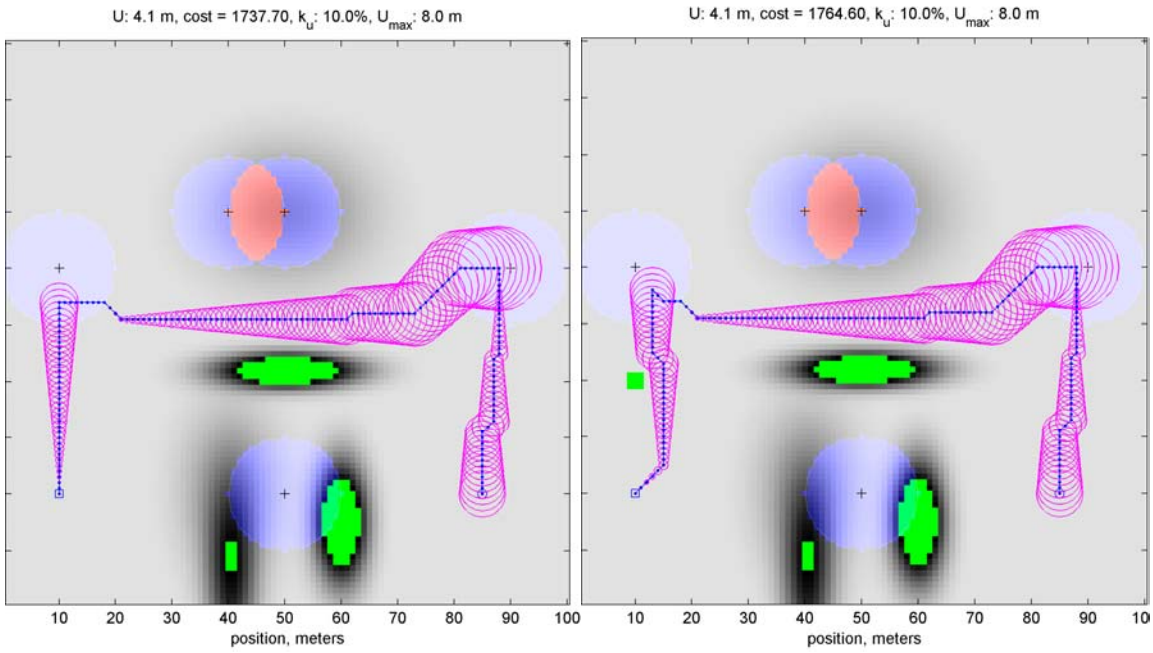

(a) (b)

Figure 34.(a) Path planned considering uncertainty in position. (b) Path updated and re-planned because of a prior map obstacle.

6.2 Sensor updates

This approach assumes that the updates in the prior map are provided by a source that is well registered with the position of the robot such as updates provided by the onboard sensors in the robot. The position of the robot with respect to these updates is known, but the position of these updates in the prior map is not.

In order to combine these two sources of information, we need to model the prior map as a *probabilistic prior*. A *probabilistic prior* is the probability distribution of the costs in the map before any sensor data is taken into account. In general, when the augmented

prior map $C_{\mathbf{r}}$ is expressed as a probabilistic prior, its representation will become $p(C_{\mathbf{r}})$, as each location (x,y,ε) will have a probability distribution of costs, instead of a single cost. When sensor data is available, the posterior distribution of the cost is

$$p(C_{\mathbf{r}}^{'}) = p(C_{\mathbf{r}} \mid C_s) = \frac{p(C_s \mid C_{\mathbf{r}})p(C_{\mathbf{r}})}{p(C_s)} \tag{6.4}$$

where $p(C_s \mid C_{\mathbf{r}})$ is the sensor model. Although many models can be used to model the prior map and sensor costs, an initial approximation would be to model them as Gaussian distributions such that:

$$\begin{aligned} p(C_{\mathbf{r}}) &\triangleq N(\overline{C}_{\mathbf{r}}, \sigma_{\mathbf{r}}) \\ p(C_s \mid C_{\mathbf{r}}) &\triangleq N(\overline{C}_s, \sigma_s) \end{aligned} \tag{6.5}$$

In such case, the posterior distribution is the product of two Gaussians, which is also a Gaussian:

$$C_{\mathbf{r}}^{'} : N(\overline{C}', \sigma') \tag{6.6}$$

where

$$\begin{aligned} \overline{C} &= \alpha \overline{C}_s + (1-\alpha)\cdot \overline{C}_{\mathbf{r}} \\ \sigma &= \frac{\sigma_s \sigma_{\mathbf{r}}}{\sqrt{{\sigma_s}^2 + {\sigma_{\mathbf{r}}}^2}} \\ \alpha &= \frac{\sigma^2}{{\sigma_s}^2} = \frac{\frac{1}{{\sigma_s}^2}}{\frac{1}{{\sigma_s}^2} + \frac{1}{{\sigma_{\mathbf{r}}}^2}} \end{aligned} \tag{6.7}$$

This update is performed for each cell in the configuration-uncertainty state space such that:

$$C_{\mathbf{r}}^{'}(\mu_x, \mu_y, \varepsilon) = \alpha \overline{C}_s(\mu_x, \mu_y, \varepsilon) + (1-\alpha)\cdot \overline{C}_{\mathbf{r}}(\mu_x, \mu_y, \varepsilon) \tag{6.8}$$

Since the sensor data is assumed to be perfectly registered with the position of the robot, its cost does not depend on ε and (6.8) can be simplified as follows:

$$C_{\mathbf{r}}^{'}(\mu_x, \mu_y, \varepsilon) = \alpha \overline{C}_s(\mu_x, \mu_y) + (1-\alpha)\cdot \overline{C}_{\mathbf{r}}(\mu_x, \mu_y, \varepsilon) \tag{6.9}$$

Using this update model, when a change at location (μ_x, μ_y) is detected, the combined map is updated by recalculating $C_{\mathbf{r}}^{'}(\mu_x, \mu_y, \varepsilon)$ for all ε values at (μ_x, μ_y). However, this change affects significantly fewer cells than prior map updates, since the configuration-uncertainty prior map $C_{\mathbf{r}}$ does not change when sensor updates are received.

The parameter α in general reflects the confidence on the sensor data. In the simplest case, the confidence in the sensor data is much higher than the confidence in the prior

map data. In such case, σ_s is small compared to σ_r and $\alpha \approx 1$, but only for cells with sensor information. For cells that don't have sensor data, $\sigma_s \to \infty$, and and $\alpha \approx 0$:

$$\alpha = \begin{cases} 1 & \textit{for cells with sensor data} \\ 0 & \textit{otherwise.} \end{cases} \tag{6.10}$$

Paths found by replanning with sensor updates are not equivalent to the paths that would have been found if the new information had been present in the original prior map, because prior map information is not registered to the robot and sensor information is.

Figure 35(a) shows the same path from Figure 34 (a), and Figure 35(b) shows the resulting path after replanning because a sensor update is received showing an obstacle to the left of the workspace. Notice how only the mean of the path avoids the obstacle, not the 2σ uncertainty contour.

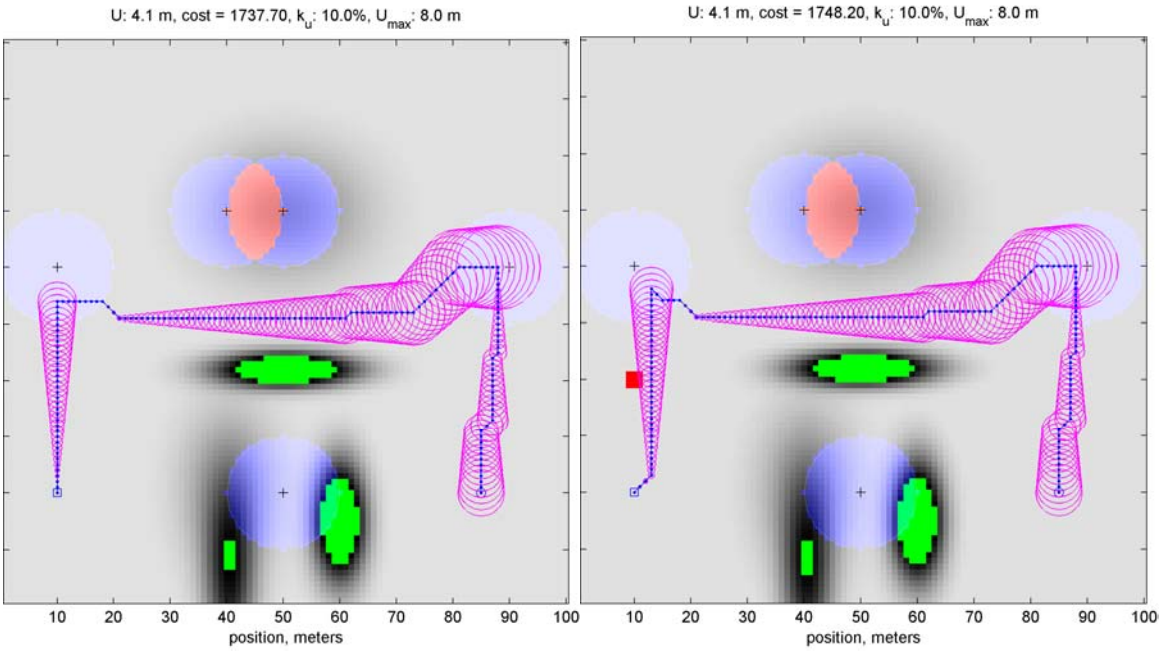

Figure 35.(a) Path planned considering uncertainty in position. (b) Path updated and re-planned because of a sensor obstacle

6.2.1 Impact of sensor updates in global route selection

While sensor updates are local, the path that the planner generates is a global route that incorporates both prior data and sensor updates. The impact of the sensor data on the global route depends on the assumptions about the sensor and prior data, and whether those assumptions are accurate or not. While these assumptions may not always be correct, the cases that have been evaluated have produced results that are consistent with the initial assumptions. One of the most interesting and representative cases for

merging prior and sensor data is the one presented by *non-detectable obstacles*. Non-detectable obstacles are obstacles that are known to exist in the prior map, but that cannot be detected with onboard sensors. A known quicksand area or a minefield are some examples of this type of obstacles, as the onboard sensors of most robots are unable to detect them, yet their location can be known from the prior map.

In order to understand how the planner handles such obstacles, it is useful to model the problem in a frame of reference centered at the most likely location of the robot. In this frame of reference there is perfect certainty about the location of the robot, but there is uncertainty about the location of the prior map obstacles. If using a non-deterministic uncertainty model in which the uncertainty region of the robot is a circle of radius ε., this model creates a configuration-uncertainty state space such that if the robot is a point at (μ_x, μ_y, ε), and the prior map obstacles are grown by ε, creating *obstacle uncertainty regions.* A path is only valid if it does not intersect any obstacle uncertainty regions. Figure 36 shows an example of the workspace and configuration-uncertainty state space views. In this example, the uncertainty along the path does not increase, which allows the obstacle-uncertainty regions to be grown with the same ε throughout the path.

If the onboard sensors detect an obstacle, this obstacle will not be grown, because its position is precisely known in the robot's frame of reference. The configuration-uncertainty state space is therefore made up of prior map obstacles that are grown by the uncertainty of the robot at each location, and of sensor obstacles that are present at each uncertainty level but are never grown. Figure 37 shows an example sensor obstacle which blocks the prior map channel and forces the planner to find a new path the prior map obstacles.

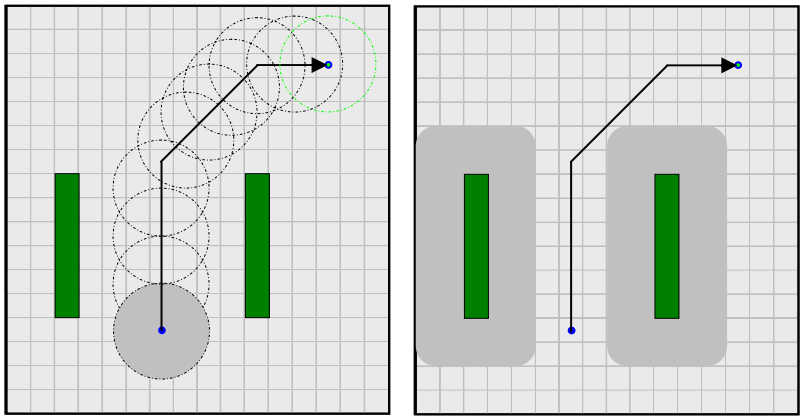

Figure 36. Dual view of uncertainty in the position of the robot as uncertainty in the position of the obstacles. Left: sample world with obstacles (green), robot (blue dot), uncertainty region for the robot (gray circle) and path (solid black). Right: view in configuration-uncertainty space, with the robot as the frame of reference. The robot is now a point, and the obstacles are grown by the uncertainty of the robot, creating an obstacle uncertainty region (gray). In this example the uncertainty along the path does not change.

If the onboard sensors detect an obstacle, this obstacle will not be grown, because its position is precisely known in the robot's frame of reference. The configuration-uncertainty state space is therefore made up of prior map obstacles that are grown by the uncertainty of the robot at each location, and of sensor obstacles that are present at each uncertainty level but are never grown. Figure 37 shows an example sensor obstacle which blocks the prior map channel and forces the planner to find a new path the prior map obstacles.

The interpretation of the combination of the prior map and sensor obstacles is however not trivial. A point in the configuration-uncertainty state space is considered non-obstacle only of it is neither in a prior map obstacle region nor in a sensor obstacle. This means that all locations that could contain a prior map obstacle are not included in the solution, even if for some positions of the obstacles there may be a valid path. Figure 38 (left) shows an example in which if obstacles are in the rightmost area of the obstacle region, there would be a path to the right of the sensor obstacle. However, since the position of the prior-map obstacle is not known, this path also needs to be valid for all possible positions of the obstacles within the obstacle region the actual position of the obstacles. The figure to the right shows that this path would not be valid if the real position of the obstacles is in the leftmost part of the obstacle region, therefore the path itself is not valid.

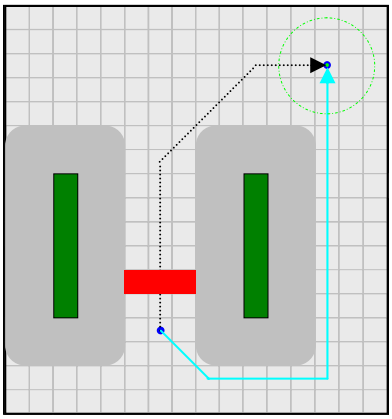

Figure 37.Sensor obstacle represented in configuration-uncertainty state space. The sensor obstacle (red) is not grown by the uncertainty of the robot because there is no uncertainty in its position. The obstacle shown blocks the guaranteed free space, therefore the new best path goes around the channel.

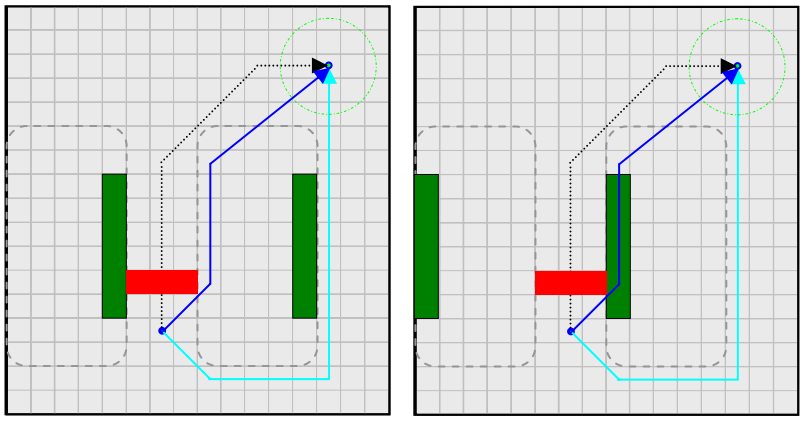

Figure 38. Possible path that is not valid. The obstacles in the map are not really located at the most likely location. If the obstacles are actually located in the rightmost part of the obstacle region, then there would be a path to the right of the sensed obstacle that could be used (blue line). However, since the actual position of the non-detectable obstacles is not known, it is also possible that the obstacles are in the leftmost part of the obstacle region. In such case, the path shown in the blue line would take the robot through an obstacle. Only a path that avoids all of the possible instances of the obstacle region can guarantee the safety of the robot.

6.3 Performance

In order to measure the performance gains achieved by using replanning vs. planning from scratch the following experiment was performed. 50 different worlds were randomly generated using a fractal world generator, varying in size from 100x100 to 1000x1000 pixels. The number of uncertainty levels was kept fixed at 100. In each of these worlds the prior map used was a low resolution version of each world. Then the robot's motion along the path was simulated and higher resolution data was obtained around the robot in a 20x20 cells area by retrieving the original, high-resolution map (see Figure 39). These data updates were incorporated into the plan as prior map updates (registered to the original map) or sensor updates (registered to the robot). The planner used for planning from scratch was the one described in Chapter 5(PUP), which is a very efficient forward planner with uncertainty in position. The simulations were performed on an Intel(R) Xeon(TM) CPU running at 3.80GHz, with 4GB of memory. While some parts of the algorithm could easily be run in parallel, the simulations only use one of the four processors present. Additional improvements in the run-time of the algorithm could be achieved by taking advantage of the additional processors available.

When using prior map updates, the performance gains were only noticeable for worlds larger than 500x500, and continuously improving for larger worlds. The best result was at 1000x1000, where planning from scratch took 50 seconds on average, while replanning

took approximately 7.5 seconds (a 7.5 times faster). Figure 40 shows the average the average online planning times (top) and the speed-up factor for different world sizes (bottom).

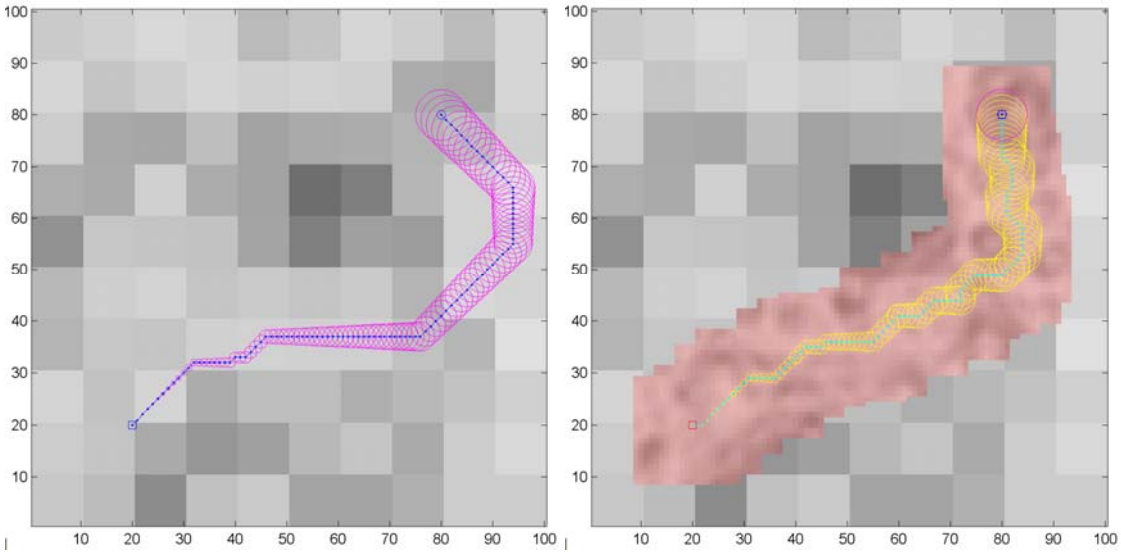

Figure 39. Initial path planned in low-resolution prior map (left) and final path followed by the robot after high-resolution sensor updates (right)

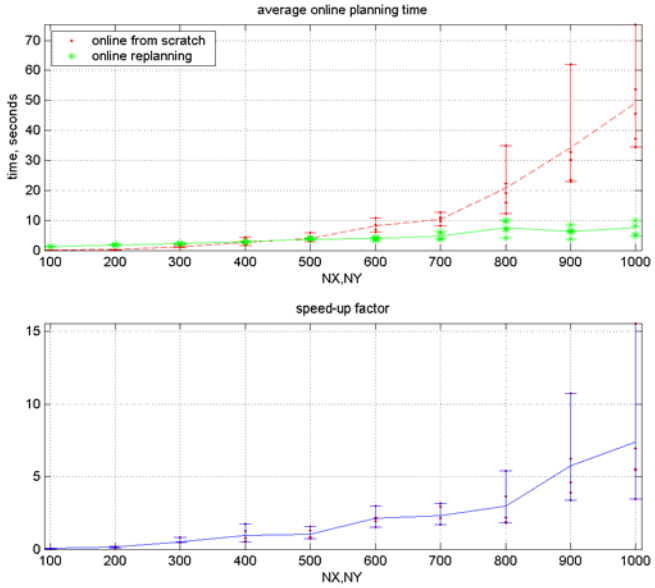

Figure 40. Average online planning time for forward search vs. re-planning with prior map updates (top). Average speed-up (bottom)

Replanning with sensor updates produced significantly better performance gains. Performance improvements were significant for worlds of size 300x300 and higher, with greater improvements in larger worlds. The best result was at 1000x1000, where planning from scratch took 38 seconds on average, while replanning took approximately 0.6

seconds (a 62 times faster). Most importantly, since the average planning time was less than one second, this planner can considered near-real-time and be used in practical applications as an on-line planner that re-plans frequently as the robot moves toward the goal. Figure 41 shows the average the average online planning times (top) and the speed-up factor for different world sizes (bottom).

While re-planning is significantly faster especially with sensor updates, it has some important disadvantages with respect to the original PUP implementation (forward search). While in forward PUP the expanded states defined a thin volume, in backward PUP with D*-Lite the search space is usually a full 3-D volume. The average thickness of the search volume in forward search is between 1 and 2 cells, while the average thickness for replanning with backward search is about 20 cells. Thus, the memory requirements for backward search are 10 to 20 times greater.

Additionally, the initial planning time when performing backward search is much longer than in forward search. Figure 42 shows the comparison between initial planning times for forward vs. backward search. The worst case is at 1000x1000, where the initial planning time for backward search is 1500 seconds (25 minutes), while for forward search is 120 seconds (2 minutes).

One possible approach to solve this problem is to pre-compute the initial path (off-line). This alternative is possible if the prior map and goal are known before the path execution begins. While in some scenarios this is possible, it is more likely that only the prior map will be known ahead of time, but the goal of the mission will not. In such scenario, it is possible to pre-compute the expected costs for each uncertainty level, which represents approximately 80% of the processing time. Figure 43 shows the initial planning time for forward and backward search when the expected costs are pre-computed. The initial planning time in the largest world is reduced from 25 minutes to 5 or 6 minutes. While this is still too long for some scenarios, in many cases it may be fast enough for practical implementations.

Figure 44 (top) shows the impact of pre-computing costs on the average online planning time with respect to forward search from scratch. For re-planning, the average online planning time remains almost unchanged, because the states that are processed in the initial path are usually the ones required to calculate the updated path during replanning. On the other hand, the online planning time for forward search from scratch is greatly improved when pre-computing expected costs. In the largest world, the planning time goes from approximately 40 seconds to about 6 seconds. While this is a significant performance improvement for the forward planner, the performance of the replanning approach is still better by a factor of 10 (see Figure 44(bottom) in the largest world).

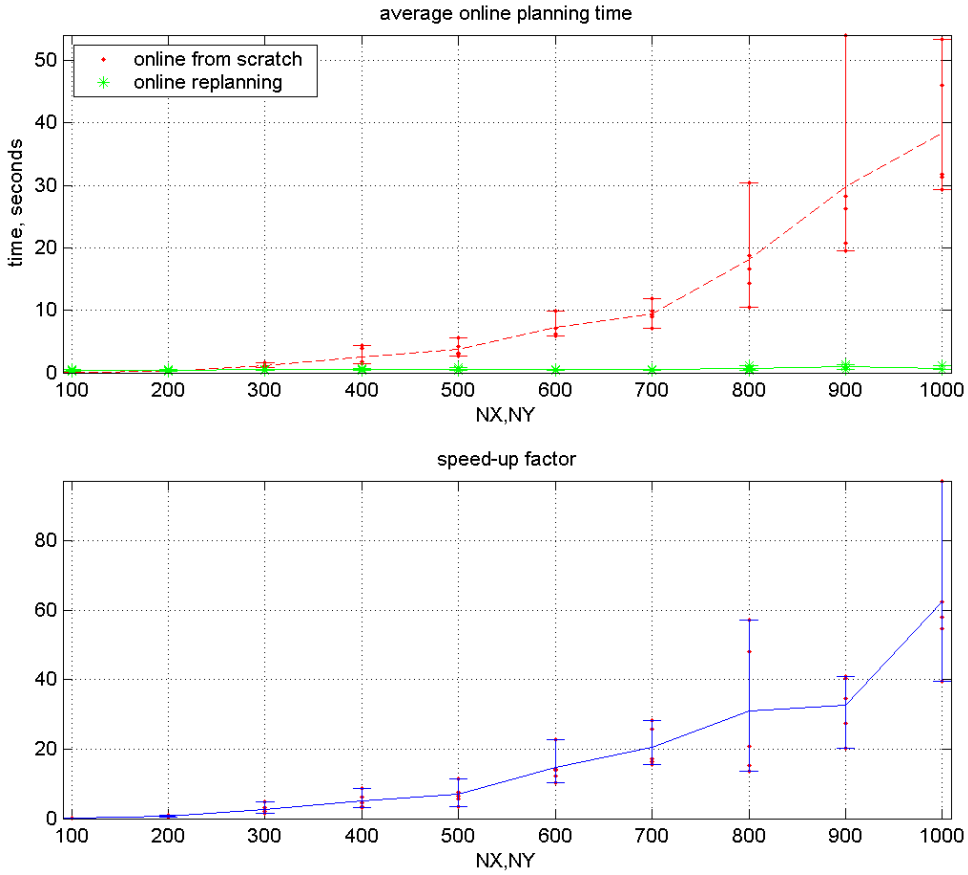

Figure 41. Average online planning time for forward search vs. re-planning with sensor updates (top). Average speed-up (bottom)

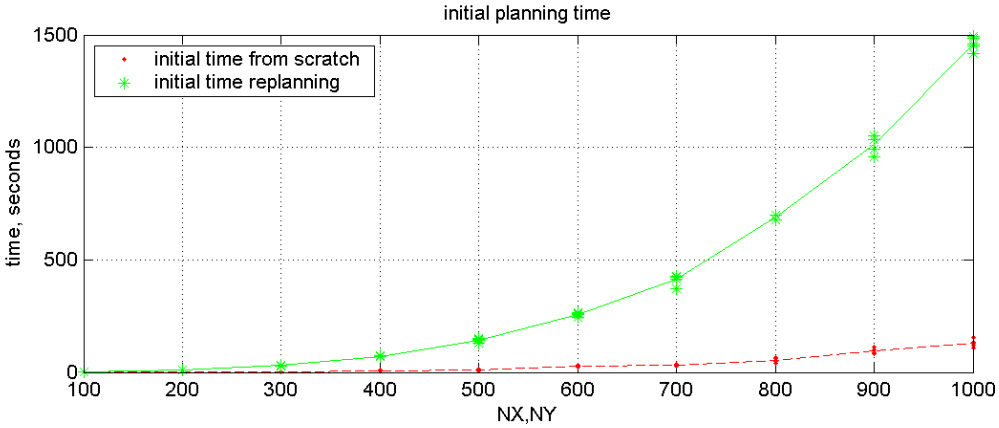

Figure 42. Average initial planning time for forward search vs. re-planning with sensor updates.

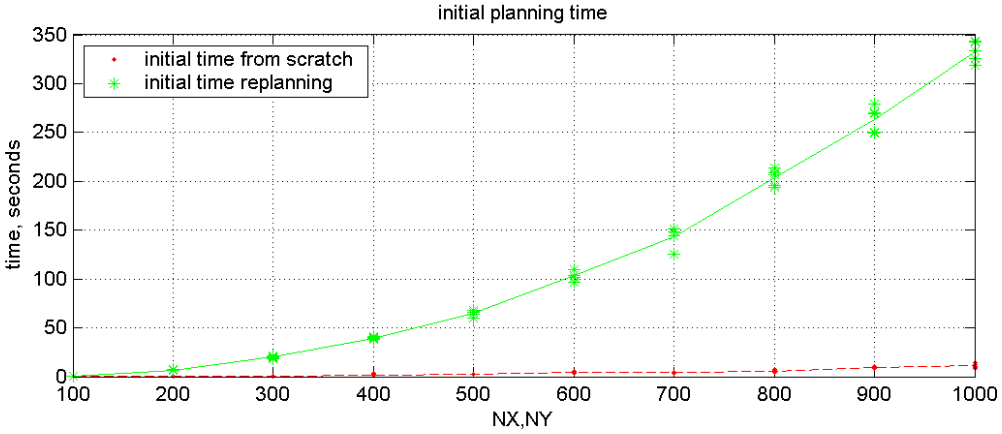

Figure 43. Average initial planning time for forward search vs. re-planning with sensor updates using pre-computed costs.

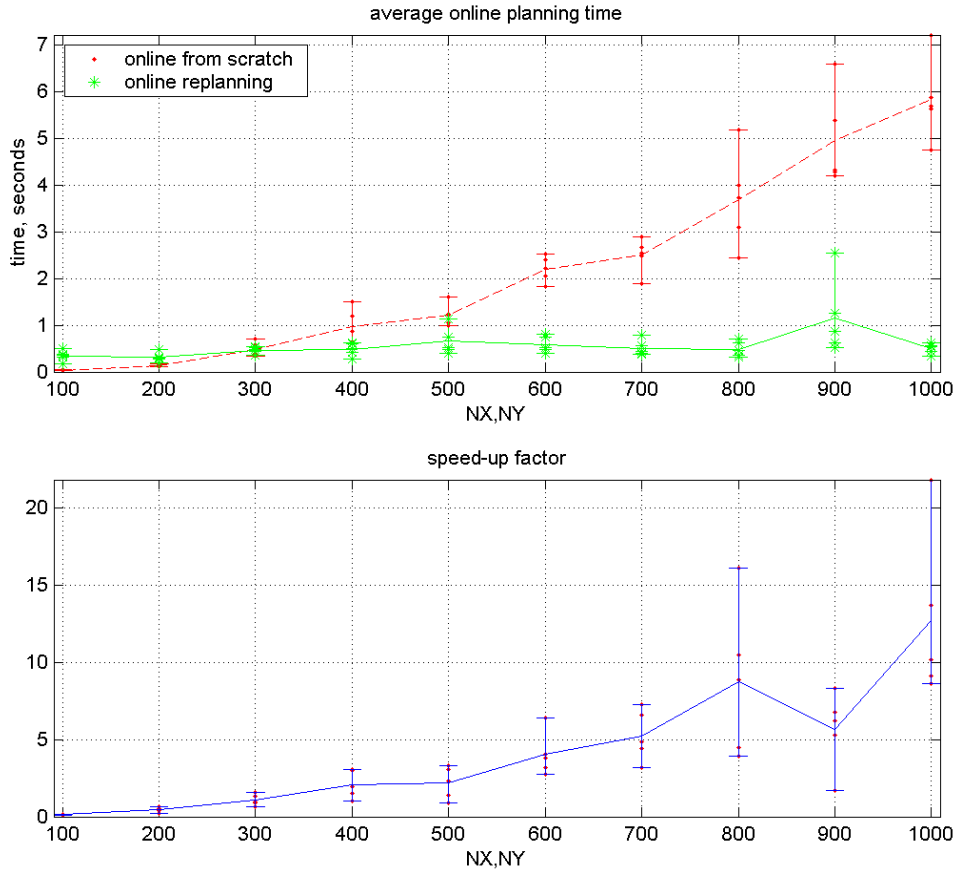

Figure 44. Average online planning time for forward search vs. re-planning with sensor updates (top). Average speed-up (bottom)

6.4 Field experiments

6.4.1 Comparison between planning with and without uncertainty

The following field tests were performed to experimentally validate the replanning approach. 10 successive runs were performed without GPS, alternating planning with uncertainty in position and planning assuming perfect position. For both sets of experiments a prior map was provided with a resolution of 1 meter/cell, with traversal costs estimated from an aerial image of the test site with a resolution of 0.3 meters/cell.

When planning with uncertainty in position, the location of known existing landmarks (light poles) was also provided to the planner, as well as an estimate of the uncertainty rate in the inertial navigation system (10% of distance traveled). With this information the planner with uncertainty in position calculated an initial path that would minimize the expected traversal cost, while guaranteeing that the goal was reached with an uncertainty of less than 5 meters (2σ confidence interval). Once execution started, sensor updates from a SICK laser range finder were incorporated in the planner, and a new global path was calculated every 1 to 2 seconds. The position of the robot was continuously estimated by a Kalman filter that incorporated the readings from the wheel encoders, the fiber-optic gyro (for heading), and the landmarks detected along the way.

While there is no ground truth data available to measure the results, the position reported a WAAS-enabled GPS can be used to estimate the quality of the solution. The accuracy of this position estimate depends on the satellites available at the time of testing, as well as other atmospheric and environmental perturbations. The GPS unit utilized for the tests reports its own estimate of accuracy for a 95% error bound.

Figure 45 shows the results of the five runs performed using replanning with uncertainty in position (RPUP). The blue line shows the difference between the position estimated by the Kalman filter and the position reported by the GPS. The green line shows the 2σ confidence interval for the position of the robot according to the Kalman filter. The red line shows the GPS's own estimate of error (which is about two meters for all runs). The gray, dotted line shows the sum of the GPS and Kalman position estimate errors.

All five runs where successfully completed, with uncertainties at the goal well below 5m. In most cases the blue line showing the difference between the robot's own estimate of its position (as reported by the Kalman filter) and the position reported by the GPS is less than the error in the GPS estimate alone (dashed red line). The exception is the second run (top right figure), where the landmark located at 250 meters from the start was not detected.

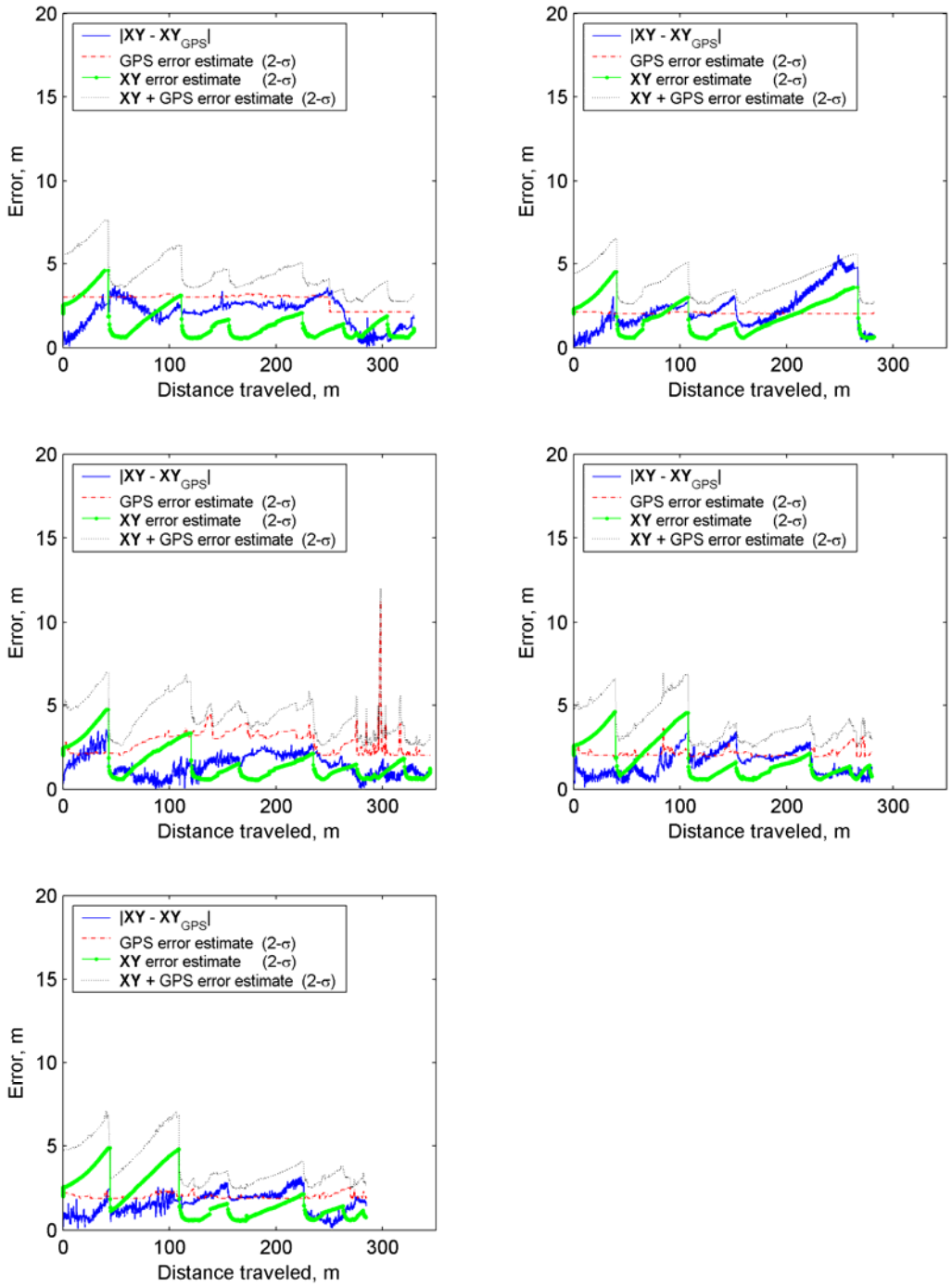

Figure 45. Error in the position of the robot in five different runs using PUP. The blue solid line is the absolute error between the robot's own estimate of its position and the position reported by the GPS (used as ground truth). The red dashed line is the GPS 2σ error estimate (as reported by the GPS unit). The green solid line with dots is the 2σ error estimate of the Kalman filter considering dead reckoning and landmarks. The dotted gray line indicates the sum of the 2σ error estimate of the Kalman filter and the GPS 2σ error estimate.

The actual error between the Kalman filter estimate and the GPS position is always bounded by the sum of the error estimates of the Kalman filter and the GPS, indicating that the model correctly bounds the errors in the system.

Figure 46 shows the results of the five runs performed assuming perfect position. The blue line shows the difference between the position estimated by the Kalman filter (without using landmarks) and the position reported by the GPS. The green line shows the 2σ confidence interval for the position of the robot according to the Kalman filter. The red line shows the GPS's own estimate of error. The gray, dotted line shows the sum of the GPS and Kalman position estimate errors.

Only four runs were completed. The first run had to be aborted because the robot got stuck near some rocks by the side of the road. Of the remaining runs, only the second run had an uncertainty at the goal below 5 meters. The other three runs had uncertainties of 10, 12 and 7 meters respectively.

In most cases the blue line showing the difference between the robot's own estimate of its position (as reported by the Kalman filter) and the position reported by the GPS is much larger than the error in the GPS estimate alone (dashed red line).

Still, the actual error between the Kalman filter estimate and the GPS position is always bounded by the sum of the error estimates of the Kalman filter and the GPS, indicating that the model correctly bounds the errors in the system.

Figure 47(a) shows the path planned by PUP, considering the uncertainty in position, the prior map and the available landmarks. Figure 47 (b) shows the actual path executed, in the first of the runs in Figure 1. The blue line is the Kalman filter position estimate, combining dead reckoning and detected landmarks. The green line is the position reported by the GPS (for reference only). Notice how the actual path differs significantly from the initial path in the top right corner of the trajectory. The onboard sensors detected that the path was blocked, and the planner calculated and alternate route that considered the prior map, the uncertainty in the position and the sensor readings.

Figure 48 (a) shows the path planned when uncertainty is not considered. Figure 48 (b) shows the actual path executed by the robot in the third of the runs from Figure 46. The blue line is the Kalman filter position estimate, using only dead reckoning. The green line is the position reported by the GPS (for reference only). Notice how the obstacles detected by the robot on the sides of the road are erroneously placed in the middle of the road on the prior map. Because of this discrepancy between the prior and the sensed data, the path that the robot follows is very treacherous.

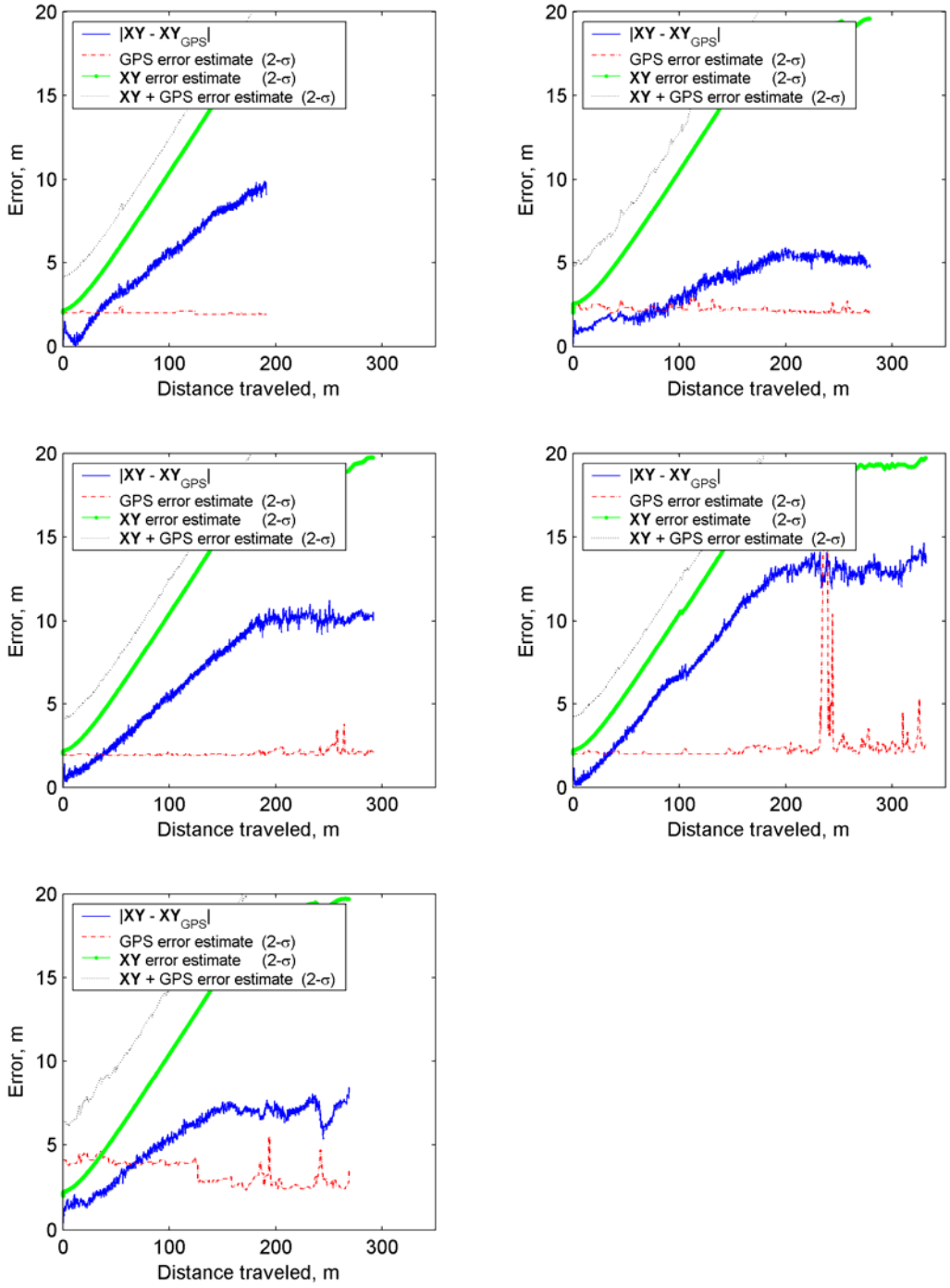

Figure 46. Error in the position of the robot in five different runs without using PUP. The blue solid line is the absolute error between the robot's own estimate of its position and the position reported by the GPS (used as ground truth). The red dashed line is the GPS 2σ error estimate (as reported by the GPS unit). The green solid line with dots is the 2σ error estimate of the Kalman filter considering only dead reckoning. The dotted gray line indicates the sum of the 2σ error estimate of the Kalman filter and the GPS 2σ error estimate.

(a) (b)

Figure 47. (a) Path planned considering uncertainty in position, with an uncertainty rate of 10%. (b) Path executed by the robot using dead reckoning and landmarks to follow the path planned. The blue line indicates the robot's own position estimate, and the green line indicates the position as reported by a WAAS GPS (for reference only)

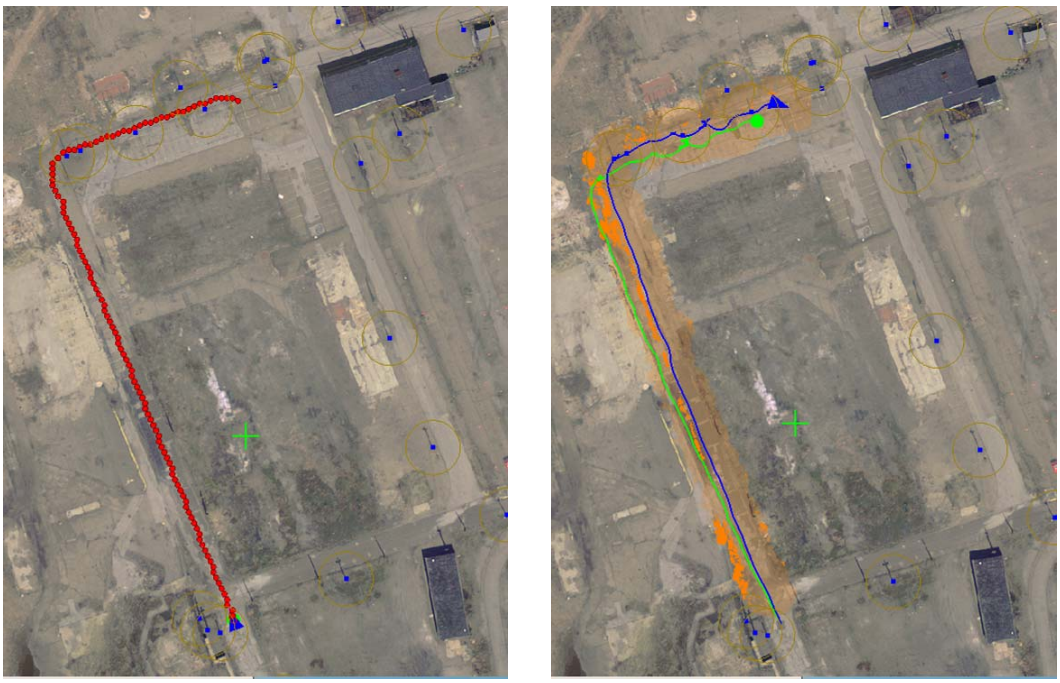

(a) (b)

Figure 48. (a) Path planned without considering uncertainty in position. (b) Path executed by the robot using only dead reckoning to follow the path. The blue line is the robot's own position estimate, and the green line indicates the position as reported by a WAAS GPS (for reference only)

Figure 49 shows the replanning times for the first of the runs using PUP. Replanning times were always less than 1.8 seconds and averaged 0.22 seconds with a standard deviation of 0.23 seconds. Figure 50 shows the same data displayed as a histogram where the horizontal axis is the replanning time and the vertical axis the number of instances for each planning time. Figure 51 is a cumulative histogram of Figure 50, where the y axis shows the percentage of cycles with replanning times less than the value on the x axis. For example, 80% of the planning cycles take less than 0.3 seconds, 90% take less than 0.5 seconds, and 99% of the cycles take less than 1 second.

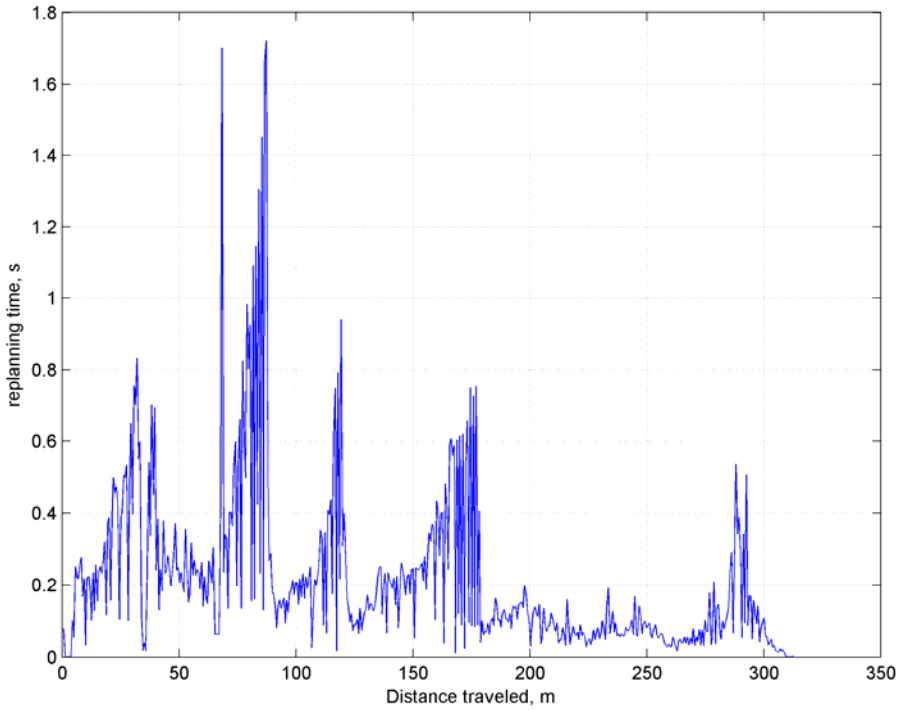

Figure 49.Replanning time during the first experiment using PUP.

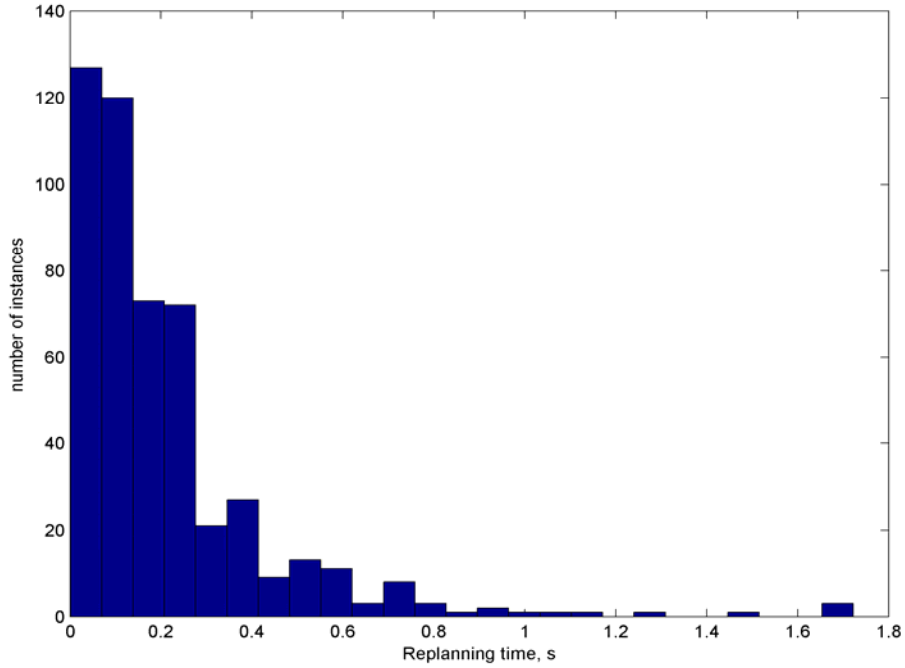

Figure 50. Histogram of replanning times during first run using PUP.

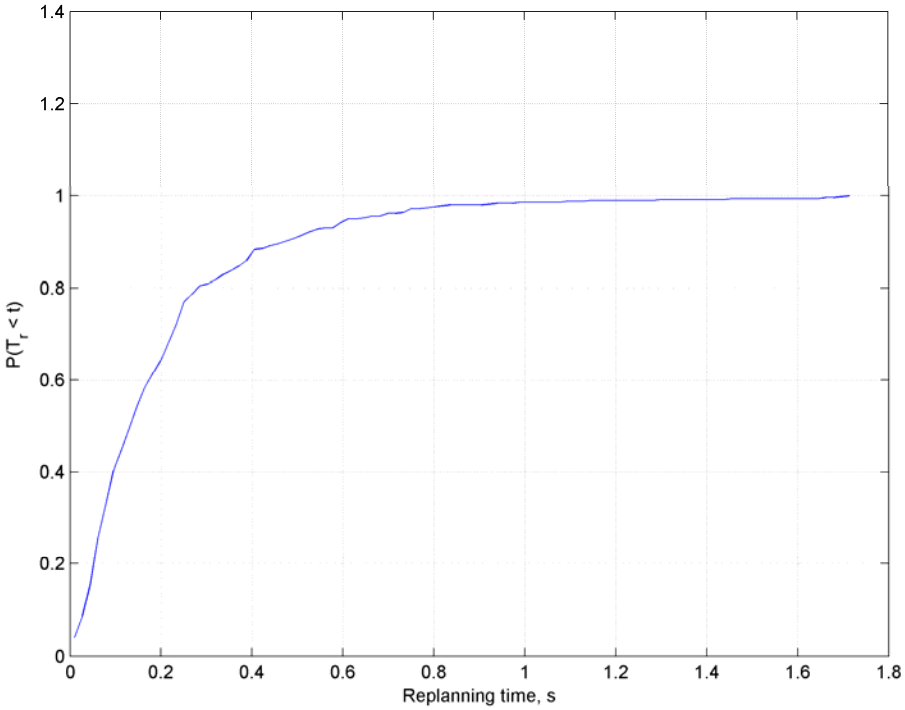

Figure 51. Cumulative histogram showing the probability of replanning time being smaller than the value on the x axis.

6.4.2 Long distance run

A single long distance run was also performed to test the ability of the approach to deal with larger worlds. The experiment setup was as follows: using a larger area of the same prior map as in previous experiments (450x350 cells, at 1 meter per cell), a start location was chosen such that the total path length would be of approximately 850 meters (Figure 52). Four artificial light poles were built and placed on the test site in order to make up for the lack of existing features in the west side of the test site.

Figure 52.Test layout for long distance run. The blue dots show the location of the landmarks. The blue triangle is the initial position of the robot. The size of the area shown is approximately 450x350 meters.

Figure 53 shows the path found by our algorithm. Notice how the path minimizes cost by staying on roads, and getting farther from known hazards when the uncertainty in position is large. The planner achieves this while visiting landmarks as needed to maintain low uncertainty. Also, notice that landmarks are only visited if they provide a significant cost reduction. For example the landmark in the bottom right corner is not

visited as the overall cost of visiting that landmark would be higher than going directly to the next landmark.

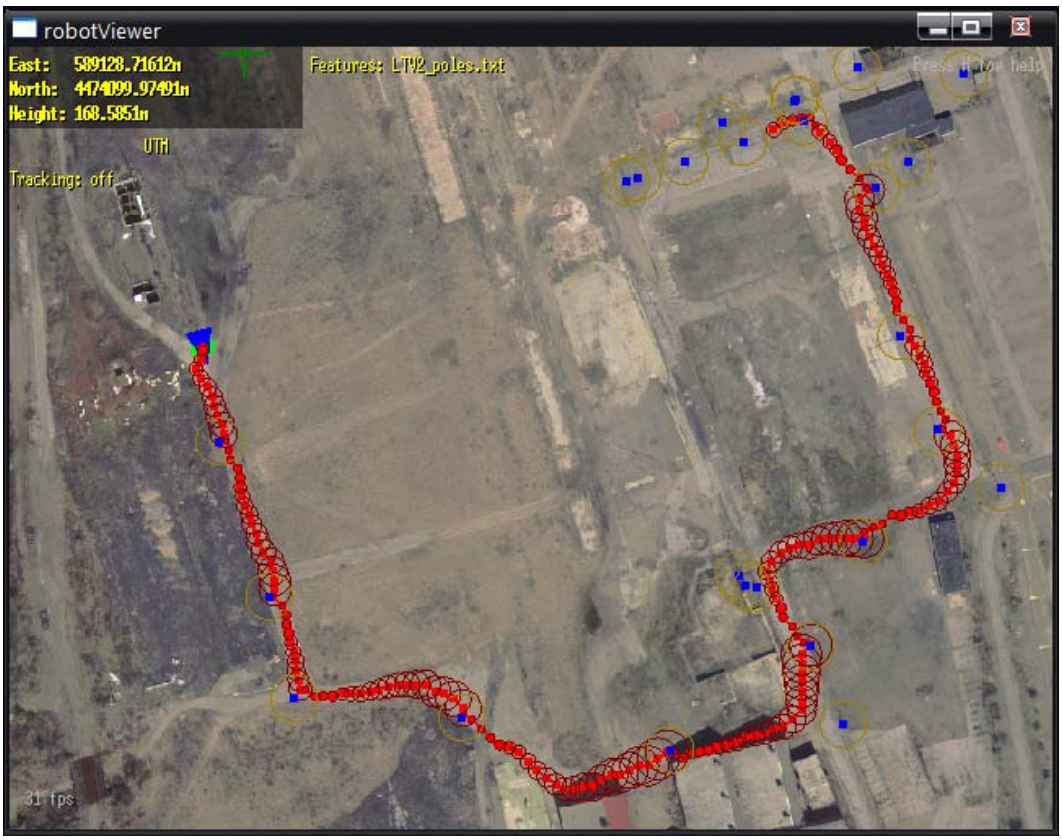

Figure 53. Path found by planner with uncertainty for long run.

Figure 54 shows the path executed by the robot. Notice how the actual path is very close to the initial path planned. Notice also how it differs significantly from the initial path in the top right corner of the trajectory (See detail in Figure 55). The onboard sensors detected that the path was blocked, and the planner calculated an alternate route that considered the prior map, the uncertainty in the position and the sensor readings.

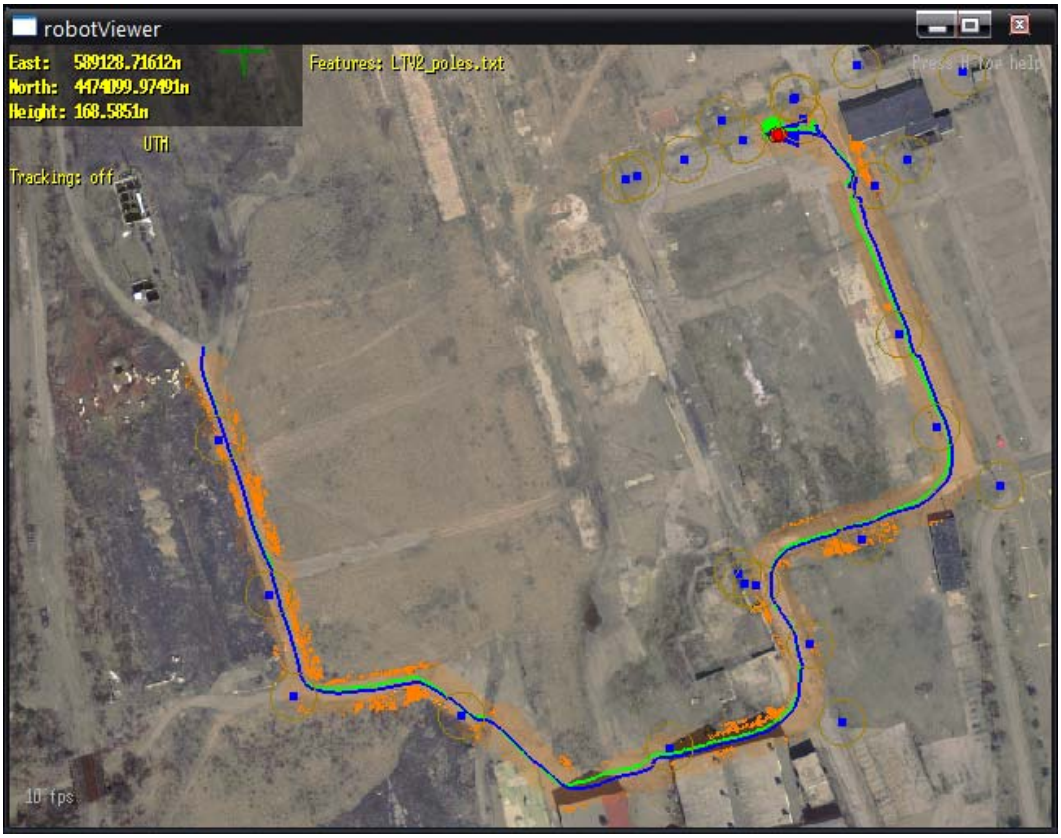

Figure 54.Path executed by robot during long distance run. The blue line shows the robot's position estimate according to the Kalman filter that combines dead reckoning and landmarks. The green line is the position reported by the WAAS GPS (for reference only)

Figure 55.Detail of the top-right area of the previous two figures. Notice how the actual path differs significantly from the initial path and, for example, goes to the left of the last landmark instead of following the original plan of going to the right. The onboard sensors detected that the path was blocked, and the planner calculated an alternate route that considered the prior map, the uncertainty in the position and the sensor readings

Figure 56 shows the different error estimates for the experiment. The blue line shows the difference between the position estimated by the Kalman filter and the position reported by the GPS. The green line shows the 2σ confidence interval for the position of the robot according to the Kalman filter. The red line shows the GPS's own estimate of error (which is about two meters for all runs). The gray, dotted line shows the sum of the GPS and Kalman position estimate errors.

In most cases the blue line showing the difference between the robot's own estimate of its position (as reported by the Kalman filter) and the position reported by the GPS is similar to the error in the GPS estimate alone (dashed red line).

The actual error between the Kalman filter estimate and the GPS position is always bounded by the sum of the error estimates of the Kalman filter and the GPS, indicating that the model correctly bounds the errors in the system

The uncertainty at the goal is approximately 2.5 meters, after traveling more than 850 meters. While there was no attempt to perform this run without using RPUP, the theoretical and experimental results shown before indicate that the error at the goal without RPUP would have been orders of magnitude larger. Furthermore, the if RPUP were not used, the prior map would be of little help once the error in uncertainty exceeds a few meters and the robot would have to depend only on onboard sensors to find its way to the goal. Instead, by using RPUP and a good prior map, we are able to navigate relatively long distance on a robot with very limited obstacle detection and avoidance capabilities.

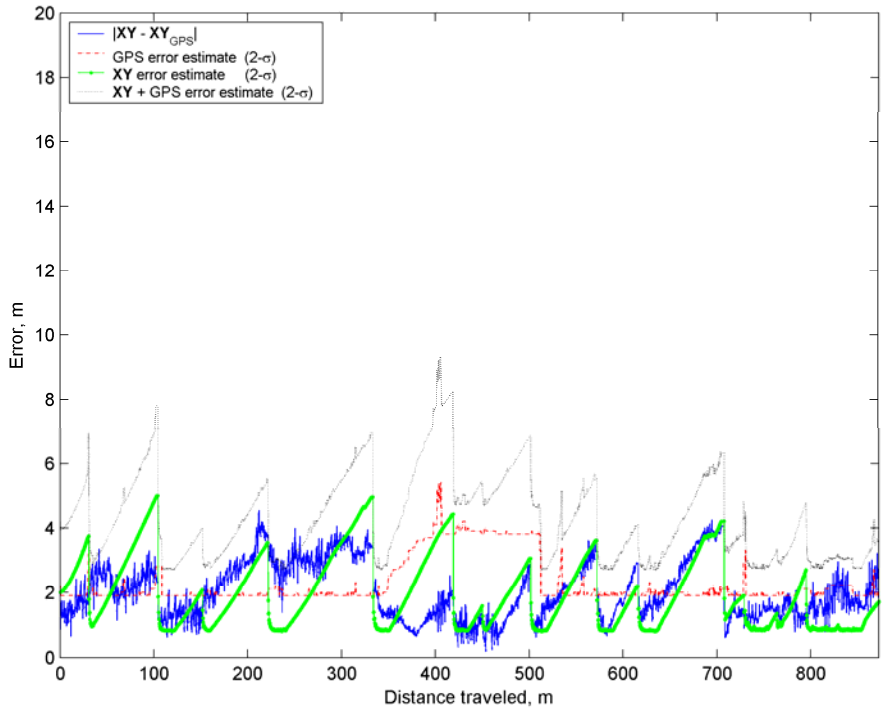

Figure 56. Error in the position of the robot in during long distance run using RPUP. The blue solid line is the absolute error between the robot's own estimate of its position and the position reported by the GPS (used as ground truth). The red dashed line is the GPS 2σ error estimate (as reported by the GPS unit). The green solid line with dots is the 2σ error estimate of the Kalman filter considering dead reckoning and landmarks. The dotted gray line indicates the sum of the 2σ error estimate of the Kalman filter and the GPS 2σ error estimate.

Figure 57 shows the replanning times for the long distance run. Replanning times were always less than 3.7 seconds and averaged 0.36 seconds with a standard deviation of 0.40 seconds. Figure 58 shows the same data displayed as a histogram where the horizontal axis is the replanning time and the vertical axis the number of instances for each planning time. Figure 59 is a cumulative histogram of Figure 58, where the y axis shows the percentage of cycles with replanning times less than the value on the x axis. For example, 80% of the planning cycles take less than 0.5 seconds, 90% take less than 0.8 seconds, and 92.6% of the cycles take less than 1 second.

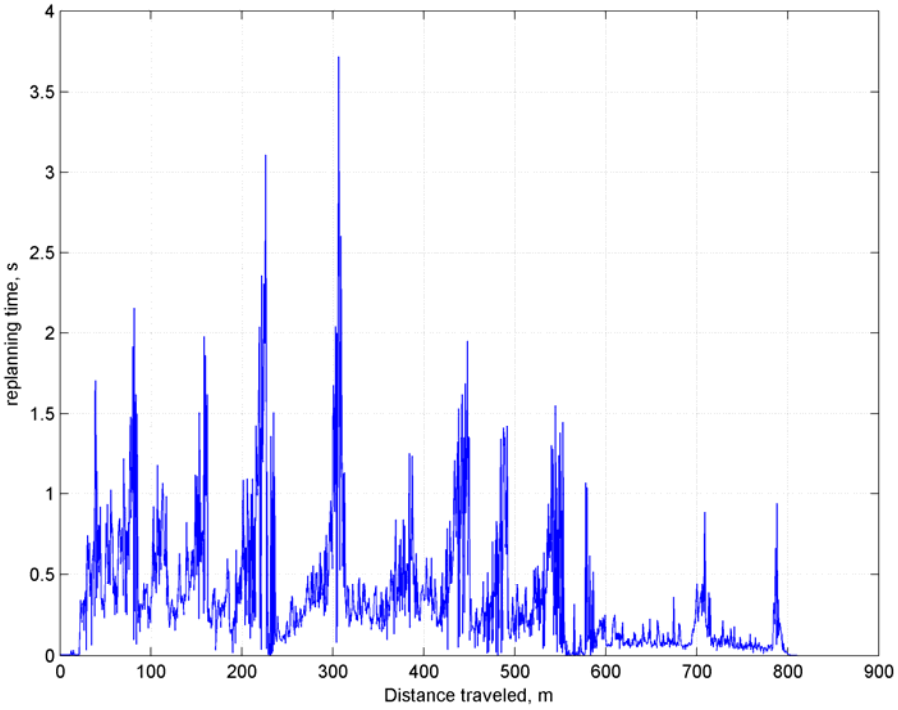

Figure 57. Replanning time during the long distance run using RPUP.

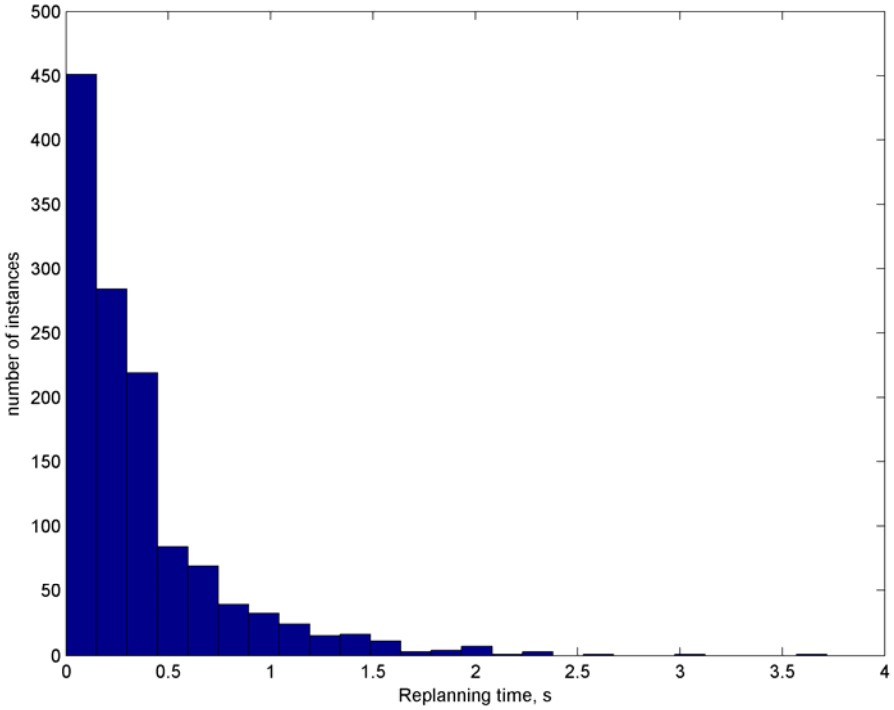

Figure 58. Histogram of replanning times during long distance run using PUP

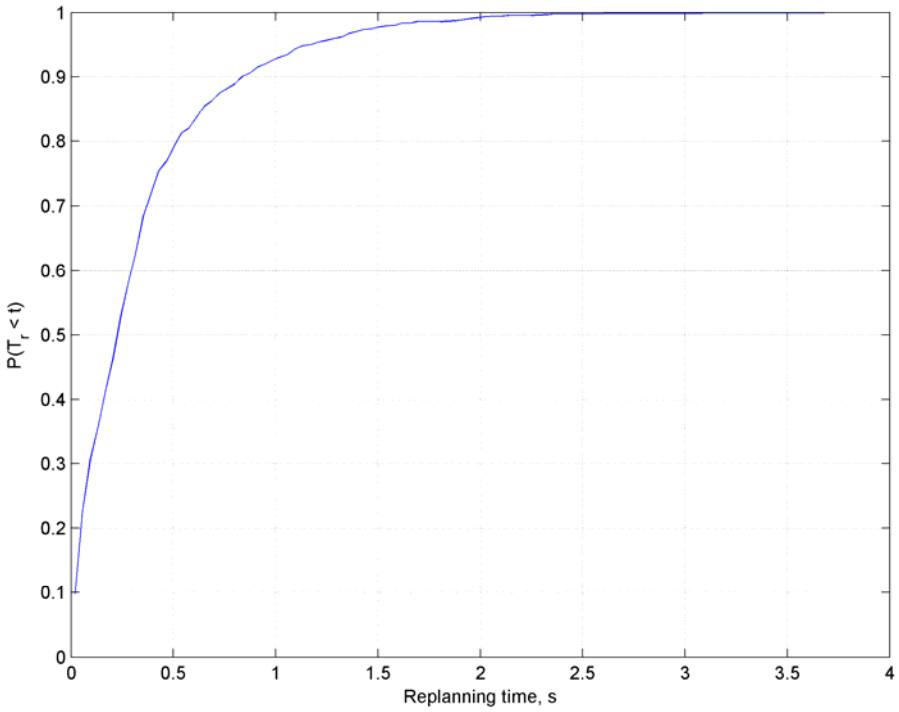

Figure 59. Cumulative histogram showing the probability of replanning time being smaller than the value on the x axis.

6.5 Discussion

The approaches presented here implement replanning within the framework of planning with uncertainty in position (PUP). This is a challenging problem as replanning for goal directed navigation requires planning backward from the goal, and many of the performance gains of PUP derive from using forward search. Two approaches are introduced. Replanning with prior map updates assumes that the updates come from source that is well registered with the prior map. Planning with sensor updates assumes that the updates are well registered with the robot, not with the prior map.

These approaches are validated through multiple simulations and field experiments. One of the field experiments is 850 meter long, and is to the best of our knowledge the longest traverse for an outdoor robot planning and navigating considering uncertainty in position and without the use of GPS.

6.5.1 Limitations

The approach proposed here handles two of the most common cases for data updates with uncertainty in position for mobile robot navigation. However, there are scenarios that fall between prior map updates and sensor updates which are not properly handled. One such scenario is if the robot were to revisit a previously sensed area. In this case, the uncertainty with respect to the previously sensed data is no longer negligible. The uncertainty in the old sensed data is not the same uncertainty as that of the prior map either. The correct way of dealing with old sensed data would be to keep track of the uncertainty of the robot with respect to each data point and to update this uncertainty as the robot moves. However this would be extremely inefficient, as all data points would change every time the robot moves.

Because the robot is assumed to be moving towards a goal, the scenario described above is not as critical as it would be for other tasks. In tasks that require sensed areas to be frequently revisited it is possible to discard sensed data after a given time or after some distance has been traveled. This would maintain the consistency of the data while keeping updates efficient.

6.5.2 Performance

The approach presented here for replanning has an average execution time that is at least two orders of magnitude faster than the approach presented in Chapter 5 for planning from scratch, which to the best of our knowledge is the fastest planner that considers uncertainty in position. Because replanning takes on average less than one second, this approach can be considered near-real-time: the planner can be implemented online incorporating real-time updates from the onboard sensors in the robot. This solves some of the problems with off-line planners that are limited to local obstacle avoidance when executing the original path.

There are, however, two important limitations in the performance of the algorithm. The first limitation is the processing time for the initial path, which can be as long as 25 minutes. While in principle all of these calculations could be performed off-line, it is more likely that only the computation of the expected costs for all uncertainties will be calculated off-line. This reduces the time to calculate the initial path to about 5 or 6 minutes, which enables a wider range of applications, but still may be a problem for scenarios requiring shorter set up time. The second important limitation is that the times reported in this chapter are average execution times. While in simulation and field tests execution times have usually been found to be very close to the results reported here, in theory it is possible for replanning to take even longer than the time required for the

initial path. Additional research is required to determine the suitability of our replanning approach to time-critical applications where there time constraints must be enforced.

Chapter 7

Planning with Uncertainty in Position using an Inaccurate Landmark Map or Imperfect Landmark Perception

The approaches presented in the previous chapters assumed that the landmarks could always be detected once the robot entered their *unique detection region*. A more realistic approach would be to allow the probability of detecting a landmark to be less than one. These imperfect landmarks can be caused either by inaccuracies in the map or by failures in the detection system.

The most general solution to planning with uncertainty in position using imperfect landmarks is to model the problem as a Partially Observable Markov Decision Process (POMDP). Within the POMDP formulation, the presence of a landmark can be modeled as a hidden variable, resulting in a policy that considers every possible combination of landmarks being present or not.

An exact solution of this POMDP would be intractable. However, some approximate solutions may produce results in an amount of time that would justify considering them.

7.1 PAO*

One of the approaches that were considered was PAO*, proposed by Ferguson *et al* [20]. In this approach most of the states in the environment have deterministic costs with the exception of a few *pinch points*. Pinch points are states that are important to the solution but whose costs are unknown (such as doors in an office environment). Instead of solving the complete POMDP problem defined by the deterministic plus non-deterministic states, PAO* has a high level graph of the unknown states and uses heuristics to determine which nodes to expand. When a node is expanded, a 2-D deterministic search is performed between the nodes involved. Using this combination of heuristics, deterministic states and pinch points, PAO* is able to find solutions to worlds with 200x200 deterministic states and 10 pinch points in less than one second on average.

Using PAO* with planning with uncertainty requires replacing the 2-D deterministic searches with paths planned considering uncertainty, and augmenting the 2-D pinch points with information about uncertainty.

However, adding uncertainty to PAO* would produce an algorithm that is not practical for large outdoor environments: PAO* starts by creating an adjacency graph containing the cost to travel between each pair of unknown cells (pinch point). This works well in 2-D search, where this graph is has $O(Np^2)$ entries (where N_p is the number of pinch points). When adding uncertainty, adjacency requires considering a third dimension N_u, and the number of entries now becomes $O(N_p{*}N_u)^2$. For typical problems, N_u is usually 100, therefore the number of entries in the adjacency graph is 10^4 times the number of entries in the 2-D adjacency graph, if we keep the number of pinch points constant. The average time to plan a path using PUP in a 200x200 world with 100 uncertainty levels and pre-computing the expected costs is about 0.2-0.3 seconds. Planning 10^4 paths would take between 30 and 50 minutes. For worlds of size 1000x1000 the average time to plan each path is between 10 and 12 seconds, and 10^4 paths would take approximately 30 hours. Additionally, the number of pinch points is likely to depend at least linearly with the dimensions of the world (or quadratically with its area). This is likely to increase the time to solve the adjacency graph to about 750 hours. Even if PAO* only required to solve 1% of this graph, the processing time is likely to be in excess of 7.5 hours.

Furthermore, the existing limitations of PAO* also would carry over an implementation that considered uncertainty. The size of the information space represented by PAO* is $m \cdot n \cdot 3^{N_p}$, which quickly diverges as N_p increases. While PAO* has numerous optimizations and only considers the hidden state elements, the exponential dependence on the number of pinch points is still an important limiting factor for this algorithm, especially when applied to large environments.

7.2 PPCP

Another approach considered was Probabilistic Planning with Clear Preferences (PPCP), by Likhachev and Stentz [63]. PPCP is an anytime algorithm for problems with hidden states that is applicable when it is clear what values of the missing information would result in the best plan. Planning with uncertainty in position is one of such problems, as the preferred outcome of each sensing attempt is for the landmark to be successfully detected. PPCP solves the underlying POMDP through a series of 2-D searches, bypassing planning in the full belief state-space altogether. As a result, the complexity of each search is independent of the number of pinch points and the number

of searches before convergence typically grows linearly or sub-linearly with the number of pinch points. However, PPCP can only guarantee optimality under certain conditions.

PPCP works as follows. A backward A*-like search is performed, incorporating at each point the cost to the goal under the preferred outcome and the best estimate of the non-preferred outcome. After the initial policy is calculated, each of the non-preferred outcomes are calculated by performing successive backward searches with a modified environment in which different unknown cells are set to the non-preferred outcome. While the algorithm can provide a policy as soon as the initial policy is computed, latter policies will have better results and higher confidence.

In order to create a version of PPCP that considers uncertainty in position, each 2-D search has to be replaced by a 3-D backward search considering uncertainty. The complexity of this search is comparable to that of the initial search required when planning the initial path in replanning with uncertainty in position, which is $O(N_x \cdot N_y \cdot N_u \cdot \log(N_x \cdot N_y \cdot N_u))$. For environments of size 1000x1000 with 100 uncertainty levels the time required to plan a path is in the order of 25 minutes. Each successive iteration is likely to take slightly less time, but still the total time for the policy to converge is likely to be a few hours, depending on the number of landmarks. While this is much better than any other POMDP-based approach, is not practical for most outdoor applications, since the prior map is only a rough estimate of the actual terrain and significant changes in the environment would have to be included at run-time based on sensor information.

7.3 Optimistic planning combined with replanning

The approach presented in Chapter 6 can be modified to deal with imperfect landmark maps or imperfect landmark detection. Using this approach, the initial path is planned still assuming that all landmarks will be detected. As the robot moves along the path, if a landmark is not found (either because it was removed or because it cannot be detected by the perception system), the path can be re-planned using the updated knowledge about the world that the landmark is not present.

The missing landmark is removed from the prior map as soon as the robot fails to detect it. Under this assumption all cells within the detection region of the missing landmark (at all uncertainty levels) are updated and new rhs values calculated.

The following is an example of replanning being used to handle missing landmarks. Figure 60 shows a sample world with four landmarks (+ signs), their detection regions (blue areas) and varying cost values. Lighter gray colors indicate lower cost areas, and darker gray indicate higher cost. Non-traversable areas are marked in green. The blue line

indicates the lowest cost path to go from the start to the goal while considering uncertainty. The purple circles show the 2σ uncertainty contour at each step along the path. As in previous chapters, this initial path is calculated assuming that all landmarks will be detected. The expected cost of this path is 1132.

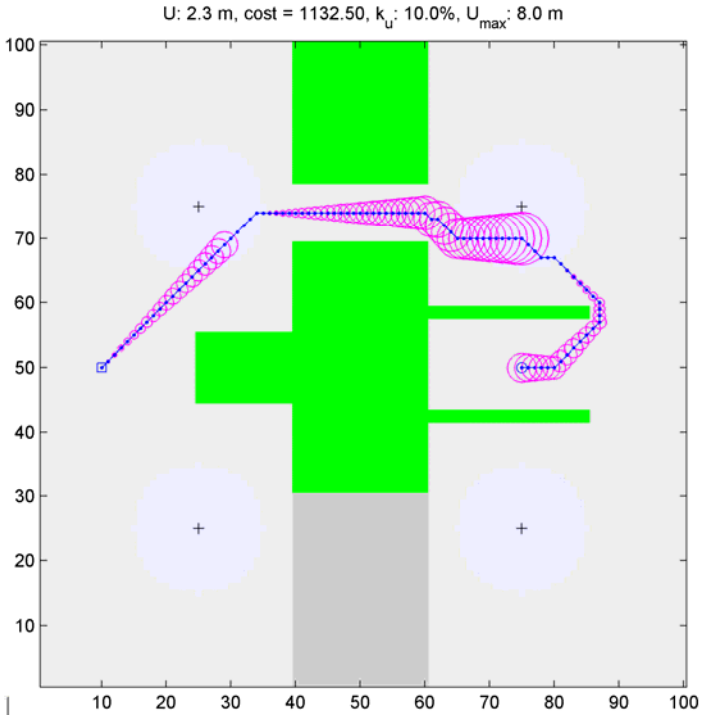

Figure 60.Initial path planned assuming all landmarks will be detected

Let us assume that the landmark in the top left corner is no longer present. When the robot reaches the detection region for the landmark it realizes that the landmark is missing and re-plans a path that no longer includes this landmark. Figure 61 shows the resulting path after replanning. The cost of this path is $C_{\sim Lg} = 2208$.

In order to understand the quality of this solution, let us analyze the different options that could have been chosen when the initial path was planned. A planner able to reason about the probability of a landmark not being present (such as PPCP) would have considered the two possible outcomes when the robot reaches the first landmark. The outcome of the landmark not being present is the one shown in Figure 61. The other possible outcome is for the landmark to be detected, shown in Figure 62. The expected cost of this path is $C_{Lg} = 851$. The overall expected cost of including the first landmark in the path is given by

$$C_{Log} = C_{oL} + p \cdot C_{Lg} + (1 - p) \cdot C_{\sim Lg} \tag{7.1}$$

Where p is the probability of detecting the first landmark, $C_{Lg} = 851$ and $C_{\sim Lg} = 2208$ are the costs explained above, and $C_{oL} = 282$ is the expected cost to reach the first landmark.

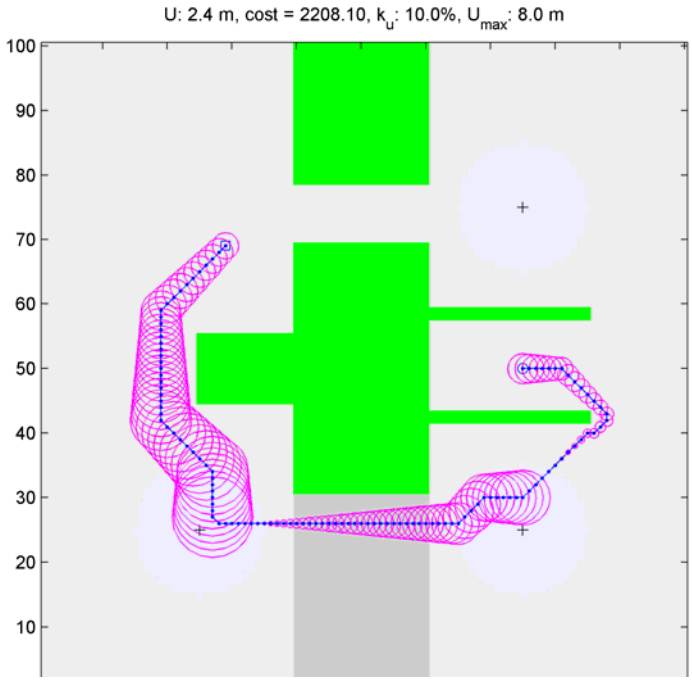

Figure 61.Resulting path after replanning when the robot fails to detect the landmark in the top left corner.

Additionally, the planner would have to consider any alternate routes that would avoid the first landmark altogether. While there are many alternate routes, the one with the lowest expected cost is the one shown in Figure 63. This path is calculated by assuming that the landmark in the top left corner is absent from the prior map when the initial path is calculated. The expected cost of this path is $C_{\sim Log} = 1979$.

As long as $C_{Log} \leq C_{\sim Log}$, the optimistic path that assumes that the landmarks will be detected will find the same path than an algorithm such as PPCP that considers all possible options. In this particular example $C_{Log} \leq C_{\sim Log}$ if $p > 0.37$. While it is not feasible to have a general rule to determine when the optimistic planner will be sufficient, in most scenarios where there is a high probability of detecting a landmark then the optimistic planner will be optimal or near-optimal.

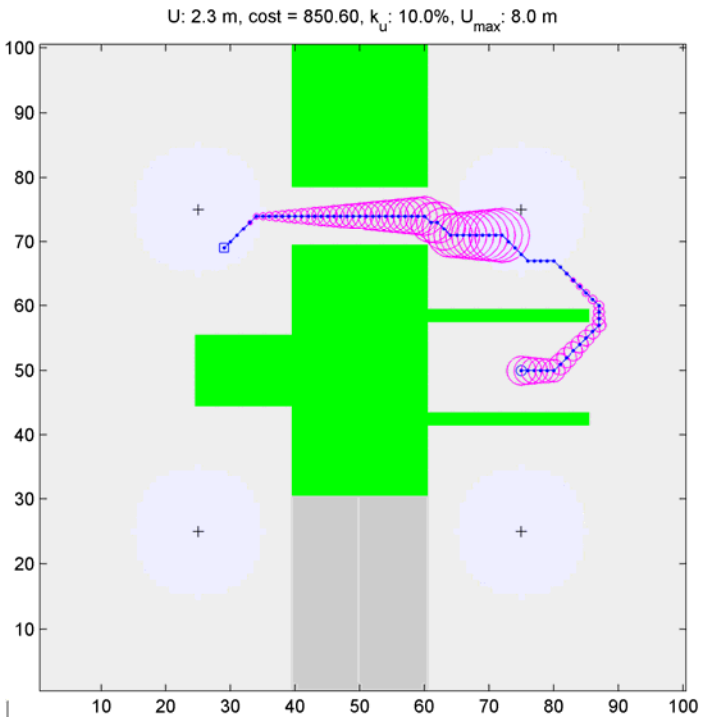

Figure 62. Resulting path after re-planning if the top left landmark is successfully detected

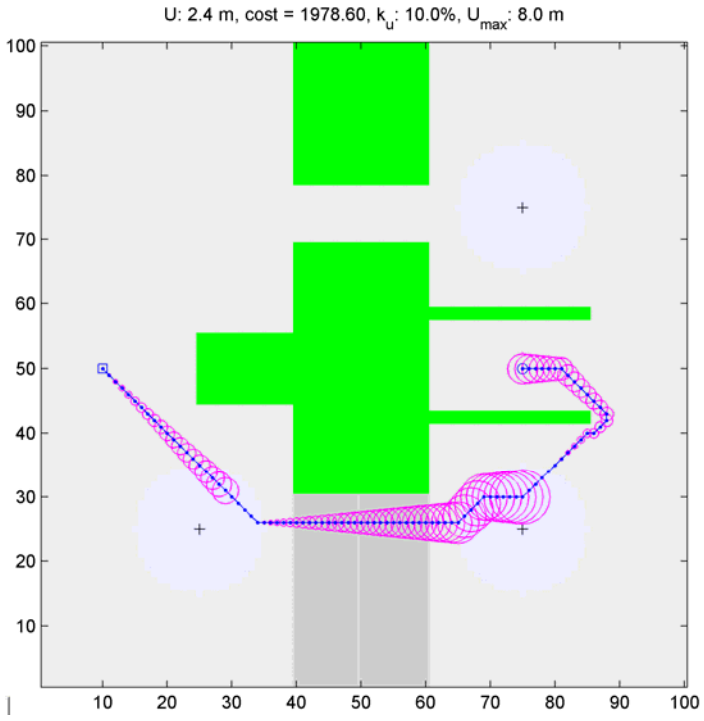

Figure 63. Initial path calculated under the assumption that the top left landmark is not present.

7.4 Planning with uncertainty in position guaranteeing a return path

While optimistic planning combined with replanning is often sufficient to deal with inaccurate landmark maps or imperfect landmark perception, there are cases where this approach fails. In the example from the previous section, if the landmark in the top right corner is not detected, the robot will be unable to reach the goal and will also be unable to go back to the start location or to any other landmark (with uncertainty smaller than the detection range)

Planning with Uncertainty in Position Guaranteeing a Return Path (PUPGR) calculates paths that guarantee that the robot will be able to return to the start location or to the last detected landmark if any landmark is not detected.

The approach works as follows. Using the same backward search as in Replanning with Uncertainty in Position (RPUP), we add a new parameter in the state space called *return uncertainty*(ε^{ret}). At the goal location (which is the start of the backward search), the return uncertainty of each cell is set to the same value as the cell's uncertainty:

$$\varepsilon_0^{ret} = \varepsilon_0 \tag{7.2}$$

As cells are expanded, both uncertainty values are updated. The regular uncertainty value is updated using:

$$\varepsilon_{k+1} = \varepsilon_k - \alpha_u d(\boldsymbol{\mu}_k, \boldsymbol{\mu}_{k+1}) \tag{7.3}$$

and the return uncertainty is updated using

$$\varepsilon_{k+1}^{ret} = \varepsilon_k^{ret} + \alpha_u d(\boldsymbol{\mu}_k, \boldsymbol{\mu}_{k+1})\,. \tag{7.4}$$

Then the expected cost to travel a cell is calculated, but instead of using only the cell's uncertainty, we now use a weighted average between the current path and the return path. For example, if the probability of using the return path (which is the probability of not detecting a landmark) is *1-p*, the expected value would be computed as

$$E_{GR}(x_k, y_k, \varepsilon_k, \varepsilon_k^{ret}) = p \cdot C_E(x_k, y_k, \varepsilon_k) + (1-p) \cdot C_E(x_k, y_k, \varepsilon_k^{ret}))\,. \tag{7.5}$$

The planner is therefore optimizing not the cost to go from the start to the goal, but the cost to go from the start to the goal and return following the same path, assuming a probability of p for the main path and a probability of (1-p) for the return path.

The *return uncertainty* also affects the way in which *unique detection regions* are processed. When using PUPGR a cell is considered to be inside a *unique detection region* if the circle of radius ε^{ret} is completely contained within the detection region. This is a stronger condition than having the circle of radius ε completely contained within the detection region, since $\varepsilon^{ret} \geq \varepsilon$. The resulting path is a path that guarantees that when moving between each pair of detection regions (*i,j*), it would be possible to return to the initial landmark i if the destination landmark j is not found or is not reachable.

Figure 64 shows the path found by PUPGR for the sample world described in the previous section. Notice how the top path is no longer chosen because it cannot guarantee a return path if the landmark in the top right is missing. The path found by PUPGR has an expected cost of 2145, almost twice the expected cost of the optimistic path. However, this path guarantees that if any of the landmarks along the path is not detected, the robot will be able to go back the previous detected landmark and to the start location.

Because PUPGR is implemented within the framework of RPUP, it allows very fast replanning, especially when using sensor updates.

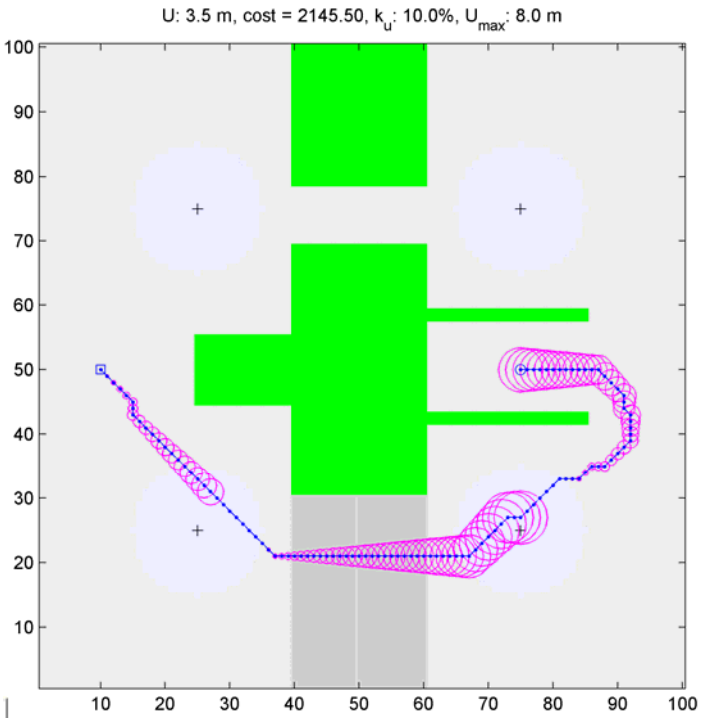

Figure 64. Path found using PUPGR. If any of the landmarks along the path are not detected, the robot always has a path to return either to the start location or to the last detected landmark.

7.5 Discussion

The approaches presented here allow a robot to plan paths considering uncertainty in position and using imperfect landmarks or imperfect landmark perception. We show that by modifying RPUP to replan when landmarks are not detected is often sufficient to deal with imperfect landmarks. This approach is called Optimistic Planning with Replanning as it first assumes that all landmarks will be detected. Optimistic Planning, however, can

lead to suboptimal paths. More importantly, it can also have the robot follow a path from which there is no return if a landmark is not detected. Planning with Uncertainty in Position Guaranteeing a return path improves on the Optimistic Planning approach by ensuring that the robot always has a return path if a landmark is missed. Both approaches allow for fast replanning when new sensor information is acquired.

The approaches presented here are likely to be much faster than any existing POMDP-based approach such as PPCP or PAO*. While no direct comparisons are available, the computational complexity estimates indicate that PUPGR is likely to be at least one order of magnitude faster than either PAO* or PPCP. In replanning mode (after the initial path has been calculated), PUPGR is likely to be two or three orders of magnidude faster than either PPCP or PAO*.

However, PUPGR also has important shortcomings. One of the most important limitations is that the planner is only considering the alternative that the robot will return along the same path it followed moving forward. It would be desirable to consider returning along a different path, or even moving forward if the probability of detecting the next landmark is high enough. While some of these alternatives could be implemented in the solution without resorting to a full POMDP solution, they would have significant implications for the performance of the algorithm.

In spite of having an overly simple model of the alternatives available, the ability to incorporate new sensor data into the path and replan quickly makes up for many of the shortcomings of the approach.

Chapter 8

Planning with Uncertainty in Position using Linear Landmarks

The main limitation of using point features for localization is that they can only be reliably detected when the uncertainty in the position of the robot is smaller than the sensor range of the vehicle. Typical sensing ranges for features such as trees and electric poles are in the order of tens of meters, which only allows for a few hundred meters of travel between landmarks. For example, with a sensing range R=10 m and an uncertainty rate k_u=10%, the maximum distance that the robot can travel without finding a landmark is $D_{\max} = R / k_u = 100\,m$.

$$D_{\max} = \frac{R}{k_u} = 100m \tag{8.1}$$

If the landmarks are spaced more than $D_{\max}$ the planner cannot use them to reduce the uncertainty in the position because their detection becomes unlikely.

In contrast, other types of landmarks can be reliably detected over greater ranges. A linear landmark such as a wall, for example, can be detected reliably over all its extent. A 100 meter wall could be detected even with an uncertainty of 50 meters. Linear landmarks are also often more widely available than point landmarks: man-made structures such as walls and roads are linear landmarks that can be easily identified in aerial images. Some geographic features such as rivers and ridges also constitute linear landmarks that can be easily identified from aerial images.

Features such a tree lines can be either point or linear landmarks, depending on the size of the robot, the scale of the map, and the separation between the features. Features with a separation smaller than the range of the vehicle can be treated as either linear features or point features. If the uncertainty of the robot when approaching the features is low, they can be used as point features and can provide complete localization. If the uncertainty of the robot when approaching the features is high, they can be used as linear features, therefore extending the range of the vehicle and allowing a longer range detection than its use as point features would allow.

We propose an approach called Planning with Uncertainty in Position using Linear Landmarks (PUPLL) that enables the use of linear landmarks for localization when planning with uncertainty in position. This approach uses forward propagation of the full (x,y,θ) covariance matrix, combined with a binning function to reduce the dimensionality of the search space. While this approach cannot guarantee optimal paths, we show that on most problems it finds optimal or near optimal solutions.

This chapter is structured as follows. We will first discuss the topology of the search space when using isometric uncertainty propagation. This provides important insight on the problem and will help explain some of the approximations proposed later in the chapter. We then explain how to propagate the full covariance matrix during the path planning process. This includes our approach to reduce the dimensionality of the search space and other approaches that have been proposed subsequently. We then discuss the effects of linear landmarks in the covariance matrix and show some performance results for the algorithm.

8.1 Planning with uncertainty in position with full covariance propagation

In order to use linear landmarks for planning with uncertainty a different error propagation model is required. Instead of the single-parameter simplified error propagation model described before, the full uncertainty propagation model from section 2.1.1 is now required:

$$\mathbf{P}(k+1) = \mathbf{F}(k) \cdot \mathbf{P}(k) \cdot \mathbf{F}(k)^T + \mathbf{L}(k) \cdot \mathbf{Q}(k) \cdot \mathbf{L}(k)^T \tag{8.2}$$

This model has 9 parameters for the covariance matrix P, of which 6 are independent. A complete planner that included P in its state space would require 8 dimensions (6 from P plus x and y), which is beyond the practical limits of most deterministic planners.

8.1.1 Using entropy to reduce the dimensionality of the search space

A planner in 8-dimensions is not practical for outdoor environments. The x and y dimensions of the planner alone can be in the order of 1000x1000=10^6 cells, and even as little as 10 cells in each of the additional dimensions would create a planner with $10^6.10^6=10^{12}$ cells.

We propose an alternative approach that performs a forward search containing the full covariance matrix and stores this result in a bin calculated by a single-number summary statistic [31]. The binning function then defines equivalency classes for P, and should be selected such that it is able to separate significantly different values of P.

This approach does not explicitly quantize P, as the full covariance matrix is propagated in each state expansion. The quantization of P takes place indirectly, when two nodes within the same bin are compared.

Let us revisit the isometric Gaussian case (1-D uncertainty representation) in order to understand how this quantization takes place. In the 1-D case, a node dominates another node if

$$(\mathbf{r}_i \trianglerighteq \mathbf{r}_j) \Leftrightarrow (\mathbf{q}_i = \mathbf{q}_j) \wedge (L^*(\mathbf{r}_o, \mathbf{r}_i) \leq L^*(\mathbf{r}_o, \mathbf{r}_j)) \wedge (\sigma_i \leq \sigma_j) \tag{8.3}$$

When comparing two nodes i and j from different bins, if i dominates j, j is deleted with no loss of information (since node i is better in cost and uncertainty). Likewise, if j dominates i, i is deleted with no loss of information. If neither one dominates, both nodes should be preserved, as one has better cost, and the other one has better uncertainty. Since each one is in a different bin, both nodes can be preserved, and no information is lost.

When comparing two nodes from the same bin, a similar process takes place. If one of them dominates the other, the dominated one is deleted and no information is lost. However, if neither one dominates, both nodes cannot be preserved. Since there is only one bin space available, only the node with lower cost is preserved, even if its uncertainty is higher. Only in this case information is lost, and some form of quantization takes place. We call this event a *collision*, and its likelihood can be made arbitrarily small by reducing the size of the quantization step in the uncertainty dimension.

The extent to which quantization affects the resulting path depends greatly on the topology of the search space. For example, if the search space is homeomorphic with the xy plane as in the example above, the planner is able to find the optimal solution no matter how large the uncertainty bins are. More frequently, however, the impact of quantization in the solution is seen when we try to achieve a certain uncertainty ε at the goal. In this case, the planner is only able to achieve such uncertainty within the tolerance of the bin size. For our experiments we use a bin size equal to the uncertainty rate, which is less than 10% of distance traveled. If the cell size is 1 meter and the uncertainty rate is 10%, the uncertainty bins are 0.1m each, which is ten times higher resolution than the world representation. While it is possible to find problems in which this resolution is not sufficient, it can be argued that such problems should not be represented on a 1-meter grid.

To generalize this analysis to the covariance matrix case we need to first extend the definition of state dominance to include covariance:

$$(\mathbf{r}_i \trianglerighteq \mathbf{r}_j) \Leftrightarrow (\mathbf{q}_i = \mathbf{q}_j) \wedge (L^*(\mathbf{r}_o, \mathbf{r}_i) \leq L^*(\mathbf{r}_o, \mathbf{r}_j)) \wedge (\Sigma_i \leq \Sigma_j) \tag{8.4}$$

As in the 1-D case, when comparing two states that are in different bins, there will be no loss of information (or quantization). The covariance matrix is calculated as a forward transformation and its full precision is preserved.

Likewise, when comparing two states that are in the same bin, no quantization will take place as long as one state dominates the other. The only case where information is lost and quantization effectively takes place is when comparing two states that belong to the same bin but that have no dominance relationship between them (a *collision*). As in the 1-D case, the state with lower cost is preserved and while final solution may no longer be optimal. Unlike the 1-D case, the likelihood of such *collision* not only depends on the size of the quantization step, but also on the choice of binning function.

A natural binning function to use is entropy, which has been successfully used in related approaches such as Roy and Thrun's [79]. Entropy is proportional to the product of the major semi-axis of the covariance matrix *P.* This binning function effectively clusters together covariances with similar dimensions, and differentiates those that have significant differences in their semi-axes. In most environments this works very well, although it is not possible to guarantee that collisions will not take place.

As in the 1-D case, the extent to which quantization affects the resulting path depends greatly on the topology of the search space. In some cases there will be no effect at all. More frequently, the impact of quantization in the solution will be seen when we try to achieve a certain uncertainty ε at the goal. In this case, the planner will only be able to achieve such uncertainty within the tolerance of the bin size.

While many other binning functions can be used, we have found that entropy produces optimal or nearly optimal results in large sets of problems analyzed. It also preserves the topology of the search space, allowing for fast queries to find neighbors.

8.1.2 Using incremental binning to preserve all dimensions

Recently Censi [14] proposed an approach for planning with uncertainty in position that allows finding minimum time or minimum covariance paths while preserving all parameters from the covariance matrix. In theory, this approach avoids quantizing the covariance matrix by using state dominance to discard unnecessary nodes, and preserving all other nodes for a given *(x,y)* location. In practice, this approach requires a finite tolerance σ_{TOL} when comparing matrices, which should be selected to be as small as possible. The author utilizes a tolerance between 1 and 5 mm. While this small tolerance is apparently insignificant, it has important theoretical and practical implications.

From a theoretical point of view, the need for this tolerance implies that rather than using a continuous representation of P, this approach is incrementally binning P in

arbitrarily small steps and defining equivalency classes of covariances that have semiaxes within σ_{TOL} of each other.

From a practical point of view, the selection of this tolerance greatly affects the performance of the algorithm. By selecting an arbitrarily small σ_{TOL} it is possible to plan with arbitrarily high resolution in the representation of *P.* However, very small values of σ_{TOL} cause the number of states at each *xy* location to increase rapidly, therefore significantly increasing the complexity and space requirements of the algorithm.

8.1.3 Combining entropy and incremental binning

The approaches described above have important strengths and weaknesses, some of which are complementary.

The main weakness of using entropy is the possibility of *collisions.* This happens, for example, when comparing two ellipses with identical semiaxes but that are rotated with respect to each other. In this case, the ellipses have the same entropy (and belong to the same bin), and the higher cost one is discarded even if it is not dominated.

The main weakness of incremental binning is that the size of the search space is not known a priori, and that it can become arbitrarily large depending on the complexity of the environment and the selection of σ_{TOL}. As the search space becomes larger, the complexity of the algorithm also becomes increasingly large. This is most noticeable in continuous cost worlds, where more alternatives are available and less pruning takes place.

We propose an approach that combines both approaches by performing a primary binning based on entropy, and then a secondary incremental binning. We define an explicit equivalence relation between covariances such that:

$$\Sigma_i \sim \Sigma_j \Leftrightarrow (\Sigma_i \leq \Sigma_j') \wedge (\Sigma_i' \geq \Sigma_j) \tag{8.5}$$

where

$$\Sigma' = \mathbf{Q}_j \begin{bmatrix} (\sigma_1 + \sigma_{TOL})^2 & 0 & 0 \\ 0 & (\sigma_2 + \sigma_{TOL})^2 & 0 \\ 0 & 0 & (\sigma_3 + \sigma_{TOL})^2 \end{bmatrix} \mathbf{Q}_j^{-1}$$

is a version of Σ in which each eigenvalue has been enlarged by σ_{TOL} (the "grow" operator described by Censi in [14]).

Rather than having only one node at each bin, each bin $q(x,y,\varepsilon)$ is allowed to hold up to n_Q nodes. If there is a *collision* between two nodes i and j at bin $q(x,y,\varepsilon)$, then their covariances are compared. If they are equivalent, the one with the lowest cost dominates and no information is lost up to a resolution σ_{TOL}. If they are not equivalent, the second

node is added to the bin. If another node k also has *collision* at bin $q(x,y,\varepsilon)$, the covariance of this new state is compared with the covariances of i and j. If neither $\Sigma_i \sim \Sigma_k$ or $\Sigma_j \sim \Sigma_k$ then this node is also added to bin. This process is repeated until n_Q nodes have been added to bin $q(x,y,\varepsilon)$. At this point, any further nodes with the same bin $q(x,y,\varepsilon)$ that have higher cost and no dominance relationship will be discarded (in a similar way as the entropy-based approach). Only at this point would a collision cause loss of information and could compromise optimality. This approach is resolution-optimal if no bins in the search exceed their capacity.

There are two design parameters that significantly affect the performance of the algorithm: n_Q and σ_{TOL}. In general, smaller values of σ_{TOL} imply higher resolution, longer execution times, and require larger values of n_Q. Finding the optimal values for these parameters is an open question. Experimentally, the following approach has shown very good results: σ_{TOL} is initially set to the uncertainty rate α_u for each bin $q(x,y,\varepsilon)$. Every time a new node is added to the bin, σ_{TOL} is doubled. Using this combined with an n_Q of 8 usually prevents exceeding the capacity of the bins and produces results equivalent to those found by incremental binning at much smaller σ_{TOL} values.

By combining entropy and incremental binning, this approach is able to limit the size of the search space in a sound manner that produces results at least as good as those produced by entropy alone. It also preserves the topology of the search space to a great extent, which is useful for neighborhood queries and other applications.

8.1.4 Other recent approaches

Other approaches have also been proposed recently, addressing some of the elements of planning with uncertainty in position.

Most of these recent approaches are limited to indoor environments. Most are also based on sampling-based planning techniques such as Probabilistic Road Maps (PRMs) or Rapidly exploring Random Trees (RRTs). PRMs and RRTs are well suited for solving some aspects of planning with uncertainty in position with full covariance propagation. Both handle multi-dimensional spaces well because of their sparse representation of the world. However, sampling-based techniques usually don't handle continuous-cost domains well, although some approaches such as hRRTs, proposed by Urmson [98], have tried to address this shortcoming with some success. Even with extensions such as hRRTs, sample-based planner are usually unable to provide the same optimality and completeness guarantees that grid-based planners do.

Missiuro and Roy's [69] approach addresses the problem of uncertainty in the position of obstacles, by replacing obstacle's vertices with Gaussian distributions. The approach, however, does not handle continuous-cost domains and does not model the uncertainty accrued while moving. Burns and Brock [11] extend Missiuro and Roy's approach to

enable the use of an arbitrary obstacle representation and many degrees of freedom. Their implementation is targeted to articulated robots. Alterovitz *et al.* [2][3] introduce the idea of a Stochastic Motion Roadmap (SMR), to steer surgical needles. The trajectory of these needles is uncertain to some extent because the tissue in which they are inserted is not completely known. However, the problem is formulated as one of avoiding binary obstacles while considering the non-holonomic constraints of the needle. Similarly, Pepy and Lambert [74] use RRTs to find safe paths considering uncertainty. Their approach uses a Kalman Filter to estimate the evolution of uncertainty and to model the effect of localization in the planning process.

Melchior *et al* [65][66] have also recently proposed an approach that uses RRTs to propagate a full covariance matrix while planning with uncertainty in position for outdoor environments. This approach is able to handle multiple hypotheses in the outcome of an action as it uses an approach similar to a particle filter to model the evolution of uncertainty during the search process. Because of this model, the planner is not limited to solving problems with low uncertainty rate. Although the approach includes a biasing term to avoid high cost regions using hRRTs [98] its results don't attempt to optimize cost. The goal is more to minimize the end error rather than to minimize the expected cost. The approach is also more tailored for short traverses, and it is unclear how well it would scale to larger environments.

8.2 Localization with linear landmarks

Although there are many types of linear landmarks, we will only focus on straight linear landmarks in order to simplify the problem and to maintain the Gaussian distribution assumption. In the limit, however, these straight piecewise linear landmarks can approximately represent any curve.

The information provided by this type of linear landmarks is not as rich as that of point landmarks. A linear landmark provides accurate information along one direction (perpendicular to the feature), but very little –if any- information along the direction parallel to the feature. They can also provide information about heading, but this information is often very noisy. Since the heading errors assumed by our approach are very small, we will not assume that linear features provide meaningful heading information.

In general, localization with a linear feature can be seen as a projection of the covariance matrix onto the localizing feature, or a marginalization of $p(x,y,\Sigma)$ along the direction n locally normal to the linear feature.

During the state expansion when the 2σ contour of a state that is being expanded approaches a linear landmark we calculate the projection of the state distribution $p(x,y,\Sigma)$ onto the 2-D plane described by expanding the feature to all values of θ within 90 degrees of the direction normal to the landmark (at the point of contact, the feature looks identical for all values of θ). Figure 65 shows an example with the 3-D ellipsoid defined by the 2σ bounds of the covariance matrix as it approaches a linear feature located at x=10. The feature creates a plane at x=10, and the covariance matrix is then projected onto that plane. In this case, the projection is equivalent to marginalizing $p(x,y,\Sigma)$ over all values of x.

Figure 66 shows the same localization process on the xy plane. It shows how the uncertainty in x is reduced, but it does not represent the uncertainty in θ.

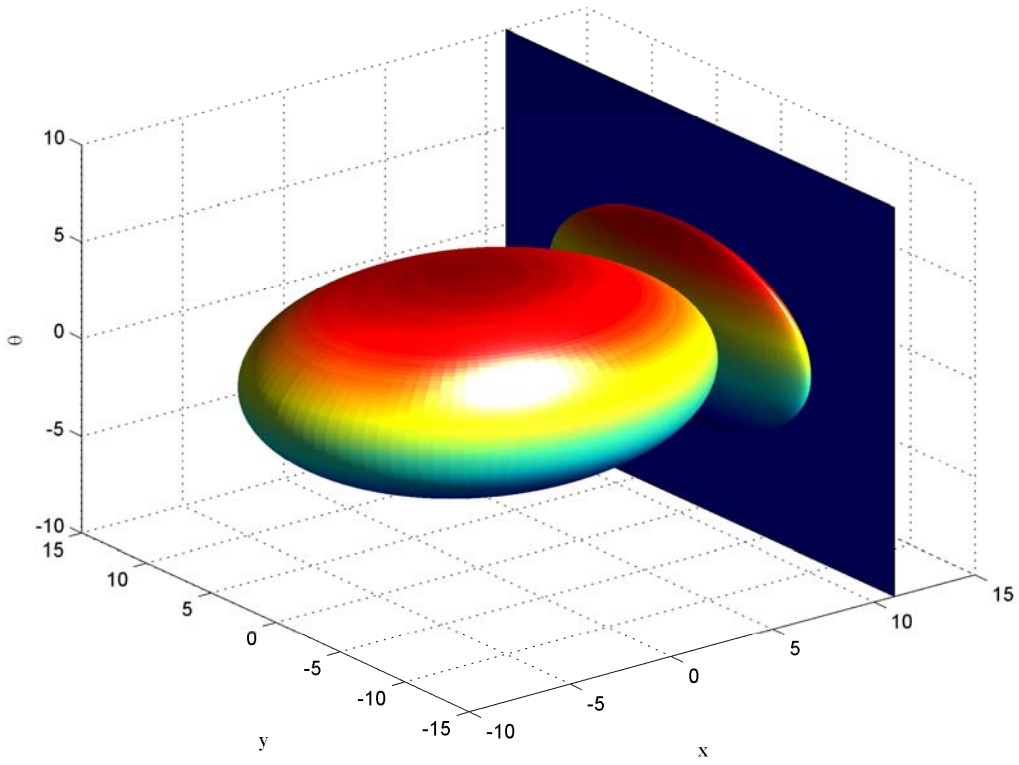

Figure 65. Localization with a linear feature: projection of the ellipsoid representing the 3-D covariance matrix in x,y and θ onto the plane defined by a linear landmark.

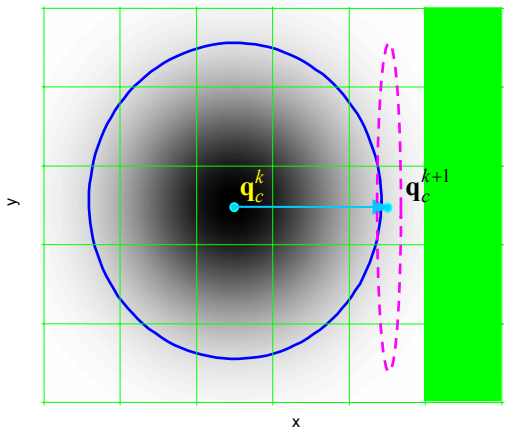

Figure 66. Localization with linear feature

8.2.1 Localizing with wall-like features

The localization approach described above assumes that, on execution, the robot will move towards the feature until the feature is found. This collapses the uncertainty in the direction normal to the feature and preserves the Gaussian assumption needed by the planner. In order to model this transition as a deterministic one we need the certainty that the feature used for localization will actually be found. While this assumption may not hold for some types of linear features, it does hold for wall-like features: features that will prevent the robot from moving when they are found. Examples of these features are walls, dense tree lines and possibly rivers. Walls and tree lines can be reliably detected with approaches such as the one proposed by Vandapel *et al* [99]. Rivers pose a much more complicated challenge as they can be obscured by vegetation and it may be dangerous to try to find a river by getting very close to it.

Figure 67 shows an example world with wall-like features and the path found by PUPLL. The robot starts with high uncertainty which would make it costly to go through the channel before the goal. The path, therefore, follows a low cost path to a vertical wall to reduce horizontal uncertainty, and then moves down to a horizontal wall to reduce vertical uncertainty. After this second localization, the uncertainty in the robot's position is very small, but the uncertainty in its heading has not changed since we do not use the walls to improve heading accuracy. The robot then accrues additional uncertainty as it moves, but is able to pass stay within the low cost area in the channel on the way to the goal.

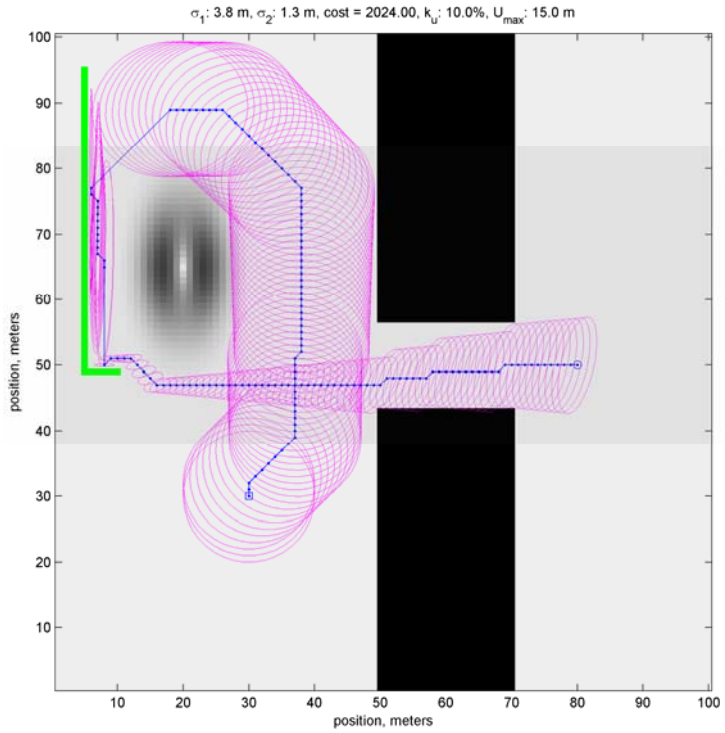

Figure 67.Path planning using wall-like features. Light gray regions are low cost regions, darker regions are higher cost regions and green areas are obstacles.

8.2.2 Localizing with roads

Localizing with roads poses some challenges not present with wall-like features. The most important challenge is that road detection is only reliable in limited situations. The most reliable type of road detection is that of structured roads (paved roads with lane markers). However, even in this case the detection is only reliable if the vehicle is on the road. Detecting a road when the robot is not on it is a challenging problem not yet solved by current approaches to road detection.

Considering these limitations, the approached proposed here to localize with roads assumes that roads can be used for localization only when the robot is on a road to begin with, or when other means of localization can be used to reduce the uncertainty within the width of the road. However, this limitations stem from the detection model, not from the planning approach used. If roads can be reliably detected under more broad circumstances, the limitations described above can be relaxed or removed.

Figure 68 shows a simple example of the planner using roads for localization. Notice how the uncertainty remains low in the direction perpendicular to the direction of travel

as long as the robot is on a road. When the robot leaves the road the uncertainty increases rapidly.

Even with this conservative approach, localization with roads is a powerful approach to planning with uncertainty in position. Because the main source of uncertainty is the error in heading and roads provide localization in the direction perpendicular to the direction of travel, it is possible to navigate very long distances without the need for any other localization approaches.

Figure 69 shows a more realistic example of the planner using roads for localization over a large area. In the example shown, the planner is able to find a path that optimizes cost and that keeps the uncertainty in position at less than 10 meters at all times over a 4.7 km path.

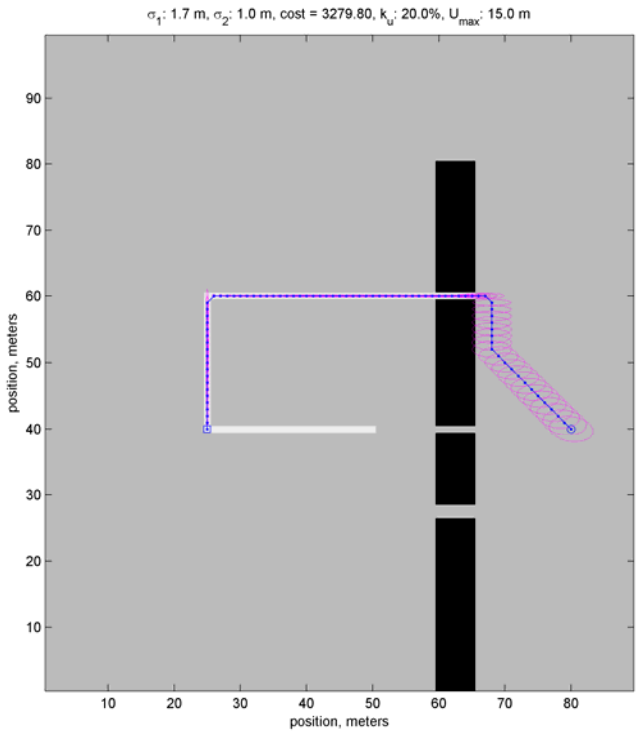

Figure 68. Path planning using roads for localization. Light gray areas are low cost roads that can be detected by the robot. Darker areas are higher cost regions.

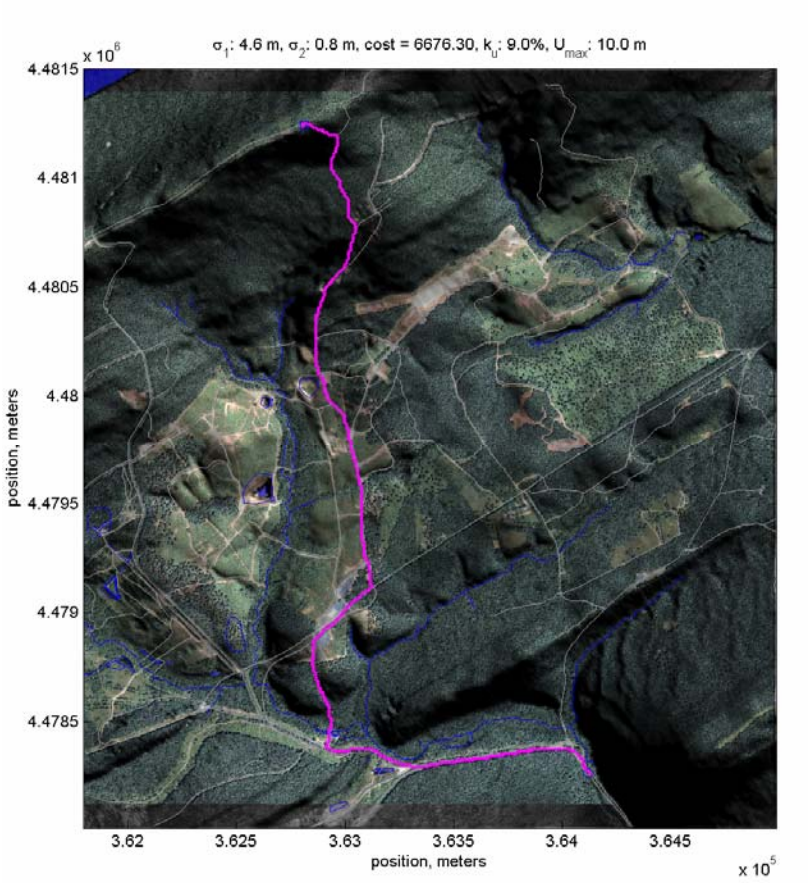

Figure 69. Localization with roads over a large area. Aerial image with shaded relief of Indiantown Gap, PA. Gray lines are roads. Blue lines are rivers. The purple line shows the path found by the planner, which minimizes expected cost and maintains the uncertainty at less than 10 meters after traveling for 4.7 km. The world size is 3.5km by 3.2 km, with 10 m cell spacing.

8.3 Performance

Although the computational complexity of the approaches presented here is similar to that of the 1-D planner, in practice their performance is not nearly as good. This is partly because of the increased overhead in the expected value calculations, and partly due to reduced caching of intermediate results.

Figure 70. shows the processing time of our approaches as well as Censi's incremental binning in simulated fractal worlds like the one in Figure 71 with sizes between 100x100 and 500x500. Our two approaches (entropy and entropy plus incremental binning) have similar performance, and are able to find a path in less than 10 seconds in worlds up to 300x300, and in a few minutes in worlds up to 500x500. Censi's approach takes between 10 and 100 times longer.

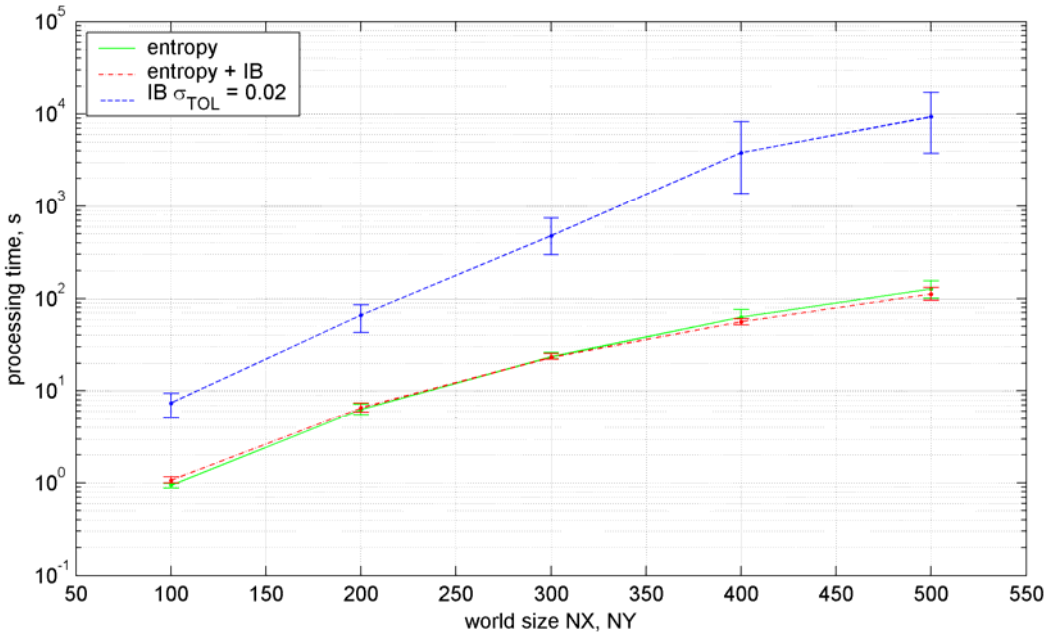

Figure 70. Processing time comparison between PUPLL and Censi's approach for fractal worlds of size 100x100 to 500x500

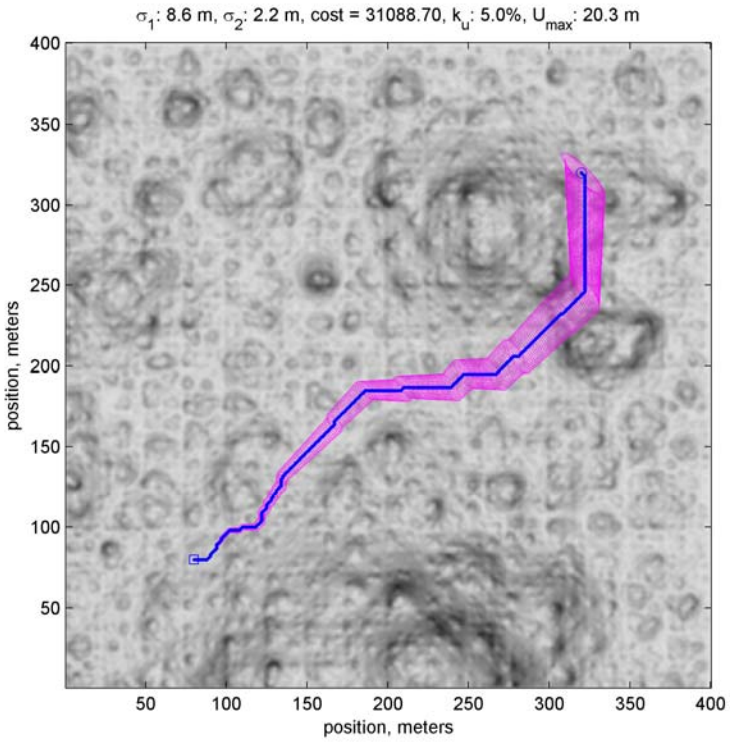

Figure 71. Sample fractal world used for performance simulations.

Another important performance metric is the optimality of the solution. Figure 72 shows a comparison between the path cost found by our approaches and Censi's approach with σ_{TOL}=0.02m, which can be considered an optimal solution. In this type of worlds both of our approaches find an optimal solution within less than 0.01% of the cost found by Censi's approach. It is important to note that even Censi's solution is only optimal in the underlying 8-connected graph that represents the world in (x,y). The solution is suboptimal in comparison with more complex graphs that are able to represent the environment without the limitations of 8-connectivity.

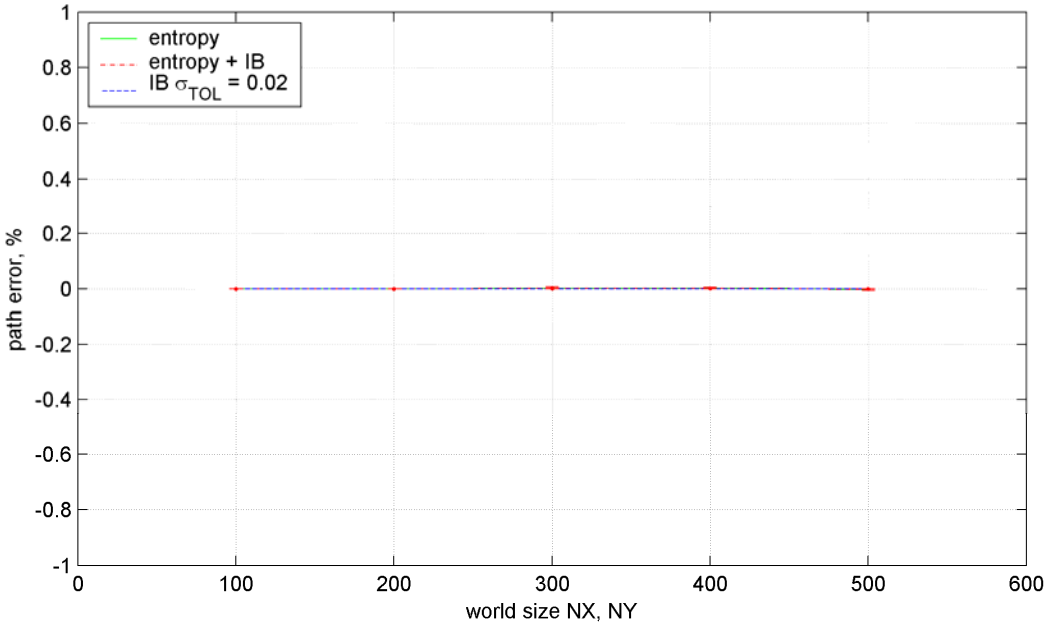

Figure 72.Error in path cost between PUPLL and Censi's approach for fractal worlds of size 100x100 to 500x500

While fractal worlds provide insights into some aspects of the performance of the algorithm, they do not cover all the space of possible configurations. Custom-designed worlds can provide insight into other important aspects of the planner.

Figure 73 shows a comparison of the processing time of our approaches and Censi's approach for different values of σ_{TOL}, for the world described in section 4.2, with maximum uncertainty of 10 meters. PUPLL is faster for σ_{TOL} smaller than 0.02, being much faster for smaller values and slightly slower for larger values. Figure 74 shows the error in the expected path cost, using Censi's approach with σ_{TOL}=0.002 as ground truth. In this example the search space is homeomorphic with the xy plane and the uncertainty's quantization does not affect the results. Both PUPLL and Censi's approach are able to find the optimal path.

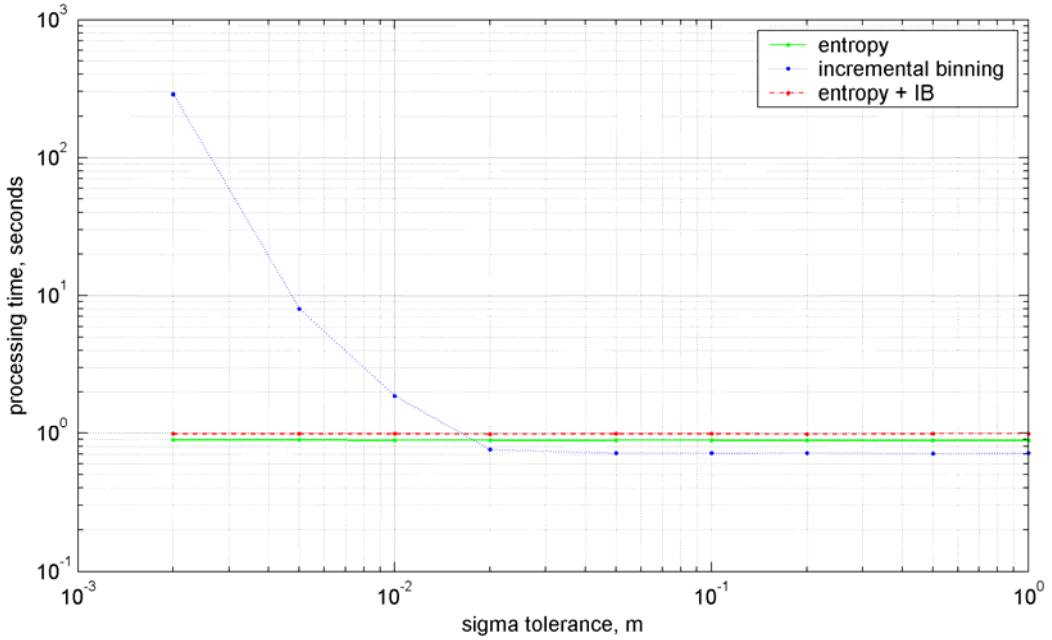

Figure 73. Processing time of PUPLL vs Censi's approach for varying σ_{TOL} values, in the world of section 4.2, with maximum uncertainty of 10 meters.

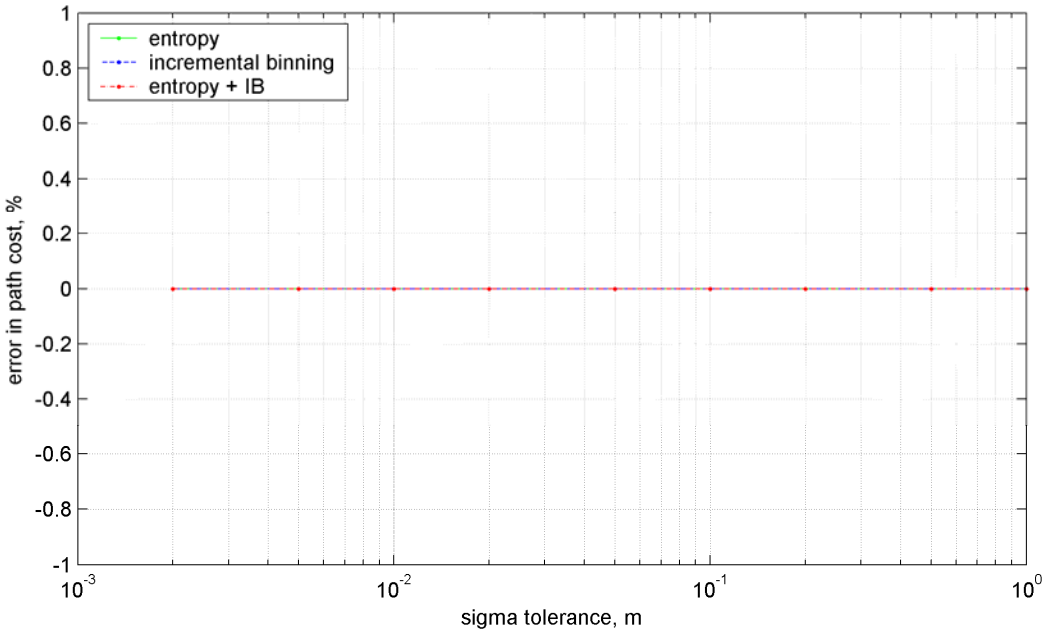

Figure 74. Path cost error of PUPLL vs Censi's approach for varying σ_{TOL} values, in the world of section 4.2, with maximum uncertainty of 10 meters.

Figure 75 shows a similar comparison, but now for the example with the maximum uncertainty of 3 meters, in which the search space is no longer homeomorphic with the xy plane. PUPLL is faster for σ_{TOL} smaller than 0.03, being much faster for smaller values and slightly slower for larger values. Figure 76 shows the error in the expected path cost,

using Censi's approach with σ_{TOL}=0.002 as ground truth. PUPLL is able to find the optimal path, and so does Censi's approach, but only when σ_{TOL} is less than 0.005. At this resolution, PUPLL is almost 100 times faster than Censi's approach.

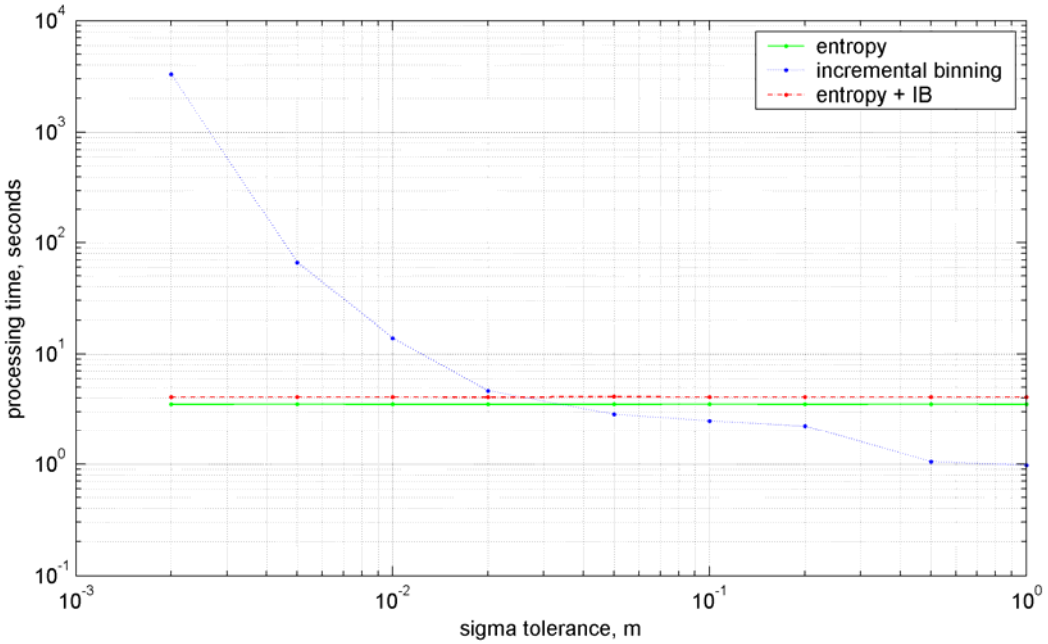

Figure 75. Processing time of PUPLL vs Censi's approach for varying σ_{TOL} values, in the world of section 4.2, with maximum uncertainty of 3 meters.

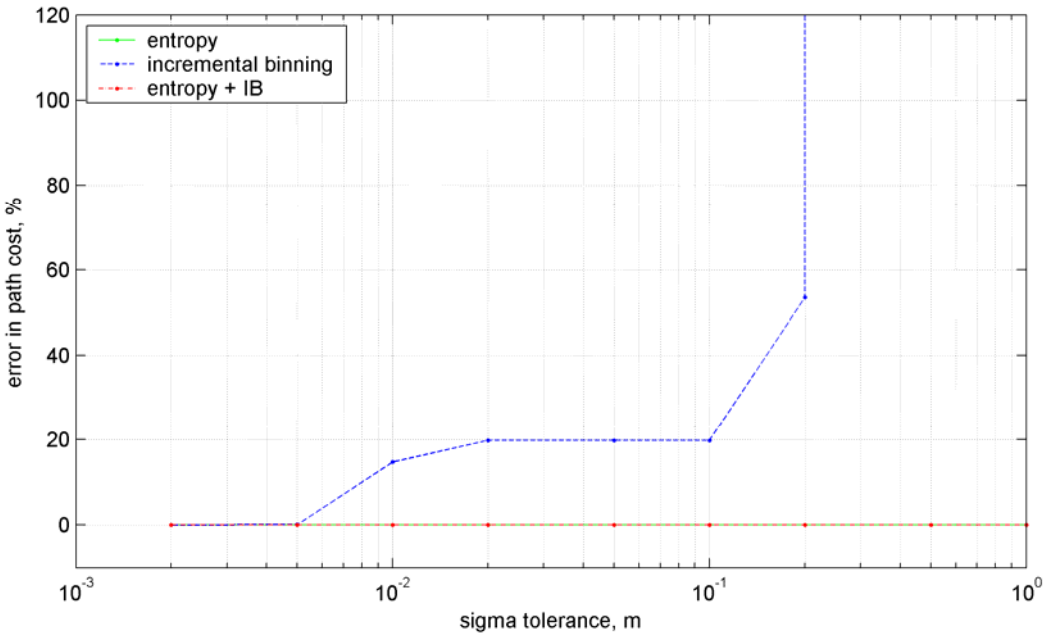

Figure 76. Path cost error of PUPLL vs Censi's approach for varying σ_{TOL} values, in the world of section 4.2, with maximum uncertainty of 3 meters.

In the previous examples, the entropy-based approach performs as well as any of the other approaches with respect to path cost. While this is not uncommon, there are environments in which using entropy alone results in suboptimal paths. Figure 77 shows one of such environments, a complex world with multiple walls in different orientations, as well as high cost areas (darker areas). Notice how the planner localizes with walls of different orientations, while staying away from high-cost regions. Notice also that the localizations only take place when needed in order to reduce cost of to get through a narrow passage, as apposed to trying to localize continuously.

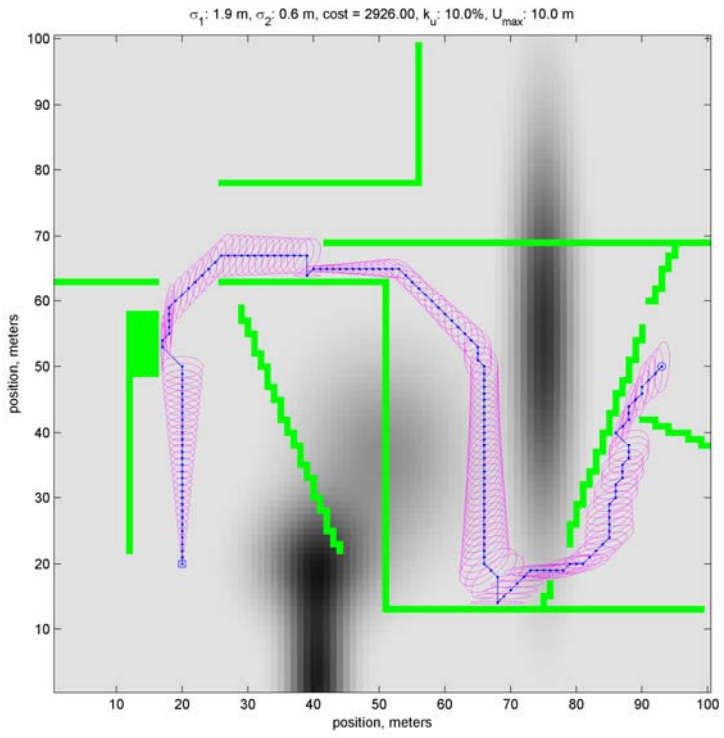

Figure 77.Complex sample world with multiple walls (green obstacles)

Figure 78 shows the path cost of Censi's approach with different values of σ_{TOL} as well as our two approaches. Notice how the entropy-based approach has a small error of about 1% with respect to the optimal path. In contrast, when using entropy plus incremental binning, the planner is able to find the optimal path. Figure 79 shows the processing time for this example. Notice how entropy is about 8 times faster than entropy plus incremental binning, and significantly faster than Censi's approach for most values of σ_{TOL}. Also notice that there are no solutions for Censi's approach when σ_{TOL} is smaller than 0.02. This is because our implementation of this approach is unable to handle more than 1000 bins, and this example requires significantly more than 1000 bin levels for σ_{TOL} smaller than 0.02.

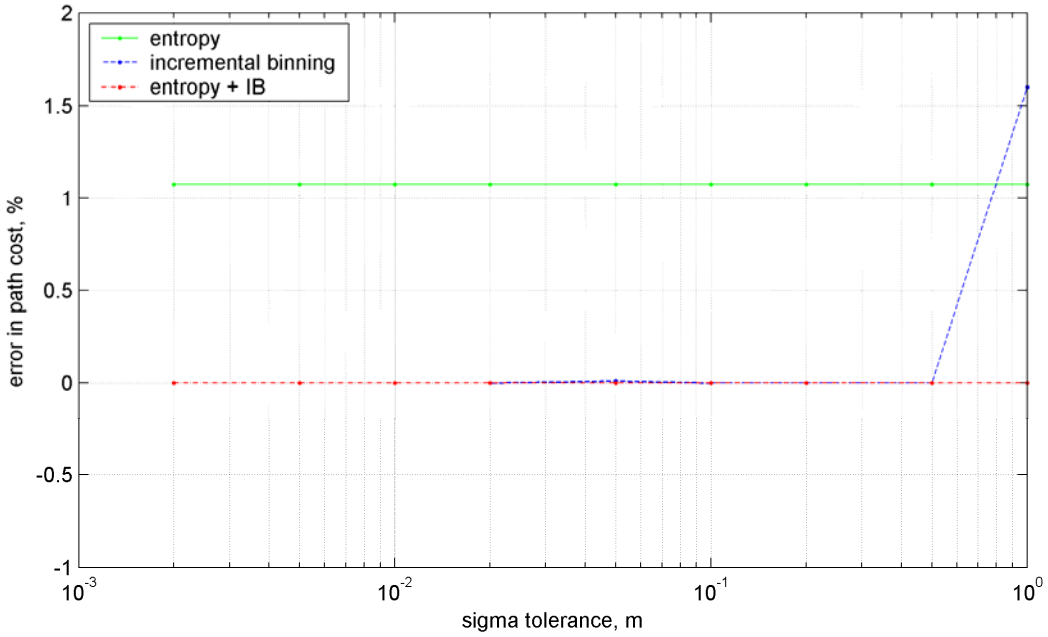

Figure 78. Path cost error of PUPLL vs Censi's approach for varying σ_{TOL} values,

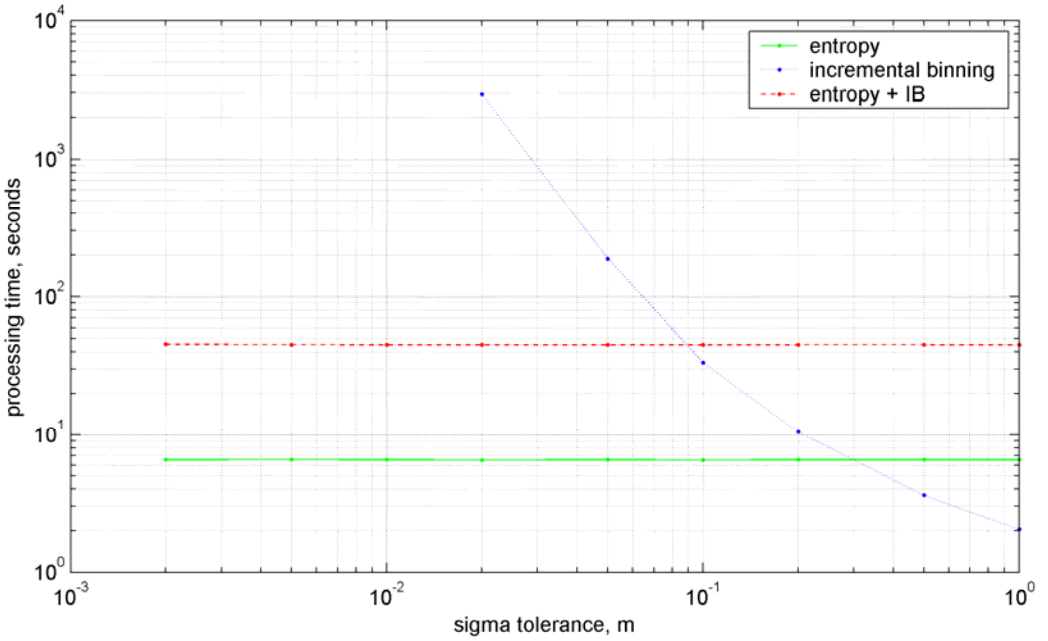

Figure 79. Processing time of PUPLL vs Censi's approach for varying σ_{TOL} values.

8.4 Discussion

The approaches presented here build on the original PUP approach and add the ability to localize with linear landmarks, which significantly improves the localization abilities of the planner. This is especially true in urban settings, since linear features are most common in man-made environments.

Having a more accurate and flexible error propagation model also allows the planner to find solutions in situations where the single-parameter approximation is too limiting, such as in narrow corridors or when the initial uncertainty is not symmetric.

However, by planning in a space that may not represent the full belief space for the problem makes the planner potentially suboptimal and incomplete. In practice, however, the paths found by the planner are usually either optimal or very near optimal (within the limitations of the resolution and the representation).

The advantages of using a single parameter to represent uncertainty are multiple. The space and computational requirements of the algorithm are several orders of magnitude lower than what would be required to plan in the complete parameter space. Also, unlike Censi's approach, the space requirements of the algorithm are clearly bounded.

We also propose an approach that combines the best features of the entropy representation and the incremental binning approach. This approach is able to find optimal paths in more complex environments than entropy alone. While this approach is somewhat slower than the entropy approach, it is still faster than incremental binning alone.

However, neither of the approaches presented are as fast as RPUP, as they do not enable re-planning. Because the approaches depend on a forward, semi-deterministic simulation to update their covariance estimates, it would be either very difficult or impossible to adapt the algorithm for backward search. Censi has proposed an algorithm that plans backwards paths with full covariance in indoor environments by backprojecting constraints, instead of covariances. If this approach can be generalized to continuous cost environments it would then be possible to implement some form of replanning as well, but it is unclear what performance gains would be achieved.

Chapter 9

Conclusion

9.1 Summary

This thesis addresses the problem of planning paths with uncertainty in position using high-resolution maps. The approaches presented here enable a robot to reliably navigate autonomously in an outdoor environment without GPS through the use of accurate, high resolution prior maps and a good dead-reckoning system.

These approaches take advantage of the low drift rate in the inertial navigation system of many outdoor mobile robots, thus enabling the use of a Gaussian distribution to model position uncertainty and the use of deterministic search to efficiently find paths that minimize expected cost while considering uncertainty in position.

9.1.1 Planning with Uncertainty in Position

Although planning with uncertainty in position without using landmarks is of limited use, this approach provides the base on which the other approaches presented in this thesis build upon. This approach is an A*-based implementation that makes use of deterministic search techniques such as lazy evaluation and state dominance. It is implemented as a forward search algorithm in order to minimize the size of the search space and the processing time.

9.1.2 Planning with Uncertainty in Position Using Point Landmarks

The approach presented here builds on the previous approach by using landmarks for localization. The current version of the algorithm uses light poles as its landmarks, and assumes that the landmarks will always be detected in both planning and execution. Because landmarks that can be reliably detected such as trees and electric poles are not

unique, we use an estimate of the position of the robot in order to disambiguate them and prevent aliasing as part of the planning process.

The planner is able to plan in less than 10 seconds for worlds up to 400x400, and in about 80 seconds in worlds of size 1000x1000. To the best of out knowledge this is the fastest planner for planning with uncertainty in position for continuous cost domains.

9.1.3 Replanning with Uncertainty in Position (RPUP)

The approach presented here has an average execution time that is up to two orders of magnitude faster than the PUP approach presented in Chapter 5. Because replanning takes on average less than one second, this approach can be considered near-real-time: the planner can be implemented online incorporating real-time updates from the onboard sensors in the robot. This solves some of the problems with off-line planners that are limited to local obstacle avoidance when executing the original path.

The approach proposed here handles two of the most common cases for data updates with uncertainty in position for mobile robot navigation: prior map updates and sensor updates. Prior map updates are assumed to be registered with the original prior map are up to one order of magnitude faster to replan than to plan from scratch. Sensor updates are assumed to be registered with the robot, and are up to two orders of magnitude faster to process than planning from scratch.

The performance of the algorithm is shown through simulations and field experiments, including a run of more than 800 meters. These experiments confirm the importance of considering uncertainty as part of the planning process, and show that the algorithm can be successfully run on-line in an autonomous robot.

9.1.4 Planning with Uncertainty in Position using an Inaccurate Landmark Map or Imperfect Landmark Perception

The approaches presented here allow a robot to plan paths considering uncertainty in position and using imperfect landmarks or imperfect landmark perception. We show that by modifying RPUP to replan when landmarks are not detected is often sufficient to deal with imperfect landmarks. This approach is called Optimistic Planning with Replanning as it first assumes that all landmarks will be detected. Optimistic Planning, however, can lead to suboptimal paths. More importantly, it can also have the robot follow a path from which there is no return if a landmark is not detected. Planning with Uncertainty in Position Guaranteeing a return path improves on the Optimistic Planning approach by ensuring that the robot always has a return path if a landmark is missed. Both approaches allow for fast replanning when new sensor information is acquired.

The approaches presented here are likely to be much faster than any existing POMDP-based approach such as PPCP or PAO*. While no direct comparisons are available, the computational complexity estimates indicate that PUPGR is likely to be at least one order of magnitude faster than either PAO* or PPCP. In replanning mode (after the initial path has been calculated), PUPGR is likely to be two or three orders of magnidude faster than either PPCP or PAO*.

In spite of having an overly simple model of the alternatives available, the ability to incorporate new sensor data into the path and replan quickly makes up for many of the shortcomings of the approach.

9.1.5 Planning with Uncertainty in Position using Linear Landmarks

This approach adds the ability to localize with linear landmarks, which significantly improves the localization abilities of the planner. This is especially true in urban settings, since linear features are most common in man-made environments.

Having a more accurate and flexible error propagation model also allows the planner to find solutions in situations where the single-parameter approximation is too limiting, such as in narrow corridors or when the initial uncertainty is not symmetric.

However, by planning in a space that may not represent the full belief space for the problem makes the planner potentially suboptimal and incomplete. In practice, however, the paths found by the planner are usually either optimal or very near optimal (within the limitations of the resolution and the representation).

The advantages of using a single parameter to represent uncertainty are multiple. The space and computational requirements of the algorithm are several orders of magnitude lower than what would be required to plan in the complete parameter space. Also, unlike Censi's approach, the space requirements of the algorithm are clearly bounded.

We also propose an approach that combines the best features of the entropy representation and the incremental binning approach. This approach is able to find optimal paths in more complex environments than entropy alone. While this approach is somewhat slower than the entropy approach, it is still faster than incremental binning alone. It is important to note, however, that the paths found by these approaches are limited by the 8-connected nature of the underlying graph used to represent the world. This means that while it is not possible to find lower cost solutions in an 8-connected graph, it may be possible to find lower cost paths if the graph is allowed to transition in arbitrary directions.

9.2 Contributions

Our approach provides the following contributions to the field of robotics

- The best approach to plan and navigate without GPS in an outdoor environment using reliable point landmarks for localization. To the best of our knowledge, PUP is the most computationally efficient planner for outdoor environments that considers uncertainty in position. On average, it also produces paths that are closer to optimal.
- The first near-real-time approach for re-planning with uncertainty in position using reliable point landmarks.
- The first approach to planning with uncertainty in position for outdoor robots to be experimentally validated in a robotic platform.
- The first approach to planning with uncertainty in position using linear landmarks in outdoor environments.
- The first near-real-time approach to planning with uncertainty in position using imperfect landmark maps or imperfect perception.

9.3 Future work

9.3.1 Implementation of an advanced feature detector

Although the experimental results shown in this thesis implement a feature detector similar to the one proposed by Vandapel *et al* [99], the resulting detector is not representative of the state-of-the-art in feature detection. Implementing a more advanced feature detector would increase the types of landmarks that could be detected, improving the applicability of the planner.

9.3.2 Explicit disambiguation of landmarks

The approaches presented here deal with ambiguity by avoiding situations in which aliasing takes place. While this approach works well, it discards solutions that may be important in some scenarios. A more thorough approach would be to add explicit disambiguation techniques to the state expansion, in order to be able to include more instances of aliased landmarks into the search.

9.3.3 Landmark search

The approach presented here for planning with point landmarks only uses a landmark when its detection region is larger than the uncertainty of the robot. In some situations, better solutions can be found if the planner is able to reason about searching for a landmark in a local neighborhood. This would enable to planner to find safe paths in situations where landmarks are sparse.

9.3.4 Planning with imperfect landmark maps or imperfect perception

The approaches presented here add significant reliability while maintaining fast replanning and the ability to incorporate new data into the path. However, the alternatives considered are overly simplistic and may be too conservative to find solutions in complicated cases. While it is important to maintain a simple model that still enables using deterministic search, the existing approach could be improved by considering more alternatives when landmarks are not detected.

9.3.5 Replanning with linear landmarks

The approach presented for planning with linear landmarks plans from scratch every time. Even though the approach is extremely efficient, its planning time is not suitable for online planning in larger environments. An important improvement to this approach would be to implement replanning. However, the challenges to implement replanning with linear landmarks are greater than those encountered when implementing replanning with point landmarks, as the backward transformations of uncertainty are not unique.

9.3.6 Generalization to a more complex graph representation

Most of the approaches presented here use an 8-connected graph to represent the (x,y) dimensions of the world. While this enables significant performance gains, it also limits the quality of the solutions, as only 8 directions of motion are allowed at each path step. Incorporating interpolation techniques such as the ones proposed in Field D*[21] or θ*[70] should improve the quality of the solution. However, these techniques also impose an overhead that can be significant depending on the domain.

9.3.7 Generalization to other planning domains

Some of the approaches presented here may be applicable to other domains. In particular, it is likely that some of the models and dimensionality reduction techniques

would be useful in non-holonomic path planning and domains with other types of uncertainty.

References

[1] E Abbott, “Land-vehicle navigation systems: An examination of the influence of individual navigation aids on system performance,” Ph.D. Dissertation, Stanford University, March 1997

[2] R. Alterovitz, A. Lim, K. Goldberg, G. Chirikjian, and A. Okamura, "Steering flexible needles under Markov motion uncertainty". Intelligent Robots and Systems, 2005. (IROS 2005). 2005 IEEE/RSJ International Conference on, , 1570-1575, 2-6 Aug. 2005.

[3] R. Alterovitz, T. Simeon, and K. Goldberg, "The Stochastic Motion Roadmap: A Sampling Framework for Planning with Markov Motion Uncertainty". Proceedings of Robotics: Science and Systems, 2007.

[4] B. Bonet and H. Geffner, "Planning with incomplete information as heuristic search in belief space," in Proceedings of the 6th International Conference on Artificial Intelligence in Planning Systems (AIPS), pp. 52-61, AAAI Press, 2000.

[5] B. Bouilly, T. Siméon, and R. Alami. “A numerical technique for planning motion strategies of a mobile robot in presence of uncertainty”. In Proc. of the IEEE Int. Conf. on Robotics and Automation, volume 2, pages 1327--1332, Nagoya (JP), May 1995.

[6] B. Bouilly. “Planification de Strategies de Deplacement Robuste pour Robot Mobile”. PhD thesis, Insitut National Polytechnique, Tolouse, France, 1997

[7] F. Bourgault, A. Makarenko, S. Williams, B. Grocholsky, and H. Durrant-Whyte, "Information based adaptive robotic exploration," in Proceedings IEEE/RSJ International Conference on Intelligent Robots and Systems (IROS), vol. 1, 2002, pp. 540—545.

[8] W. Burgard, D. Fox, D. Hennig, and T. Schmidt. “Estimating the absolute position of a mobile robot using position probability grids”. In Proc. of the Thirteenth National Conference on Artificial Intelligence, 1996

[9] W. Burgard, D. Fox, and D. Hennig. “Fast grid-based position tracking for mobile robots”. In Proc. of the 21th German Conference on Artificial Intelligence, Germany. Springer Verlag, 1997

[10] W. Burgard, D. Fox, and S. Thrun. “Active mobile robot localization”. In Proceedings of IJCAI-97. IJCAI, Inc., 1997

[11] B. Burns and O. Brock, "Sampling-Based Motion Planning With Sensing Uncertainty". Robotics and Automation, 2007 IEEE International Conference on, 3313-3318, 10-14 April 2007.

[12] A. Cassandra, L. Kaelbling, and M. Littman, “Acting optimally in partially observable stochastic domains”. In Proceedings of the National Conference on Artificial Intelligence (AAAI), 1023—1028, 1994

[13] A. Censi, "On achievable accuracy for range-finder localization". Proceedings of the IEEE International Conference on Robotics and Automation (ICRA), 4170-4175,2007.

[14] A. Censi, "Robot Motion Planning with Uncertainty". Universita degli Studi di Roma La Sapienza, 2007.

[15] F. Dellaert, D. Fox, W. Burgard, and S. Thrun, “Monte Carlo Localization for Mobile Robots,” IEEE International Conference on Robotics and Automation (ICRA99), May, 1999.

[16] C. Dima, N. Vandapel, and M. Hebert, "Classifier Fusion for Outdoor Obstacle Detection," International Conference on Robotics and Automation, IEEE, April, 2004

[17] M. Dissanayake, P. Newman, S. Clark, H. Durrant-Whyte, and M. Csorba. “A solution to the simultaneous localization and mapping (SLAM) problem”. IEEE Transactions on Robotics and Automation, 2001

[18] G. Dudek, K. Romanik and S. Whitesides. “Localizing a robot with minimum travel”. In Proc. 6th ACM-SIAM Symp. on Discrete Algorithms, 437-- 446, 1995

[19] M.E. El Najjar, P. Bonnifait, “A Road-Matching Method for Precise Vehicle Localization Using Belief Theory and Kalman Filtering”. Autonomous Robots 19(2): 173-191, 2005

[20] D. Ferguson, A. Stentz, and S. Thrun, “PAO* for Planning with Hidden State,” Proceedings of the 2004 IEEE International Conference on Robotics and Automation, April, 2004.

[21] D. Ferguson and A. Stentz, "Using Interpolation to Improve Path Planning: The Field D* Algorithm". Journal of Field Robotics, 23, 79-101, February 2006.

[22] D. Fox, “Markov Localization: A Probabilistic Framework for Mobile Robot Localization and Navigation”. Ph.D. Dissertation, University of Bonn, Germany, 1998.

[23] D. Fox, W. Burgard, and S. Thrun. “Active markov localization for mobile robots”. Robotics and Autonomous Systems, 1998

[24] D. Fox, W. Burgard, F. Dellaert, and S. Thrun, "Monte Carlo Localization: Efficient Position Estimation for Mobile Robots," Proceedings of the Sixteenth National Conference on Artificial Intelligence (AAAI'99)., July, 1999.

[25] Th. Fraichard and R. Mermond "Integrating Uncertainty And Landmarks In Path Planning For Car-Like Robots" Proc. IFAC Symp. on Intelligent Autonomous Vehicles March 25-27, 1998.

[26] Th. Fraichard and R. Mermond. “Path Planning with Uncertainty for Car-Like Robots”. In: Proc. of the IEEE Int. Conf. on Robotics and Automation, volume 1, pages 27-32, Leuven (BE), May 1998

[27] Th. Fraichard & Mermond, R. - Path Planning with Kinematic and Uncertainty Constraints. - In: Intelligent Autonomous Systems, pages 30-37. International Scientific Issue, Ufa State Aviation Technical University (RU), 1998.

[28] R.L. French, “Map Matching Origins, Approaches and Applications”. In Proceedings of the Second International Symposium on Land Vehicle Navigation, pages 91-116

[29] A. Gelb, Applied Optimal Estimation, MIT Press, Cambridge, MA, 1974.

[30] K. Goldberg, M. Mason, and A. Requicha. “Geometric uncertainty in motion planning”. Summary report and bibliography. IRIS TR. USC Los Angeles, 1992.

[31] J.P. Gonzalez, Planning with Uncertainty in Position Using High-Resolution Maps - Thesis Proposal, tech. report CMU-RI-TR-06-45, Robotics Institute, Carnegie Mellon University, October, 2006.

[32] J.P. Gonzalez and A. Stentz, “Planning with Uncertainty in Position: an Optimal Planner”, tech. report CMU-RI-TR-04-63, Robotics Institute, Carnegie Mellon University, November, 2004.

[33] J.P. Gonzalez and A. Stentz, "Planning with Uncertainty in Position: An Optimal and Efficient Planner," Proceedings of the IEEE International Conference on Intelligent Robots and Systems (IROS '05), August, 2005.

[34] J.P. Gonzalez and A. Stentz, “Planning with Uncertainty in Position Using High-Resolution Maps”, tech. report CMU-RI-TR-06-33, Robotics Institute, Carnegie Mellon University, August, 2006.

[35] J.P. Gonzalez and A. Stentz, "Planning with Uncertainty in Position Using High-Resolution Maps," In Proceedings of the IEEE Int. Conference on Robotics & Automation (ICRA) 2007, April, 2007.

[36] A. Hait and T. Simeon, “Motion planning on rough terrain for an articulated vehicle in presence of uncertainties,” in IEEE International Conference on Robots and Systems, Osaka (Japan), November 1996.

[37] A. Haït, T. Simeon, and M. Taïx, "Robust motion planning for rough terrain navigation".Published in IEEE Int. Conf. on Intelligent Robots and Systems Kyongju, Korea, 1999.

[38] S. Honey, W. Zavoli, K. Milnes, A. Phillips, M. White and G. Loughmiller, “Vehicle navigational system and method”. US Patent 4,796,191, 1989

[39] A. Howard and L. Kitchen. Navigation using natural landmarks. Robotics and Automous Systems, 26:99--115, 1999

[40] K. Iagnemma, F. Genot, and S. Dubowsky, "Rapid physics-based rough-terrain rover planning with sensor and control uncertainty". Robotics and Automation, 1999. Proceedings. 1999 IEEE International Conference on, 3, 2286-2291 vol.3, 1999.

[41] M. Jabbour and P. Bonnifait, "Global Localization Robust to GPS Outages using a Vertical Ladar". Control, Automation, Robotics and Vision, 2006. ICARCV '06. 9th International Conference on, 1-6, 5-8 Dec. 2006.

[42] R.R. Joshi, "A new approach to map matching for in-vehicle navigation systems: the rotational variation metric," Proceeding of IEEE Intelligent Transportation Systems, Oakland, CA, 2001.

[43] Kaelbling, L., Littman, M., and Cassandra, A. “Planning and acting in partially observable stochastic domains,” Artificial Intelligence, 1998.

[44] R.E. Kalman, "A new approach to linear filtering and prediction problems," Transactions of the ASME--Journal of Basic Engineering, vol. 82, no. Series D, pp. 35--45, 1960.

[45] A. Kelly, “Linearized Error Propagation in Odometry”, The International Journal of Robotics Research. February 2004, vol. 23, no. 2, pp.179-218(40).

[46] S. Koenig and M. Likhachev. Improved fast replanning for robot navigation in unknown terrain. Technical Report GITCOGSCI -2002.

[47] S. Koenig and M. Likhachev, "D*lite". Eighteenth national conference on Artificial intelligence, American Association for Artificial Intelligence, 476-483, 2002.

[48] S. Koenig, M. Likhachev and D. Furcy, "Lifelong planning A*". Artificial Intelligence, Elsevier Science Publishers Ltd., 155, 93-146, 2004.

[49] S. Koenig, R.G Simmons, "Real-Time search in non-deterministic domains," In Proceedings of IJCAI-95, pp. 1660-1667, 1995

[50] S. Koenig and R.G. Simmons, "Solving robot navigation problems with initial pose uncertainty using real-time heuristic search". In Proceedings of the International Conference on Artificial Intelligence Planning Systems, 1998, pp 154—153.

[51] J. Lalonde, N. Vandapel, and M. Hebert, "Automatic Three-Dimensional Point Cloud Processing for Forest Inventory", tech. report CMU-RI-TR-06-21, Robotics Institute, Carnegie Mellon University, July, 2006

[52] A. Lambert and T. Fraichard, "Landmark-based safe path planning for car-like robots". Robotics and Automation, 2000. Proceedings. ICRA'00. IEEE International Conference on, 3, 2000.

[53] A. Lambert and D. Gruyer, "Safe path planning in an uncertain-configuration space". Robotics and Automation, 2003. Proceedings. ICRA '03. IEEE International Conference on, 3, 4185-4190 vol.3, 14-19 Sept. 2003.

[54] J.C. Latombe, A. Lazanas, and S. Shekhar, "Robot Motion Planning with Uncertainty in Control and Sensing," Artificial Intelligence J., 52(1), 1991, pp. 1-47.

[55] J.C. Latombe, A. Lazanas and S. Shekhar, "Motion Planning with Uncertainty: Practical Computation of Non-maximal Preimages," in Proceedings of the IEEE International Workshop on Intelligent Robots and Systems, Tsukuba, Japan, 1989.

[56] J.C. Latombe, *Robot Motion Planning*. Kluwer Academic Publishers. 1990

[57] S.M. LaValle, "Planning Algorithms", Cambridge University Press, 2006. Also online, http://planning.cs.uiuc.edu

[58] S. LaValle and S. Hutchinson, "An objective-based framework for motion planning under sensing and control uncertainties". International Journal of Robotics Research, 17(1):19--42, 1998.

[59] A. Lazanas, and J.C. Latombe, "Landmark-based robot navigation". In Proc. 10th National Conf. on Artificial Intelligence (AAAI-92), 816--822. Cambridge, MA: AAAI Press/The MIT Press.

[60] M. Likhachev, D. Ferguson, G. Gordon, A. Stentz, and S. Thrun, "Anytime Dynamic A*: An Anytime, Replanning Algorithm". Proceedings of the International Conference on Automated Planning and Scheduling (ICAPS), 2005.

[61] M. Likhachev, G. Gordon, and S. Thrun, "ARA*: Anytime A* with provable bounds on sub-optimality". Advances in Neural Information Processing Systems (NIPS), 2003.

[62] M. Likhachev and S. Koenig, "Lifelong Planning for Mobile Robots". Revised Papers from the International Seminar on Advances in Plan-Based Control of Robotic Agents,, Springer-Verlag, 140-156, 2002.

[63] M. Likhachev and A. Stentz, "PPCP: Efficient Probabilistic Planning with Clear Preferences in Partially-Known Environments," Proceedings of the National Conference on Artificial Intelligence (AAAI), 2006

[64] T. Lozano-Perez, M. Mason and R. Taylor, "Automatic Synthesis of Fine-Motion Strategies for Robots," in proceedings, International Symposium of Robotics Research, Bretton Woods, NH, August 1983.

[65] N. Melchior, J. Kwak, and R. Simmons, "Particle RRT for Path Planning in Very Rough Terrain," Proceedings of the NASA Science Technology Conference 2007 (NSTC-07), May, 2007.

[66] N. Melchior and R. Simmons, "Particle RRT for Path Planning with Uncertainty," 2007 IEEE International Conference on Robotics and Automation, April, 2007, pp. 1617-1624.

[67] G.A. Mills-Tettey, A. Stentz, and M.B. Dias, "DD* Lite: Efficient Incremental Search with State Dominance," Twenty-First National Conference on Artificial Intelligence (AAAI-06), July, 2006, pp. 1032-1038.

[68] N.J. Nilsson. "Principles of Artificial Intelligence". Tioga publishing company, Wellsboro, PA, 1980

[69] P. Missiuro and N. Roy, "Adapting probabilistic roadmaps to handle uncertain maps". Robotics and Automation, 2006. ICRA 2006. Proceedings 2006 IEEE International Conference on, , 1261-1267, May 15-19, 2006.

[70] A. Nash, K. Daniel, S. Koenig, and A. Felner, "Theta*: Any-Angle Path Planning on Grids". Proceedings of the AAAI Conference on Artificial Intelligence, Menlo Park, CA; Cambridge, MA; London; AAAI Press; MIT Press; 1999, 22, 1177, 2007.

[71] I. Nourbakhsh, R. Powers, and S. Birchfield. Dervish an office-navigating robot. AI Magazine, 16(2):53--60, 1995.

[72] J.M. O'Kane and S.M. LaValle, "Almost-Sensorless Localization," in Proceedings of the 2005 IEEE International Conference on , vol., no.pp. 3764- 3769, 18-22 April 2005

[73] L. Page and A. Sanderson, "Robot motion planning for sensor-based control with uncertainties". Robotics and Automation, 1995. Proceedings., 1995 IEEE International Conference on, 2, 1995.

[74] R. Pepy and A. Lambert, "Safe Path Planning in an Uncertain-Configuration Space using RRT". Intelligent Robots and Systems, 2006 IEEE/RSJ International Conference on, , 5376-5381, Oct. 2006.

[75] J. Pineau, G. Gordon & S. Thrun "Point-based value iteration: An anytime algorithm for POMDPs". International Joint Conference on Artificial Intelligence (IJCAI). Acapulco, Mexico. pp. 1025-1032. Aug. 2003.

[76] J. Pineau, "Tractable Planning Under Uncertainty: Exploiting Structure", doctoral dissertation, tech. report CMU-RI-TR-04-32, Robotics Institute, Carnegie Mellon University, August, 2004.

[77] M. Rao, G. Dudek, and S. Whitesides. Randomized algorithms for minimum distance localization. In Proc. Workshop on Algorithmic Foundations of Robotics, pages 265–280, 2004

[78] N. Ratliff, D. Bradley, J. Bagnell, and J. Chestnutt, "Boosting Structured Prediction for Imitation Learning," Advances in Neural Information Processing Systems 19, MIT Press, Cambridge, MA, 2007.

[79] N. Roy, and S. Thrun, "Coastal navigation with mobile robots". In Advances in Neural Processing Systems 12, volume 12, pages 1043—1049, 1999.

[80] N. Roy and G. Gordon. "Exponential Family PCA for Belief Compression in POMDPs". Advances in Neural Information Processing (15) NIPS, Vancouver, BC. Dec. 2002

[81] N. Roy, Finding Approximate POMDP solutions Through Belief Compression, doctoral dissertation, tech. report CMU-RI-TR-03-25, Robotics Institute, Carnegie Mellon University, September, 2003

[82] N. Roy, Private Conversation. September 1, 2004

[83] C. Scott, "Improved gps positioning for motor vehicles through map matching," In Proceedings of ION GPS-94, 1994.

[84] D. Silver, B. Sofman, N. Vandapel, J. Bagnell, and A. Stentz, "Experimental Analysis of Overhead Data Processing To Support Long Range Navigation," IEEE International Conference on Intelligent Robots and Systems (IROS), October, 2006.

[85] R. Sim and N. Roy, “Global A-Optimal Robot Exploration in SLAM”, in proceedings of the IEEE International Conference on Robotics and Automation (ICRA), Barcelona, Spain, 2005.

[86] R. Simmons and S. Koenig. “Probabilistic robot navigation in partially observable environments”. In Proc. of the International Joint Conference on Artificial Intelligence, 1995.

[87] R.G. Simmons, R. Goodwin, K.Z. Haigh, S. Koenig, J. O'Sullivan, and M.M. Veloso. “Xavier: Experience with a layered robot architecture”. ACM magazine Intelligence, 1997

[88] B. Sofman, J. Bagnell, A. Stentz, and N. Vandapel, “Terrain Classification from Aerial Data to Support Ground Vehicle Navigation”, tech. report CMU-RI-TR-05-39, Robotics Institute, Carnegie Mellon University, January, 2006

[89] B. Sofman, E. Lin, J. Bagnell, N. Vandapel, and A. Stentz, "Improving Robot Navigation Through Self-Supervised Online Learning," Proceedings of Robotics: Science and Systems, August, 2006.

[90] C. Stachniss and W. Burgard. “Exploring unknown environments with mobile robots using coverage maps”. In Proc. of the Int. Conf. on Artificial Intelligence (IJCAI), 2003

[91] A. Stentz, "The Focussed D* Algorithm for Real-Time Replanning," Proceedings of the International Joint Conference on Artificial Intelligence, August, 1995.

[92] A. Stentz, "Optimal and Efficient Path Planning for Partially-Known Environments," Proceedings of the IEEE International Conference on Robotics and Automation (ICRA '94), Vol. 4, May, 1994, pp. 3310 - 3317.

[93] H. Takeda and J.C. Latombe, “Sensory uncertainty field for mobile robot navigation,” Robotics and Automation, 1992. Proceedings., 1992 IEEE International Conference on , vol., no.pp.2465-2472 vol.3, 12-14 May 1992

[94] H. Takeda, C. Facchinetti, and J.C. Latombe. Planning the motions of a mobile robot in a sensory uncertainty field. IEEE Trans. on Pattern Analysis and Machine Intelligence, 16:1002--1015, 1994

[95] J. Tanaka, K. Hirano, T. Itoh, H. Nobuta, and S. Tsunoda, “Navigation system with map-matching method”. In SAE Technical Paper Series (SAE No. 900471), 45-50. Warrendale, PA: Society of Automotive Engineers, 1990.

[96] S. Thrun, D. Fox, and W. Burgard. “A probabilistic approach to concurrent mapping and localization for mobile robots”. Machine Learning and Autonomous Robots (joint issue), 1998

[97] S. Thrun, W. Burgard, and D. Fox. “Probabilistic Robotics”. MIT Press, Cambridge, MA, 2005.

[98] C. Urmson and R. Simmons, "Approaches for Heuristically Biasing RRT Growth," IEEE/RSJ IROS 2003, October, 2003.

[99] N. Vandapel, D. Huber, A. Kapuria, and M. Hebert, "Natural Terrain Classification using 3-D Ladar Data," IEEE International Conference on Robotics and Automation, April, 2004.

[100] P. Whaite and F. P. Ferrie. Autonomous exploration: Driven by uncertainty. IEEE Transactions on Pattern Analysis and Machine Intelligence, 19(3):193--205, March 1997